TAMPEREEN TEKNILLINEN YLIOPISTO
TAMPERE UNIVERSITY OF TECHNOLOGY

Anne-Marie Haaparanta

Highly Porous Freeze-Dried Composite Scaffolds for Cartilage and Osteochondral Tissue Engineering

Julkaisu 1290 • Publication 1290

Tampere 2015

Tampereen teknillinen yliopisto. Julkaisu 1290
Tampere University of Technology. Publication 1290

Anne-Marie Haaparanta

Highly Porous Freeze-Dried Composite Scaffolds for Cartilage and Osteochondral Tissue Engineering

Thesis for the degree of Doctor of Science in Technology to be presented with due permission for public examination and criticism in Tietotalo Building, Auditorium TB109, at Tampere University of Technology, on the 17th of April 2015, at 12 noon.

Tampereen teknillinen yliopisto - Tampere University of Technology
Tampere 2015

ISBN 978-952-15-3484-3 (printed)
ISBN 978-952-15-3491-1 (PDF)
ISSN 1459-2045

Abstract

Cartilage lesions are known to heal poorly and their tissue engineering with optimal scaffolds are widely studied. If the cartilage lesion is deep, there is a need to also repair the underlying bone (i.e. subchondral bone) and the lesion is called an osteochondral lesion. There are several methods used for osteochondral tissue engineering and various scaffold compositions are being studied. The studied scaffold compositions include the one scaffold method, where only one scaffold is used for the osteochondral lesion, or independent structures for cartilage and bone. These two scaffolds could be combined during processing, before surgery or in surgery to obtain osteochondral solutions for cartilage repair.

In this thesis, freeze-drying was used to manufacture highly porous scaffolds with an interconnected pore structure. Natural polymer-based scaffolds often lack the required mechanical stability. Therefore, natural polymer-based hybrids with improved stiffness were manufactured for cartilage tissue engineering scaffolds. Synthetic polymer-based composites with improved osteoconductivity were manufactured for bone or osteochondral tissue engineering scaffolds. The scaffolds were studied to determine the structure of the scaffolds, the effect of the fibrous filler mesh or filler particles on the characteristics of the hybrids or composites, and the suitability of the hybrids for cartilage tissue engineering and the composites for bone or osteochondral tissue engineering. The majority of the studied scaffolds were also cultured with cells *in vitro* to define the suitability of the scaffolds for tissue engineering.

The results show the freeze-drying method to be useful for manufacturing highly porous hybrid and composite scaffolds with improved properties compared with plain polymer scaffolds. Also, all the studied scaffolds had an interconnected porous structure. Improved wettability characteristics showed the method of cross-linking collagen post freeze-drying to be more effective way of cross-linking collagen compared to cross-linking collagen prior to freeze-drying. Synthetic polymer-based composites with an inhomogeneous scaffold structure with β-tricalcium phosphate (TCP) or bioactive glass (BG) filler particles showed improved osteoconductivity. TCP was found to improve the cell proliferation and alkaline phosphatase (ALP) activity of adipose stem cells (ASCs) over plain poly(L/D,L)lactide 70/30 (PLA70) scaffolds or PLA70+BG composites. A porous polymer matrix with a highly porous fibrous filler was successfully combined into highly porous freeze-dried hybrids with a natural polymer matrix (collagen/chitosan and poly(L/D)lactide 96/4 fibres (PLA96)) and composites with a synthetic polymer matrix (poly(D,L-lactide-co-glycolide)70/30 (PLGA)) with bioactive

glass fibres (BGf). The PLA96 fibrous mesh improved the penetration of the chondrocytes into the hybrids compared with plain natural polymer scaffolds.

The manufactured scaffolds were found to be applicable for cartilage, bone and osteochondral tissue engineering applications. Based on the structures developed in this thesis, more optimal scaffold structures are currently being studied.

Acknowledgements

The work presented in this thesis was performed at the Tampere University of Technology, Department of Electronics and Communications Engineering (formerly Department of Biomedical Engineering).

I wish to express my sincere gratitude to my supervisor, professor Minna Kellomäki for her support throughout this thesis and for giving me the opportunity to work under her guidance. I am also most grateful to the official pre-examiners, professor Anna Finne Wistrand and associate professor Showan N. Nazhat for their effort and constructive comments for improving the thesis.

I would like to thank all my co-authors, especially Suvi Haimi, Niina Hopper, Ville Ellä, Susanna Miettinen, Juha Koivurinta, Eija-Riitta Hämäläinen, Elina Järvinen, Ibrahim Fatih Cengiz, Ilkka Kiviranta, Peter Uppstu and Markus Hannula for their contributions to my research and for sharing their expertise with me. For all my colleagues at the university especially the Biomaterial and Tissue Engineering group I owe my deepest gratitude for the pleasant work atmosphere. There have been so many good friends working at the department during these years and I am truly grateful getting to know all of you! Especially I would like to express my gratitude to the entire laboratory and technical personnel of the department for all their valuable help during these years. I would like to thank professor Jari Viik for his help with statistical analysis and I am also very grateful to Peter Heath for all his help with language editing.

I am extremely grateful for the financial support of the Finnish Funding Agency for Technology and Innovation (TEKES) and Jenny and Antti Wihuri Foundation.

I owe my deepest gratitude to my parents, Jorma and Sinikka Hannula, for their never-ending love and support. I would also like to thank all my closest relatives and friends for believing in me and for all their support through all these years.

My dear husband Jari, thank you for all your love and support, you always believed in me and found the words to encourage me to go on during these years.

Aada and Jimi, the biggest loves of my life, thank you for making my life complete!

This thesis is dedicated to my beloved late granny, Kerttu, who always believed in me.

Kangasala, February 2015 Anne-Marie Haaparanta

Table of contents

List of original publications

This thesis is based on the following publications that are later referred to in the text as Publications I–V. The publications are reprinted with the permission of the publishers.

I Haaparanta, AM., Koivurinta, J., Hämäläinen, ER. and Kellomäki, M. The effect of cross-linking time on a porous freeze-dried collagen scaffold using 1-ethyl-3-(3-dimethylaminopropyl)carbodiimide as a cross-linker, Journal of Applied Biomaterials & Biomechanics, **6** (2008), 89-94

II Haimi, S., Suuriniemi, N., Haaparanta, AM., Ellä, V., Lindroos, B., Huhtala, H., Räty, S., Kuokkanen, H., Sándor, GK., Kellomäki, M., Miettinen, S. and Suuronen, R. Growth and osteogenic differentiation of adipose stem cells on PLA/bioactive glass and PLA/β-TCP scaffolds, Tissue Engineering, **15** (2009), 1473-1480

III Haaparanta, AM., Haimi, S., Ellä, V., Hopper, N., Miettinen, S., Suuronen, R. and Kellomäki, M. Porous polylactide/β-tricalcium phosphate composite scaffolds for tissue engineering applications, Journal of Tissue Engineering and Regenerative Medicine, **4** (2010), 366-373

IV Haaparanta, AM., Järvinen, E., Cengiz, IF., Ellä, V., Kokkonen, HT., Kiviranta, I. and Kellomäki, M. Preparation and characterization of collagen/PLA, chitosan/PLA, and collagen/chitosan/PLA hybrid scaffolds for cartilage tissue engineering, Journal of Materials Science: Materials in Medicine, **25** (2014), 1129-1136

V Haaparanta, AM., Uppstu, P., Hannula, M., Ellä, V., Rosling A. and Kellomäki, M. Improved dimensional stability with bioactive glass fibre skeleton in poly(lactide-co-glycolide) porous scaffolds for tissue engineering, Materials Science and Engineering C: Materials for Biological Applications, *submitted*

Author's contribution

The author's contribution to the publications was the following.

I The author was responsible for writing this paper, planning the work together with the co-authors, manufacturing all the studied scaffolds and analysing the data.

II The author was responsible for writing this paper together with the first two authors, planning the work together with the co-authors, manufacturing of all the studied scaffolds and analysing the material characterization data.

III The author was responsible for writing this paper, planning the work with co-authors, manufacturing of all the studied scaffolds and analysing the data.

IV The author was responsible for writing this paper, planning the work with the co-authors and analysing the data.

V The author was responsible for writing this paper, planning the work with the co-authors, manufacturing of some of the studied scaffolds and analysing of the data.

Abbreviations

2D	Two-dimensional
3D	Three-dimensional
β-TCP	β-Tricalcium phosphate
ASC	Adipose stem cells
ALP	Alkaline phosphatase
BG	Bioactive glass
CA	Contact angle
CaP	Calcium phosphate
DSC	Differential scanning calorimeter
ECM	Extracellular matrix
EDC	1-ethyl-3-(3-dimethylaminopropyl)carbodiimide hydrochloride
ESEM	Environmental scanning electron microscopy
GAG	Glycosaminoglycan
GPC	Gel permeation chromatography
HA	Hyaluronic acid
HAp	Hydroxyapatite
HCl	Hydrochloric acid
i.v.	Inherent viscosity
kGy	KiloGray, SI unit for radiation dose
M_n	Number average molecular weight
M_w	Weight average molecular weight
MSC	Mesenchymal stem cell
NHS	N-Hydroxysuccinimide
OA	Osteoarthritis
PBS	Phosphate buffered saline solution
PCL	Polycaprolactone
PGA	Polyglycolide
PLA	Polylactide
PLGA	Poly(lactide-co-glycolide)
PLLA	Poly(L-lactictide)
PLCL	Poly(lactide-co-ε-caprolactone)
PTFE	Polytetrafluoroethylene (Teflon)
PVA	Poly(vinyl alcohol)
RT	Room temperature

SEM	Scanning electron microscopy
T_d	Denaturation temperature
T_g	Glass transition temperature
TGA	Thermogravimetric analysis
v/v	Volume to volume
w/v	Weight to volume

The abbreviations for different scaffold types.

To be noted: the most frequently studied collagen scaffolds with 1.0 wt% of collagen cross-linked with EDC+NHS post freeze-drying are marked simply as “Col”.

Abbreviation	Scaffold materials	Matrix material	Filler	Cross-linking	Publi-cation
Natural polymer-based scaffolds					
Col0.3NoE	Collagen	0.3 wt% collagen	No	No	I
Col0.3(E)	Collagen	0.3 wt% collagen	No	EDC prior	I
Col0.3E	Collagen	0.3 wt% collagen	No	EDC post	I
Col0.5NoE	Collagen	0.5 wt% collagen	No	No	I
Col0.5(E)	Collagen	0.5 wt% collagen	No	EDC prior	I
Col0.5E	Collagen	0.5 wt% collagen	No	EDC post	I
Col1.0NoE	Collagen	1.0 wt% collagen	No	No	I
Col1.0(E)	Collagen	1.0 wt% collagen	No	EDC prior	I
Col1.0E	Collagen	1.0 wt% collagen	No	EDC post	I
Col	Collagen	1.0 wt% collagen	No	EDC+NHS post	IV
Col2.0	Collagen	2.0 wt% collagen	No	No	I
Col2.0(E)	Collagen	2.0 wt% collagen	No	EDC prior	I
Col2.0E	Collagen	2.0 wt% collagen	No	EDC post	I
Chi	Chitosan	1.0 wt% chitosan	No	No	IV
C1C1	Collagen+Chitosan	1.0 wt% collagen and chitosan 1:1 (v/v)	No	EDC+NHS post	IV
C2C1	Collagen+Chitosan	1.0 wt% collagen and chitosan 2:1 (v/v)	No	EDC+NHS post	IV
ColPLA	Collagen+PLA96/4	0.5 wt% collagen	PLA mesh	EDC+NHS post	IV
ChiPLA	Chitosan+PLA96/4	0.5 wt% chitosan	PLA mesh	EDC+NHS post	IV
C1C1PLA	Collagen+ Chitosan+PLA96/4	0.5 wt% collagen and chitosan 1:1 (v/v)	PLA mesh	EDC+NHS post	IV
C2C1PLA	Collagen+ Chitosan+PLA96/4	0.5 wt% collagen and chitosan 2:1 (v/v)	PLA mesh	EDC+NHS post	IV
Synthetic polymer-based scaffolds					
PLA2	PLA70/30	2.0 wt% PLA70/30	No	No	II, III
PLA3	PLA70/30	3.0 wt% PLA70/30	No	No	III
PLA2TCP5	PLA70/30+β-TCP	2.0 wt% PLA70/30	5 wt% β-TCP	No	III
PLA2TCP10	PLA70/30+β-TCP	2.0 wt% PLA70/30	10 wt% β-TCP	No	II, III
PLA2TCP20	PLA70/30+β-TCP	2.0 wt% PLA70/30	20 wt% β-TCP	No	II, III
PLA3TCP5	PLA70/30+β-TCP	3.0 wt% PLA70/30	5 wt% β-TCP	No	III
PLA3TCP10	PLA70/30+β-TCP	3.0 wt% PLA70/30	10 wt% β-TCP	No	III
PLA3TCP20	PLA70/30+β-TCP	3.0 wt% PLA70/30	20 wt% β-TCP	No	III
PLA2BG10	PLA70/30+BaG0127	2.0 wt% PLA70/30	10 wt% BaG	No	II
PLA2BG20	PLA70/30+BaG0127	2.0 wt% PLA70/30	20 wt% BaG	No	II
PLGA1	PLGA1	5.0 wt% PLGA1	No	No	V
PLGA2	PLGA2	5.0 wt% PLGA2	No	No	V
PLGA1BG1	PLGA1+BG1	3 wt% PLGA1	BG mesh	No	V
PLGA2BG2	PLGA2+BG2	3 wt% PLGA1	BG mesh	No	V

The following abbreviations are used to mark out the different forms of BG components in the scaffolds:

BGf	Bioactive glass fibre
BGp	Bioactive glass particle

Definitions

Allogenic	From individuals of the same species
Allograft	Graft from a donor of the same species as the recipient but not genetically identical
Autograft	Graft obtained from one part of a patient's body for use on another part
Autologous	Originating from the recipient rather than from a donor
Avascular	Lacking blood vessels
Bioabsorbable	Capable of being degraded or dissolved and subsequently metabolized within an organism
Biodegradation	Capable of being decomposed by bacteria or other biological means
Blend	A uniform combination of two or more materials
Carding	Mechanical process that disentangles, cleans and intermixes fibres to produce a continuous randomly oriented web, i.e. a carded mesh
Composite	A combination of two or more distinctly different materials where each component contributes positively to the properties of the final product
Hybrid	A combination of two or more materials or of material and space to allow a superposition of their properties
In vitro	Taking place in a test tube, culture dish, or elsewhere outside a living organism
In vivo	Taking place in a living organism
In situ	In the natural, original, or appropriate position
Modulus	A force exerted under specific strain
Needle punching	A process that uses needles with barbs along the shaft of the needle that grabs the top layer of fibres and tangles them with the inner layers of fibres as the needle enters the carded mesh
Osteoblast	Bone-forming cell
Osteoclast	A large multinucleate bone cell which absorbs bone tissue during growth and healing
Osteoconductive	Supports bone growth and encourages the ingrowth of surrounding bone
Osteocyte	A bone cell that is formed when an osteoblast becomes embedded in the material it has secreted

Osteoid	Un mineralized organic component of bone
Osteoinductive	Capable of promoting the differentiation of progenitor cells down an osteoblastic lineage
Osteointegration	Integrates into surrounding bone
Strength	Ability of a material to withstand an applied load without failure

1 Introduction

There is a growing need to find adequate tissue replacements for damaged or diseased tissues. The best tissue replacement would in general be autologous tissue, an autograft, from the patient. However, on many occasions this is not possible because of a shortage of tissue or a lack of undamaged replacement tissue. Tissue engineering has become one of the most promising ways to regenerate new tissues and to overcome the lack of donor tissues for use as tissue transplants and to avoid possible undesirable tissue reactions (Langer 2000). Tissue engineering scaffolds serve as a template for new tissue formation. Since material properties, scaffold geometries as well as the types of cells and their seeding procedures all affect the formation of new tissue, there are still numerous studies to be done to find out the best possible scaffolds for different tissue engineering applications (Fisher & Mauck 2013).

Cartilage tissue is avascular by nature and it possesses relatively low cell number density. Therefore, cartilage defects are known to heal poorly because cartilage tissue does not possess the ability to heal after trauma (Kinner et al. 2005). The use of autologous transplants would be an optimal way to replace the damaged tissue. However, the need for a second operation to collect the tissue to be transplanted is always a risk and an inconvenience. Because the healing of native cartilage is challenging, the tissue engineering of new cartilage tissue is also rather challenging. If the cartilage lesion is deep, the underlying bone can also be affected, making the lesion an osteochondral lesion. In this case, there is also the need to repair the underlying bone as well (Panseri et al. 2012). For load bearing applications such as cartilage and bone tissue, there is a need for more mechanically stable constructs that can keep their porosity open even after loading. In addition, highly biomimetic materials and structures are required for optimal scaffolds. On many occasions, one particular type of material is not enough to obtain the best scaffold properties, and a more complex scaffold structure manufactured using multiple or combined processing methods may be required. Therefore, scaffolds with more than one material component and with more complex structures, composites, with two or more components have been studied for the purpose (Chen et al. 2002; Seo & Park 2010).

Current treatments for articular cartilage repair are autologous chondrocytes implantation (ACI) and matrix-assisted chodrocyte implantation (MACI) (Nukavarapu & Dorcemus 2013). However, the current repair techniques for damaged articular cartilage are inadequate and need development since they mainly result in fibrotic cartilage formation. In addition, the scaffolds currently used are thin membranes that have limited biomechanical properties, and act mainly as a cover to keep the blood clot at the repair site. The main challenge has been to manufacture highly porous scaffolds with adequate mechanical properties. An optimal cartilage tissue engineering scaffold would give structural support to the lesion during healing. Such a scaffold would also allow early load bearing, giving the tissue mechanical stimulus as well as shortening recovery time. Therefore, there is still a need for dimensionally, mechanically and functionally optimal scaffolds for articular cartilage tis-

sue engineering (Kock et al. 2012). The manufacturing of dimensionally and mechanically stable, highly porous and functional scaffolds is studied in this thesis in order to obtain an optimal tissue engineering scaffolds for cartilage or osteochondral lesions.

Many kinds of manufacturing methods have been applied in the manufacture of porous tissue engineering scaffolds, such as particulate leaching, different textile technologies, phase separation, high pressure based methods, melt based technologies and rapid prototyping (Gomes & Reis 2004). This thesis focuses on freeze-drying, a thermally induced phase separation, where highly porous tissue engineering scaffolds with interconnected pore structures can be manufactured from both natural and synthetic bioabsorbable polymers (Liu et al. 2007). In addition, composite structures manufactured from different filler materials as well as different filler compositions can also be processed by freeze-drying. To achieve the best properties for cartilage or bone tissue engineering scaffolds, it is important to find out the optimal material properties, the required geometry of the scaffold and the optimum combination of different structures for the application (Hutmacher 2000). Materials that best mimic the target tissue are often the naturally occurring components of the native tissue. However, these materials cannot usually be used on their own as scaffolds because they lack some other necessary property such as the required mechanical stability.

To overcome the limitations of current cartilage repair scaffolds with poor mechanical properties, this thesis focuses on the manufacturing of freeze-dried composite structures with highly porous structures, biomimetic components and improved biomechanical properties. The literature review provides an overview of the manufacturing of porous scaffolds for cartilage and osteochondral tissue engineering. In the experimental part, highly porous scaffolds were manufactured by freeze-drying in order to find ways to improve the properties of the freeze-dried scaffolds to meet the requirements of the high demanding tissues of cartilage and bone. Different natural and synthetic polymer-based composite scaffolds were manufactured, and the effects of particle or fibrous fillers were studied as composite structures and compared with plain polymer scaffolds. The tissue engineering scaffolds were studied to determine the structure of the manufactured composite scaffolds, to find out the characteristics of the composites, and to assess the feasibility of the composites for cartilage, bone or osteochondral tissue engineering applications.

2 Porous scaffolds for tissue engineering

2.1 Scaffold composition

Tissue engineering scaffolds require many specific characteristics. For example, highly flexible, stiff, rigid or soft components may be required, depending on the application. Also, for some applications, some specific materials are shown to induce tissue regeneration and, therefore, would be best suited for the application. To achieve the optimal characteristics for the scaffold, different kinds of composite structures have been developed in order to mimic the characteristics of native tissue as well as possible (Mohamad Yunos et al. 2008; Moutos & Guilak 2008). No ideal combination of a specific composite structure, composite materials or composite filler exists because different tissue engineering applications require different properties from the scaffold. This means that different scaffold materials manufactured with different kinds of fabrication methods are often combined to achieve the goal.

2.1.1 Scaffold microstructure

The microstructure of a scaffold is a crucial factor for a tissue engineering construct to work properly. Generally, the majority of the cell culture studies are carried out in two-dimensional (2D) surroundings such as in well plates or Petri dishes. However, almost all tissue cells in the body exist in 3D constructs in a native extracellular matrix (ECM) (Lee et al. 2008). Therefore, almost all tissue engineering scaffolds are 3D structures. The microstructure of the scaffold has a great effect on cell-material interaction. Four different types of microstructures, each with associated advantages and disadvantages, are listed below (Gibson et al. 2010):

1) One-dimensional (1D) fibre structures:
   Cells cultured on individual fibres (length and diameter of the fibres can vary)
2) Impermeable, two-dimensional (2D) substrates:
   Cells cultured in a 2D environment. Assessment of material chemistry, mechanics and micro-scale patterning
3) Three-dimensional (3D), nanoporous hydrogel scaffolds:
   Cells on top of hydrogel (i.e. interacting with 2D substrate with nano-scale surface) or encapsulated inside 3D structure (the cells have to degrade the surrounding hydrogel to move or extend process)
4) Three-dimensional (micro-porous) scaffolds:
   Cells are able to spread in three dimensions because of high porosity (typically >90%) and, depending on scaffold pore size, they can either be aligned along one-dimensional scaffold struts or attached to multiple struts and spread in three dimensions

The porosity and pore size of scaffolds are thought to be one of the major properties for tissue-engineered scaffolds (Yang et al. 2001). High porosity, over 90%, is thought to enhance cell integration and nutrition exchange in tissue engineering scaffolds. The optimal pore size in the scaffold is more or less determined by the application and the type of cell used. The optimal pore sizes are typically in the range of 20–500 µm (Gibson et al. 2010). High porosity, pore size and interconnectivity play significant roles in the migration of cells inside the scaffold, as well as nutrition and waste exchange (Hutmacher 2000). The properties of an ideal tissue engineering scaffold depend on the application, but nevertheless, various mutual properties are still required.

A tissue engineering scaffold should:

- be biocompatible to support cell viability and biodegradable so that the new tissue replaces the scaffold after time
- be a highly porous 3D structure with interconnected pores in order to allow cells to migrate inside the scaffold
- have appropriate porosity for the used cells, so that the cells stay inside the scaffold, proliferate and form new tissue
- have appropriate strength for the application, for the mechanical stimuli to be as close as possible to the native tissue
- have an appropriate degradation time for the application, assisting the tissue in growth and subsequently forming new tissue (Chen et al. 2002; Lee et al. 2008; Yang et al. 2001; Mikos & Temenoff 2000; Ma 2004; Jagur-Grodzinski 2006; Tsang & Bhatia 2006; Weigel et al. 2006; Liu et al. 2007)

The majority of tissue engineering scaffolds are made of polymers because of the easy control over biodegradability and processability they offer (Chen et al. 2002). However, there is a growing trend towards the use of composite scaffolds. Tissue engineering composites can be either polymer-polymer constructions, or, for example, polymer-ceramic or polymer-bioactive glass constructions. To ideally mimic the structure of the native tissue to be replaced, it is often necessary to rely on composite structures rather that just one-component scaffolds. Also, one more specific composite structure, hybrid structures, which combine the advantages of both synthetic and natural biomaterials, have attracted attention for the development of tissue engineering scaffolds (Chen et al. 2002; Liu et al. 2007). Furthermore, it might not be possible to manufacture the eligible geometry of the scaffold with only one component structure because the structure may lack some essential property such as the required mechanical strength. It may also not be possible to manufacture the geometry required with only one component because, for example, not all polymers can be processed into fibres.

2.1.2 Composites and hybrids

Composites

A composite is a combination of two or more distinctly different materials, where each component contributes positively to the properties of the final product. A composite is usually a construct with a matrix (the major component in the system) and filler (acting often as reinforcement). Composites can be divided into different categories based on the matrix material used (polymer, ceramic or metal). The filler material in the composites can be in various forms such as particles (nano- or microparticles), fibres (short or long) or textiles (Hull & Clyne 1996). Four basic types of composite structures are represented in Figure 1.

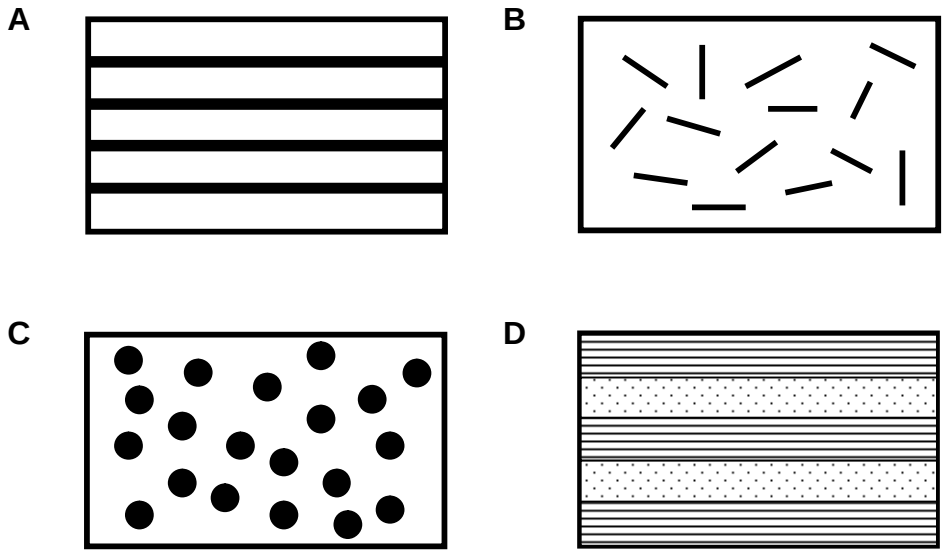

Figure 1. Schematic representations of basic composite structures. A) Long-fibre composite, B) short-fibre composite, C) particle reinforced composite, and D) laminate. (In all figures, matrix in white and filler/reinforcement in black.)

The composite can be reinforced with long fibres (Figure 1A), where the fibres are continuous throughout the matrix. The packing of fibres is more irregular and misalignment of the fibres is more likely for lower fibre contents. Short-fibre composites contain short fibres dispersed in the matrix (Fibre 1B). The orientation of short fibres is more random than for long fibres and fibre orientation changes during processing especially when extensional flow and shear flow is present in melt processing. Particle-reinforced composites contain particles (for example nano- or microparticles), randomly dispersed into the matrix (Figure 1C). A laminate structure comprises separate layers or laminae stacked in a pre-determined arrangement (Figure 1D). Each laminae may contain long or short fibres and they can be aligned in one or more directions or be randomly distributed in two or three dimensions. Textiles fabricated by using conventional textile technology processes (weaving, braiding and knitting) can also be used as reinforcements. Woven, non-woven, braided and knitted structures are examples of textiles used for composite reinforcement. Some of the tex-

tiles can be thought of as long-fibre reinforcement and some as laminate reinforcement structures, depending on the application. (Hull & Clyne 1996)

Usually, it is not possible to achieve the required properties and structure for an ideal tissue engineering scaffold using only one component scaffold or only one material. Therefore, composites with at least two different materials or two different components (matrix and filler) are often needed to achieve an optimal tissue engineering scaffold and to mimic the natural ECM environment (Moutos & Guilak 2008; Mohamad Yunos et al. 2008). The property of the composite is highly depended on the quality of matrix-filler interface. The interfacial bond strength of the matrix and filler can be influenced in multiple ways, such as with coupling agents or interfacial chemical reactions (Hull & Clyne 1996).

Composite structures can be used for tailoring the functional or mechanical properties of the scaffold. Examples of additional functionality for tissue engineering scaffolds are bioactivity, tailored degradation profile or controlled drug release. Many kinds of reinforcements are used to enhance the mechanical properties of scaffolds, and many times the reinforcing phase is used to transfer the load from the mechanically weaker matrix (Hull & Clyne 1996). For example, long bioactive glass fibres are used to improve the mechanical and degradation properties of polylactide-based scaffolds for load-bearing applications (Lehtonen et al. 2013b). In addition, bioactive glass fibre-reinforced starch-polycaprolactone (SPCL) composites have been manufactured using compression moulding of SPCL in layers with bioactive glass fibres to enhance the initial mechanical properties of the polymer (Jukola et al. 2008). Multilayered and fibre reinforced polymer composites have been manufactured for spinal surgery in order to obtain a bioresorbable composite with a bioactive agent for potential osteoconductive properties and adequate compressive properties for the application (Huttunen et al. 2006). Particle fillers can be used, for example, to modify the degradation 6ehaveiour and to neutralize the acidic degradation products of self-reinforced polylactide in composites containing osteoconductive bioceramic particles (Niemelä 2005). The drug release of multiple drugs with a multilayer composite was developed to release the active agents in different phases (Nikkola et al. 2008). Osteoconductive, biodegradable bone filling composite releasing rifampicin was manufactured for the treatment of osteomyelitis with an improved drug release profile using bioceramic filler (Ahola et al. 2012). As an example of textile reinforcement, polylactide knitted mesh was used together with copolymer of caprolactone and lactic acid as a film to obtain a flexible membrane with different layers to enhance more rapid tissue ingrowth onto the porous mesh and to prevent tissue growth on the other side of the film (Kellomäki et al. 2000). Highly porous structures often suffer from low mechanical strength. Therefore, different composite structures are widely studied for 3D tissue engineering scaffolds for load-bearing applications such as cartilage or bone (Chen et al. 2003; Maquet et al. 2004; Navarro et al. 2006; Gentile et al. 2012a; Gentile et al. 2012b).

Hybrids

A hybrid material is a combination of two or more materials or of material and space so as to allow a superposition of their properties. By using hybridisation, it is possible to meet the design requirements for the desired construct that is not possible using a single material. Figure 2 shows the four scenarios of making a hybrid from two materials. Point A represents the ideal hybrid with the best properties of both components: "the best of both" scenario. Point B represents the best that can be obtained as an arithmetic average of the properties of the components, i.e., the bulk properties are combined: "the rule of mixtures" scenario. In point C, the properties of the hybrid fall below those of the rule of mixtures with less spectacular gains, but still somehow useful: "the weaker link dominates" scenario. Point D represents something we do not want: "the worst of both" scenario (Ashby & Bréchet 2003).

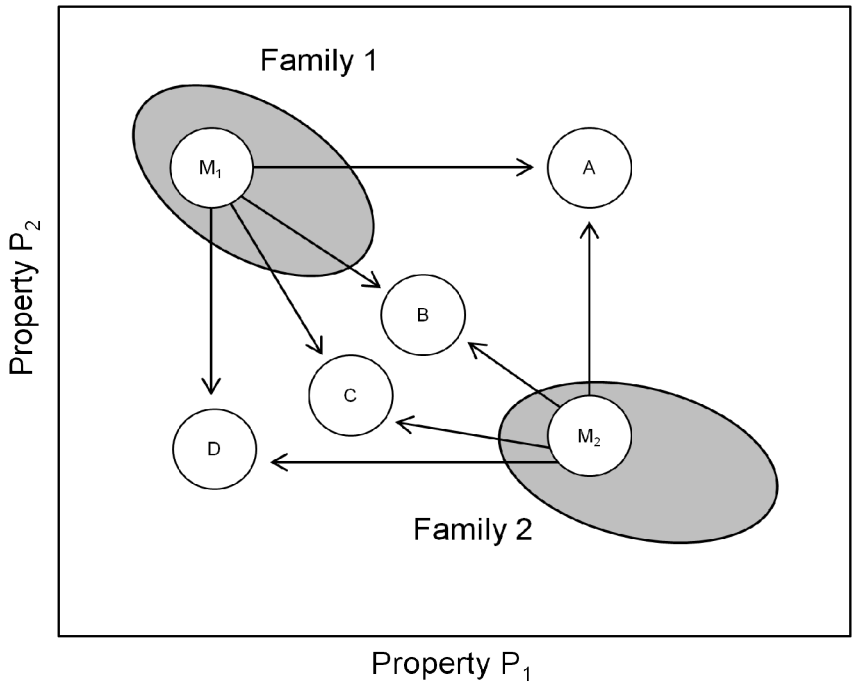

Figure 2. Hybridisation possibilities. Four classes of hybrids (A–D) made of two families of materials (M_1 and M_2) plotted in a chart with properties P_1 and P_2 as axes (adapted from Ashby & Bréchet 2003).

Hybrids include fibrous and particulate composites, foams and lattices, sandwich structures and almost all natural materials (Ashby & Bréchet 2003). The design variables of hybrids are listed in Table 1. The potential of hybrid materials is in the choice of components and their relative volume, their configuration and in the way they are connected to each other. The creation of new "materials" with specific property profiles is made possible by the new variables expanding the design space (Ashby 2013). As scaffolds, hybrids have emerged as a promising alternative for tissue engineering, for example, as a combination of a synthetic polymer construct (like sponge or mesh) combined with a porous natural polymer matrix (Chen et al. 2004; Chen et al. 2006; Dai et al. 2010; Hokugo et al. 2006; Lu et al. 2012).

Table 1. The design variables of the hybrid design (Ashby 2013).

Components	The choice of materials to be combined
Relative volumes	The volume fraction of each component
Configuration	The shapes and relative placing of the components
Connectivity	The number of connections between components
Scale	The length-scale of the structural unit

The classification of scaffolds into composites or hybrids is diverse. A composite is a material comprised of two or more different components or phases (Hull & Clyne 1996). Therefore, the term composite includes more or less all the variations of different combinations of two or more materials applied in one system. However, the combination of material and space is not thought to be composite but it can be a hybrid. Therefore, some hybrids (but not all) are composites and vice versa. The term composite is generally used in this thesis more often since all the studied scaffolds in this thesis were composites although some, but not all, were also hybrids. In tissue engineering, the hybrids are often thought of as inorganic-organic compounds with a chemical bond, or as a combination of natural and synthetic component structures. The hybrids in this thesis are the combinations of natural and synthetic materials in one scaffold.

2.2 Scaffold materials

2.2.1 Natural bioabsorbable polymers

Several natural bioabsorbable polymers have been studied as tissue engineering scaffolds (Nair & Laurencin 2006; Malafaya et al. 2007; Mano et al. 2007) and they can be considered as the first biodegradable biomaterials used clinically (Nair & Laurencin 2007). The use of natural polymers often relies on their natural characteristics of being similar to biological macromolecules and, therefore, similar to natural ECM (Mano et al. 2007). Being enzymatically degradable polymers, the *in vivo* degradation rate varies significantly with implantation site and depends on the availability and the concentration of the enzymes (Nair & Laurencin 2007). Natural polymers can be divided into three groups according to their chemical structure: proteins, polysaccharides and polyhydroxyalkanoates. Natural polymers are mainly extracted from plant and animal sources or from algae. However, they can also be obtained from the fermentation of microorganisms or produced *in vitro* by enzymatic processes (Mano et al. 2007). Some of the most commonly used natural bioabsorbable polymers, their origin and some examples of their use for tissue engineering applications are listed in Table 2. Although natural polymers are often the first choice to be used for tissue engineering applications because of their ability to highly mimic the natural tissue environment, there are some factors that limit their use such as variability from batch to batch, poor mechanical properties, a possibility of animal residues and limited processability (Malafaya et al. 2007; Mano et al. 2007; Nair & Laurencin 2007).

Table 2. Natural bioabsorbable polymers and their origin and applications in tissue engineering (Nair & Laurencin 2006; Malafaya et al. 2007; Mano et al. 2007; Nair & Laurencin 2007; Van Vlierberghe et al. 2011).

	Origin	TE applications
Proteins		
Collagen	Derived from animal tissues or produced by recombinant technologies	Bone, cartilage, skin, vascular, adipose, intervertebral disc, cardiovascular, dental, urological, liver, neural, pancreas
Gelatin	Derived from collagen	Bone, cartilage, osteocohdral, skin, vascular, adipose, intervertebral disc, liver, neural, pancreas
Elastin	Derived from animal tissues or produced by recombinant technologies	Bone, skin, vascular, neural, ocular
Fibrin	Produced from autologously harvested fibrinogen	Bone, osteochondral, skin, vascular, intervertebral disc, cardiovascular, spinal cord, peripheral nerve
Silk fibroin	Spun into fibres by some *lepidoptera* larvae such as silkworms, spiders, scorpions, mites and flies.	Bone, cartilage, osteochondral, skin, adipose
Polysaccharides		
Chitosan	Derived by deacetylation of chitin found in exoskeleton of arthropod or cell wall of fungi	Bone, cartilage, osteochondral, skin, vascular, peripheral nerve
Chondroitin sulphate	Derived from animal tissues	Bone, cartilage, vascular, heart valve, kidney
Hyaluronic acid	Derived from animal tissues or produced by bacterial fermentation	Bone, cartilage, osteochondral, skin, vascular, adipose, spinal cord
Starch	Derived from plants	Bone, vascular

Collagen

Collagen is the most abundant protein in the ECM and is the major component of skin and other musculoskeletal tissues. At least 28 different types of collagen have been identified to date (Ramshaw et al. 2009; Gordon & Hahn 2010). All collagens have a triple-helical structure where three individual chains, each in a left-handed polyproline II-helix, are coiled together to form a right handed, super coiled triple helix with a rope-like structure. In this structure, collagens show a characteristic repeating sequence, glysine-X-Y, where glysine is a small enough amino acid to pack into the centre of the triple-helical structure. X and Y positions can be any amino acid, but X is often proline and Y is frequently hydroxyproline (Ramshaw et al. 2009). Collagens can be divided into different groups based on their structure and supramolecular organization. These groups are fibril-forming collagens, fibril-associated collagens (FACIT), network-forming collagens, anchoring fibrils, transmembrane collagens, basement membrane collagens and others, each with a unique function. The most abundant group of collagens are the fibril-forming collagens with about 90% of the total collagen. Collagen type I is the most abundant and the best studied collagen and forms more than 90% of the organic mass of bone and is the major collagen in tendons, skin, ligaments, cornea

and many interstitial connective tissues, with the exception of only a few tissues such as hyaline cartilage, brain and vitreous body. Type II collagen, on the other hand, is the characteristic and predominant component of hyaline cartilage, but it is also found in the vitreous body, the corneal epithelium, notochord, the nucleus pulposus of intervertebral discs and embryonic epithelial-mesenchymal transitions (Gelse et al. 2003).

Collagen possesses high mechanical strength, good biocompatibility, low antigenicity and the ability to cross-link, which enables the tailoring of the mechanical, degradation and water uptake properties of collagen. When fabricated into highly porous scaffolds, the cross-linking of collagen is necessary to fabricate scaffolds with adequate mechanical properties and degradation rate (Malafaya et al. 2007; Mano et al. 2007). Collagen has been extensively studied for use in various medical applications and a wide range of tissue engineering applications such as bone, cartilage and skin tissue engineering. Modifying or combining collagen with other degradable polymers improves the potential of collagen as a biomaterial (Ulery et al. 2011). The principal collagen that can be readily prepared in a pure form in commercial quantities is type I collagen. It is the most widely used collagen for tissue engineering applications. Collagen scaffolds offer an alternative way to provide biological information to the growing construct, unlike biodegradable synthetic polymers. While using collagen scaffolds, a wide range of cell adhesion and other signals that will enhance the quality of the tissue-engineered products is achieved (Ramshaw et al. 2009). Generally, freeze-drying or stereolithography methods are used for fabricating porous, collagen-based scaffolds and carbodiimide is often applied for cross-linking. Porous collagen scaffolds are often combined with other components such as, bioceramics or synthetic biodegradable polymers (Van Vlierberghe et al. 2011). Collagen is already available in a variety of commercial medical products, such as a bioprosthetic heart valve or as a wound dressing. The use of collagens can be divided into two different categories: tissue-based devices where natural, stabilised tissue is used as a device (a bioprosthetic heart valve) and purified collagen, where collagen is made soluble through an enzyme digestion step and reconstituted into various products (a wound dressing). Recombinant collagens are emerging as the most interesting development since they offer a way to produce high purity and disease-free collagens with the possibility to produce all types of collagens, even those with very low abundance in natural tissue (Ramshaw et al. 2009).

Chitosan

Chitosan is a linear polysaccharide composed of β(1–4) linked glucosamine with randomly located *N*-acetyl-glucosamine groups, depending on the degree of deacetylation of the polymer. Chitosan is a deacetylated form of chitin, the second most abundant natural biopolymer. Chitin is a fully acetylated polymer extracted from the exoskeletons of arthropods and also from cell walls and the ECM of most fungi. The degree of deacetylation of chitosan can vary from 30% to 95% (Di Martino et al. 2005; Domard & Domard 2001) and molecular weight from 300 to over 1000 kD (Di Martino et al. 2005). Chitosan, unlike chitin, is soluble in dilute acids (pH<6.0) when the protonated free amino

groups on glucosamine facilitate the solubility of the molecule. The degree of deacetylation and the molecular weight of chitosan can vary greatly, depending on the source and the preparation procedure of the polymer. Chitin and chitosan in their polymeric form are completely absent in numerous animals including mammals. However, the *N*-acetyl-glucosamine unit is widely found in the chemical structure of other glycosaminoglycans (GAGs) and in glycoconjucates such as glycoproteins and glycolipids (Domard & Domard 2001). Chitosan is primary degraded by lysozyme enzyme *in vivo* through hydrolysis of acetylated residues. The degree of deacetylation is related to its degradation rate and, as a consequence, highly deacetylated chitosan degrades more slowly *in vivo* (Di Martino et al. 2005).

Chitosan is often processed for tissue engineering scaffolds by freeze-drying, supercritical fluid technology or stereolithography (Van Vlierberghe et al. 2011). The glass transition and the melting temperatures of dry, solid chitosan are both higher than its temperature of thermal decomposition. Therefore, it is necessary to process chitosan from solutions (Domard & Domard 2001). The qualities that make chitosan a versatile polymer for tissue engineering applications are its good biocompatibility, its ability to be processed into various forms, its antibacterial activity and its ability to bind anionic molecules such as the growth factors, GAGs and DNA. Chitosan has cationic nature which enables electrostatic interactions with GAGs, proteoglycans and other negatively charged molecules (Di Martino et al. 2005). Chitosan has been used, for example, in bone, cartilage and skin tissue engineering in various forms and it is also often combined with other natural polymers such as collagen, with ceramics, or with synthetic polymers (Van Vlierberghe et al. 2011; Di Martino et al. 2005; Muzzarelli 2009). Especially, as a positive aspect for cartilage tissue engineering, chitosan has been found to maintain the round morphology of chondrocytes. This is a normal phenotypic characteristic of chondrocytes and preserves their capacity to synthesize cell-specific ECM (Muzzarelli 2009).

2.2.2 Synthetic bioabsorbable polymers

Synthetic bioabsorbable polymers are widely studied as tissue engineering scaffolds (Jagur-Grodzinski 2006; Nair & Laurencin 2006; Nair & Laurencin 2007; Gunatillake et al. 2003; Ulery et al. 2011). Their controllable chemistry and properties as well as their characteristic of being easily reproducible have exceeded their use as scaffold materials. Synthetic bioabsorbable polymers can be divided into various subgroups such as esters, orthoesters, anhydrides, carbonates and amides, depending on their functional group's susceptibility to hydrolysis. In particular, polyesters have been used in a number of clinical applications because of their ease of degradation by hydrolysis of ester linkage. Also, their degradation products are in some cases resorbed through the metabolic pathways, and they possess the potential to alter their degradation rates by tailoring their structures. For these reasons, polyesters are also studied for tissue engineering applications (Gunatillake et al. 2003). Some of the most widely and earliest studied synthetic bioabsorbable polymers used in tissue engineering are poly(α-esters). Their synthetisation methods and applications in the field of tissue

engineering are listed in Table 3. The uniqueness of poly(α-esters) lies in their vast diversity and synthetic versatility. In the class of poly(α-esters), the poly(α-hydroxy acid)s, which include polyglycolide (PGA) and the stereoisomeric forms of polylactide (PLA), are the most widely studied polymers. Although many groups of bioabsorbable polymers have been studied for biomaterial applications, only a few of them are generally used for tissue engineering scaffolds. The main reasons for this are that many of them cannot be used in load bearing applications because their degradability is too fast or too slow, or they cannot be processed into 3D structures. This is why copolymerization is often used to overcome these limitations (Nair 2007).

Table 3. Poly(α-esters), their synthetisation method and applications in tissue engineering scaffolds (Jagur-Grodzinski 2006; Nair & Laurencin 2006; Nair & Laurencin 2007; Gunatillake et al. 2003; Ulery et al. 2011).

	Synthetisation method	**TE applications**
Poly(α-esters)		
Polyglycolide (PGA)	Ring-opening polymerization of glycolide, the cyclic dimer of glycolic acid, with solution or melt polymerization	Bone, cartilage, dental, tendon, vaginal, intestinal, lymphatic, spinal regeneration
Polylactide (PLA)	Condensation polymerization of lactic acid [poly(lactic acid)] or ring-opening polymerization of lactide [poly(lactide)]	Bone, cartilage, vascular, neural, tendon
Poly(lactide-co-glycolide) (PLGA)	Copolymerization of lactic and glycolic acid	Bone, cartilage, skin, liver, neural, tendon
Polycaprolactone (PCL)	Ring-opening polymerization of the cyclic monomer ε-caprolactone	Bone, cartilage, skin, vascular, neural, ligament

Polylactides

PLAs are thermoplastic, biodegradable polymers produced either by condensation polymerization from lactic acid, derived from the fermentation of sugars from carbohydrate sources such as corn, sugarcane and tapioca or by ring-opening polymerization from lactide, the cyclic dimer of lactic acid. Because of its chiral carbon atom, lactic acid exists in two enantiomeric forms referred to as L-lactic acid (*S*), which occurs in the metabolism of all animals and microorganisms, and D-lactic acid (*R*). With condensation polymerization, only low molecular weight PLA is usually obtained. High molecular weight PLA can be obtained by ring-opening polymerization in which the polycondensation of lactic acid is followed by depolymerisation into the dehydrated cyclic dimer, lactide. The optically active lactide can be found either as D-lactide, L-lactide or as *meso*-lactide (D,L-lactide). In addition to the three diastereomeric structures, racemic lactide, a racemic mixture of D-lactide and L-lactide also exists (Södergård & Stolt 2002; Groot et al. 2010).

The structure and composition of the polymer chains, and in particular the ratio of the L- to the D-isomer of lactic acid, affect the processing, crystallization and degradation behaviour of PLA. By

using copolymerization of L-lactide and *meso*-, D- or racemic lactide, high molecular weight amorphous or semicrystalline polymers with a melting point from 130 to 185 °C can be obtained. Poly(L-lactide) (PLLA), a homopolymer comprising only L-lactide, is a semicrystalline and has the highest melting point, whereas PLA copolymers with higher D-isomer content exhibits lower melting points and dramatically lower crystallization behaviour, becoming amorphous at D-contents higher than 12–15% (Groot et al. 2010).

PLA is an aliphatic polyester and is, therefore, susceptible to hydrolytic degradation because of the ester groups present in its structure. The hydrolytic degradation behaviour, rate and mechanism are controllable by varying the molecular and higher order structures and by medium factors such as temperature, pH and the catalytic species (for example alkali and enzyme) of PLA. The *in vivo* hydrolytic degradation rate is comparable to *in vitro* degradation and, therefore, the *in vivo* degradation can be predicted to a certain extent from *in vitro* degradation behaviour and rate (Tsuji 2010). PLA does not require the presence of enzymes to catalyse the hydrolysis. Lactic acid occurs in the metabolism of living organisms and, as a result, the degradation products of PLA are non-toxic (Gupta & Kumar 2007). The hydrolysis of aliphatic polyesters starts with a water uptake into the matrix that is followed by the hydrolytic splitting of the ester bonds. The initial degree of crystallinity affects the hydrolytic degradation rate as the amorphous parts have the higher rate of water uptake and the crystal segments reduce the water permeation in the matrix (Södergård & Stolt 2002). Also, the autocatalytic effect of a PLA specimen has been reported. The autocatalysis is due to the increasing number of compounds containing carboxylic end groups in the centre of a specimen when low molar mass compounds cannot permeate the outer shell where the degradation products dissolve in the surrounding solution (Gupta & Kumar 2007; Li et al. 1990).

PLAs can be processed into various forms due to their thermoplastic nature. Melt processing is the most widely used method for PLA. In addition, injection moulding and extrusion are widely used methods to fabricate PLA films and fibres for different nonwovens or textiles. Also, the electrospinning of PLA is used for medical applications to produce thin fibres that can be used as medical tissue scaffolds, wound dressings, carriers for drugs, protective fabrics and nanocomposite materials (Lim et al. 2010). The wide range of medical applications of PLAs includes orthopaedic screws, tissue engineering scaffolds, sutures, protein encapsulation and delivery, microspheres and drug delivery systems (Gupta & Kumar 2007). PLLA is a slow-degrading polymer (between 2 to over 5 years for total resorption *in vivo*) with good tensile strength, low extension and high modulus. That is why PLLA is considered to be ideal for load bearing applications such as orthopaedic fixation devices. PDLLA, on the other hand, degrades faster and loses its strength within 1–2 months and, when hydrolysed, undergoes a loss in mass within 12–16 months. It also has lower tensile strength compared with PLLA. For that reason, PDLLA is preferred as drug delivery vehicles and as a low strength scaffold material for tissue engineering (Nair & Laurencin 2007; Ulery et al. 2011). At the moment, PLLA (semi crystalline), PLDLA (amorphous), P(L/DL)LA 70/30 (amorphous) and

P(L/D)LA 96/4 (semi crystalline) are the most commonly used PLA polymers in the medical industry (Ellä 2012).

Polylactide-based co-polymers

One of the oldest and most successful approaches to vary the properties of a polymer is copolymerization with suitable comonomers. The stereocopolymers of D- and L-lactide are a special case for PLA copolymers, but other copolymers with PLAs are extensively studied as well. In the case of PLAs, the most widely used comonomers of L- or DL-lactide are glycolide (GA) and ε-caprolactone (CL). The GA enhances the rate of degradation of the polymer, and hence poly(lactide-co-glycolide) (PLGA) is often designed for pharmaceutical applications such as controlled drug release. In the case of poly(lactide-co-ε-caprolactone) (PLCL), the incorporation of CL reduces the rate of hydrolytic degradation and lowers the glass transition temperature and thus enhance the flexibility of the end product (Kricheldorf 2001).

PLGA is the most studied degradable polymer for biomedical applications. Because PLA and PGA have significantly different properties, different copolymer compositions allow PLGA to be optimized for different applications. With 25–75% lactide composition, PLGA forms amorphous polymers that are very hydrolytically unstable compared with the more stable homopolymers. A number of different processing techniques have been used for PLGA scaffold manufacturing such as gas foaming, microsphere sintering, porogen leaching, electrospinning and polymer printing. Because of the rapid degradation of PLGA compared with other polyesters, PLGA has been especially used as sutures and drug delivery devices. PLGA has also been fabricated into tissue engineering scaffolds since it demonstrates great cell adhesion and proliferation properties (Nair & Laurencin 2007; Ulery et al. 2011).

2.3 Fabrication methods of porous scaffolds

The fabrication parameters of a tissue-engineered scaffold depend mostly on the geometry and the mechanical properties of the tissue to be replaced. The scaffold should mimic the natural ECM environment. This is essential if the cells are to function in the simulated environment as they would *in vivo*. The material to be processed may present some processing limitations because not all biodegradable polymers are suitable for processing into 3D matrices or at least not in all processing methods (Lee et al. 2008). For this reason, it is important to know the limitations and advantages of the fabrication method to be used in order to process applicable scaffolds for the required application. Fabrication methods can be divided into different categories based on the process feature used, for example, under high temperatures or through the use of solvents or gases during processing. The used process feature can also be an advantage or disadvantage as not all materials can be processed in all conditions. Tissue engineering requires highly porous 3D scaffolds. Table 4 summarizes some

Table 4. Fabrication methods applied for porous polymeric tissue engineering scaffolds (Yang et al. 2001; Mikos & Temenoff 2000; Ma 2004; Weigel et al. 2006; Liu et al. 2007; Peltola et al. 2008; Shah Mohammadi et al. 2014).

	Process feature	Process method	Used polymer	Advantages	Disadvantages
Textile technologies	Transient temperature[a]	Usually melt extruded fibres produced into fabrics with textile technology methods	Synthetic polymers (if melt extruded fibres are used)	Easy to process, high porosity, variable pore size, large surface area	Heat needed for the fibre processing, two-step process
Electrospinning	Solvent based[b]	Usually polymer is dissolved into proper solvent and using high-voltage electrostatic field the fibre is formed	Synthetic or natural polymers	No heat, ultrafine fibres (micro- or nanoscale), a wide range of pore size distribution, high porosity and a high surface area	Low mechanical strength because of micro- or nanoscale fibres, possibility of solvent residues
Particulate-leaching	Solvent based	Polymer solution cast with water soluble particulates and afterwards salt is leached from the system using water	Synthetic or natural polymers	Easy to process, no heat, pore size can be controlled by the size of the salt crystals and the porosity by the salt/polymer ratio	Inter-pore openings may not be controlled, possible solvent residues
Freeze-drying	Transient temperature, solvent based	Solvent in polymer solution is removed by sublimation under very low pressure	Synthetic or natural polymers	High porosity, no heat used in processing, architecture of the scaffold can be controlled by phase separation conditions	Possible solvent residues
CO_2 gas techniques	Gas-aided[c], transient temperature	Solid piece of polymer (usually thermoplastic) is foamed with high-pressure CO_2 gas	Synthetic or natural polymers	No toxic solvents used	Nonporous surface, mixed open and closed pores
Rapid prototyping techniques	Transient temperature, solvent based	Computer-aided design fabricated into scaffold usually with layer-by-layer grown constructions	Synthetic or natural polymers	Porosity, pore size, interconnectivity, and geometric stability precisely controlled	Specific material properties needed, limited by the resolution of the used machine

[a]Transient temperature: Temperature change is used for processing (raised temperature for melt processing or lowered temperature for processes where material is frozen), [b]Solvent based: Solvent is used for processing (dissolving of used material), [c]Gas-aided: Gas is used for processing (foaming of the material)

of the most commonly applied fabrication methods for porous polymeric tissue engineering scaffolds.

Each of the fabrication processes has its own unique advantages in the manufacturing of tissue engineering constructs. No standard fabrication method is superior to any other method and, therefore, new methods are being researched (Lee et al. 2008). The future of the fabrication of tissue engineering scaffolds could rely on combining multiple processing methods to achieve the best scaffold structure for each tissue engineering application (Mikos & Temenoff 2000; Weigel et al. 2006). Though new fabrication methods are being introduced, the potential for the future development of scaffolds could also rely on the advancement and adaptation of conventional fabrication methods or their combination (Weigel et al. 2006).

2.3.1 Freeze-drying

Freeze-drying, also known as lyophilisation, has been used in the food and pharmaceutical industry because of its favourable property of being a low-temperature drying method (Franks 1998). Freeze-drying is nowadays also widely used for the fabrication of tissue engineering scaffolds. It is, therefore, known as one of the conventional methods for fabricating biomaterials into scaffolds (Liu et al. 2007). Freeze-drying is a processing method based on the sublimation phenomenon. Sublimation of the solvent, the formed ice crystals, produces a highly porous scaffold as an anhydrous or almost anhydrous state (Franks 1998). Unlike other drying methods, freeze-drying is a process where the material is solidified prior to drying and the removal of the major amount of water occurs through direct conversion of water from the solid state to the vapour state (Flink & Knudsen 1983).

Freeze-drying is a three-step process divided into freezing, primary drying and secondary drying periods. First (step 1), the liquid material is cooled into its solid form in the freezing period. Then (step 2), the frozen liquid, ice, is subsequently dried under vacuum in a freeze-dryer. Finally (step 3), the strongly bound water is removed from the product (secondary drying). The last two steps occur simultaneously in a freeze-dryer at different locations in the sample (Flink & Knudsen 1983). The properties of the dried sample can only be affected by the three different process parameters in the freeze-dryer that can be directly controlled: condenser temperature, chamber pressure and freeze-drying time. In addition to the freeze-dryer properties, the properties of the sample can also be affected by the material properties prior to freeze-drying as well as by the freezing temperature. The composition/formulation/concentration of the used material, the solid content and the fill volume all affect the properties of the sample (Franks 1998). In brief, the higher the freezing temperature or the slower the freezing results in a smaller number of larger ice crystals and also a more oriented structure into the sample. On the other hand, rapid freezing or a lower freezing temperature results in a large number of small ice crystals not oriented in one direction (Flink & Knudsen 1983).

To date, various polymers and various kinds of scaffolds have been fabricated by freeze-drying, and it is still one of the most commonly used methods to fabricate highly porous scaffolds for tissue engineering. By freeze-drying, it is possible to manufacture many kinds of polymers, natural and synthetic, and different kinds of composite structures are also possible. From natural polymers collagen (Pieper et al. 2002; Pieper et al. 1999; Park et al. 2002; Schoof et al. 2001; Von Heimburg et

al. 2001; Powell & Boyce 2006; Harley et al. 2007) and chitosan (Madihally & Matthew 1999; Francis Suh & Matthew 2000b; Ma et al. 2001; Nettles et al. 2002; Xia et al. 2004), for example, are widely studied as scaffold materials for freeze-drying. From synthetic polymers, the most used polymers are polyesters such as polylactide-based polymers. Also, different kinds of polymer blends such as collagen-chitosan blends (Ma et al. 2003; Wang et al. 2003; Wu et al. 2007; Zhu et al. 2009a; Zhu et al. 2009b; Arpornmaeklong et al. 2008; Wang et al. 2011), as well as different composite structures or hybrid structures with natural and synthetic components (Chen et al. 2003; Chen et al. 2004; Dai et al. 2010; Sato et al. 2001; Lee et al. 2006; Lee et al. 2004; Hiraoka et al. 2003; Lin et al. 2009; Ficai et al. 2010; Sionkowska & Kozłowska 2010; Akkouch et al. 2011; Xu et al. 2011) have been studied.

3 Cartilage and bone tissue engineering

3.1 Physiology and function of cartilage and bone

Because of the high variation between cartilage and bone tissue compositions and structures, it is very important to find the optimum tissue engineering construct to be used in osteochondral lesions. Cartilage is categorized as soft tissue. On the other hand, bone is categorized as hard tissue and, therefore, many approaches for osteochondral tissue engineering have concentrated on the different compositions and mechanical properties of each of the tissues (Martin et al. 2007; Castro et al. 2012). There are two distinct approaches for interfacial tissue engineering: by bridging two tissues as an independent interface or by transitioning from one tissue to another with a specific "tissue unit" as one component. The use of an autologous tissue transplant is an example of the latter approach that includes both cartilage and subchondral bone components (Castro et al. 2012).

3.1.1 Cartilage

Cartilage exists in various places in the body such as the articular surface of long bones, the trachea, ears, nose and intervertebral discs. Three types of cartilage exist: hyaline cartilage, elastic cartilage and fibrocartilage. Hyaline cartilage is the most abundant type of cartilage present in the human body. Hyaline cartilage exists, for example, on the articular surface of bones and in the trachea; whereas, elastic cartilage can be found in the ears and in fibrocartilage in the intervertebral discs (Meyer & Wiesmann 2006). The articular cartilage (hyaline cartilage) in the ends of bones is normally only ~3 mm thick, and it permits a smooth motion and minimal friction between the bones forming the joint (Kinner et al. 2005; Chiang & Jiang 2009). Loss of cartilage and especially articular cartilage is a problem from which millions of people suffer worldwide. The failure of articular cartilage may be caused by injury or disease and is a major problem as it may lead to severe pain and disability of the joint. (Kinner et al. 2005; Temenoff & Mikos 2000) Many joint diseases can cause these lesions, but the primary cause of losing articular cartilage is osteoarthritis (OA) (Temenoff & Mikos 2000; Hunziker 2002; Risbud & Sittinger 2002). Therefore, the regeneration of articular cartilage by therapeutic approaches would improve the quality of life for many people. This is why several approaches have been made in order to improve the outcome of the loss of articular cartilage. However, there is still no optimal way of regenerating fully functional articular cartilage (Kinner et al. 2005; Iwasa et al. 2009; Vinatier et al. 2009).

Cartilage tissue possesses only limited or almost no regenerative properties on its own. This is mainly due to its avascular, aneural and alymphatic nature and because cartilage contains a relatively low number of cells, mainly chondrocytes, in its structure. The chondrocytes are placed in lacunas and are therefore surrounded by dense ECM and not by other cells as in many other tissues. Cartilage ECM is mainly composed of collagen type II and proteoglycans that give the tissue its

unique mechanical properties. The articular cartilage comprises three distinct layers: the superficial, the middle and the deep zone. Each layer varies in structure and function and responds to different stimuli and secretes different proteins. For example, with increased depth, an increase in collagen is observed, and superior mechanical properties in the deep zone compared with the superficial zone are provided. (Chung & Burdick 2008)

Because of the low healing capability of articular cartilage, many attempts have been made in order to produce proper cartilage tissue. The most used so-called conventional cartilage repairing techniques are the microfracture technique, mosaicplasty, osteochondral autologous grafts and autologous chondrocyte implantation. However, these techniques can lead to fibrocartilage repair tissue, the morbidity of the donor site is a concern and the surgical procedures are complex (Iwasa et al. 2009). Nowadays, the tissue engineering approach has been found to posses the best abilities for cartilage regeneration. For example, to further improve the quality of autologous chondrocyte implantation by also using appropriate scaffolds (Iwasa et al. 2009; Chung & Burdick 2008). Even though cartilage tissue is an anisotropic tissue composed of different layers, the use of homogenous constructs has been the most used method for cartilage tissue engineering (Chung & Burdick 2008).

3.1.2 Bone

Bone serves as a mineral reservoir in the body and, more importantly, it provides the mechanical stability that is needed by the skeleton for load bearing, locomotion and also for the protection of internal organs. (Kneser et al. 2006) In general, bone possesses the intrinsic ability to self-repair itself as a response to injury or during skeletal development, or continuous remodelling to maintain mechanical integrity and to respond to the changing demands of the body. Trauma, infection, tumour resection or skeletal abnormalities may, however, need assisted bone regeneration in load bearing and non-load bearing skeletal sites. Also, the normal regenerative process of bone might be compromised, for example, by avascular necrosis, osteoporosis or rheumatoid arthritis. (Dimitriou et al. 2011; Holland & Mikos 2006)

The structure of bone is highly vascularized and it has the ability to regenerate itself without forming scar tissue. An adult skeleton contains two types of bone: trabecular (cancellous) and cortical (compact) bone. Cortical bone, 80% of all bones, is arranged in a compact pattern with almost solid, less than 10% porosity and is generally present in long, short and flat bones. Trabecular bone, 20% of all bones, is arranged in a porous sponge-like pattern (up to 50–90% porous) and it can be found in a large part of the bone marrow and is essentially present in the methaphysis of long bones, the iliac crest and the vertebral bodies. Bone tissue is mainly composed of three different cell types: osteoblasts, osteocytes and osteoclasts. (Kneser et al. 2006; Mistry & Mikos 2005) Osteoblasts are derived from mesenchymal stem cells (MSCs) and they secrete collagenous proteins that form the organic matrix of bone, the osteoid. When surrounded by osteoid, the mature osteoblasts stop secreting matrix and become osteocytes. Osteoclasts, derived from hematopoietic cells of the marrow, secrete acids and proteolytic enzymes that dissolve mineral salts and digest the organic matrix of

bone. The inorganic-organic structure of bone is composed of roughly 60% inorganic mineral, 30% organic material and 10% water (Mistry & Mikos 2005). The inorganic phase is composed of calcium phosphate, mainly hydroxyapatite (HAp), while the organic phase is mainly composed of collagens but also glycoproteins, proteoglycans and sialoproteins. (Mistry & Mikos 2005; Kneser et al. 2006) HAp crystals provide compressive strength to the inorganic-organic composite structure, while collagen fibres give tensile properties to the structure (Mistry & Mikos 2005).

Current treatments in bone repair are based on bone grafts, mainly autologous grafts, and allografts or metal or ceramic-based constructs. However, autologous grafts are limited due to their number and donor site morbidity. Allografts carry the risk of immune reactions. Metals exhibit poor overall integration and may also cause infections. Ceramics have very low tensile strength and are brittle. As a result, several clinical conditions still require enhancement of bone regeneration and various methods are used for this purpose. Nevertheless, more work is still needed to find the optimised outcome for bone tissue regeneration for the required purposes (Dimitriou et al. 2011).

3.2 Scaffolds for cartilage and bone tissue engineering

3.2.1 Cartilage tissue engineering scaffolds

The unique structure of cartilage has set many limitations on cartilage tissue engineering. The ideal materials used for cartilage tissue engineering could be the major components in cartilage tissue, collagen and proteoglycans. Collagen type II makes up the majority in articular cartilage (90–95% of the collagen in the matrix) but other collagens V, VI, IX and XI are also present. Proteoglycans, composed of about 95% polysaccharide and about 5% protein are not chemically bound between collagen fibres in the cartilage ECM, but aggregation prevents the diffusion of the proteoglycans out of the matrix during loading of the joint. (Temenoff & Mikos 2000) The collagen fibre structure gives the cartilage ECM its ability to withstand tensile stresses and proteoglycans withstand compressive loads and have the ability to contain water and, therefore, swell again after the load is released (Kinner et al. 2005). However, tissue engineering scaffolds fabricated from collagen and/or proteoglycans often lack the mechanical properties necessary to properly mimic the cartilage ECM. Therefore, several scaffold constructions have been studied to date, and many are under investigation for optimal cartilage tissue engineering (Iwasa et al. 2009; Chung & Burdick 2008). Articular cartilage has relatively high water content 60–80% of the wet weight of the tissue (Kinner et al. 2005). The scaffold should maintain its structure during the mechanical loading-unloading phenomenon and also be able to reabsorb the lost liquid into the scaffold *in situ*. This is important because the main exchange of nutrients and oxygen happens in cartilage ECM during this phenomenon (Temenoff & Mikos 2000; Ge et al. 2012). Furthermore, the mechanical stimulus of a tissue engineered scaffold during cell culturing affects the outcome of the newly formed tissue (Kinner et

al. 2005; Vinatier et al. 2009). As pointed out here, there are still many things to be studied before an ideal cartilage tissue engineering construct is discovered.

3.2.2 Bone tissue engineering scaffolds

The optimal materials to be used for bone tissue engineering should preferably be *osteoinductive*, capable of promoting the differentiation of progenitor cells down an osteoblastic lineage, *osteoconductive*, supports bone growth and encourages the ingrowth of surrounding bone, and capable of *osseointegration*, integrates into surrounding bone (Stevens et al. 2008). Several materials such as metals, ceramics and biodegradable polymers, both synthetic and natural, have been studied for bone tissue engineering. Metals and most of the ceramics are not biodegradable. Therefore, the most suitable materials to be studied for the application rely on biodegradable polymers and a small number of ceramics (Salgado et al. 2004). Collagen and especially type I collagen is a widely used material for bone tissue engineering because it is one of the major organic components in bone ECM. Also, osteogenic differentiation and mineralization have been shown to be provoked in type I collagen matrices (Ignatius et al. 2005; Ferreira et al. 2012). However, collagen scaffolds lack the mechanical properties essential for bone tissue engineering, and, therefore, they are not the best choice for the application on their own. Synthetic biodegradable polyesters, poly(α-hydroxy acids), and especially polylactide copolymers (PLAs), are widely used and well studied polymers for numerous biomedical applications and also for bone tissue engineering. More and more bone tissue engineering applications are using PLAs together with inorganic components, as they enhance the mechanical and degradation properties and can modify the biological behaviour of the scaffold. Because the structure of the native ECM of bone is a composite, many kinds of composite scaffolds are studied for bone tissue engineering (Navarro et al. 2006). Scaffolds composed of bioactive ceramics, bioactive glasses, natural or synthetic polymers or composites of the above are the most studied components for bone tissue engineering (Stevens et al. 2008). The pore size and porosity of a bone tissue engineering scaffold are crucial factors for proper scaffold geometry. A bone tissue engineering scaffold needs a highly porous structure with relatively large pores (diameter preferably over 100 μm). The high porosity is needed because the scaffold needs relatively fast cell migration into the scaffold and also vascularisation throughout the scaffold with high oxygenation. However, the porosity of the scaffold should not exceed the limit of the mechanical properties of the scaffold material or the scaffold construct. Also, the degradation of the scaffold should be taken into account. The scaffold should not be too porous when rapidly degrading materials are used, especially if the scaffold is used in load-bearing applications (Karageorgiou & Kaplan 2005).

4 Approaches for osteochondral tissue engineering

Since osteochondral tissue engineering requires the repair of both the cartilage and subchondral bone, the approach towards osteochondral scaffolds can vary in several ways. To repair an osteochondral defect, one must take into account all of the three variables: cartilage, bone and the cartilage-bone interface. A scaffold used for osteochondral tissue engineering may be composed of one, two or even more components, depending on the used materials and their compositions. Osteochondral scaffolds can be either single phase, layered or graded structures (Nukavarapu & Dorcemus 2013).

The major limitation in osteochondral tissue engineering is that it relies on the regeneration of the complex structure of the interface between cartilage and bone. Many different approaches including different scaffold materials, scaffold fabrication methods and the used cell types and compositions have been studied for osteochondral tissue engineering (Panseri et al. 2012; Martin et al. 2007; Castro et al. 2012).

4.1 Cartilage defects

If the cartilage defect affects the underlying subchondral bone, the defect is said to be an osteochondral defect. The osteochondral lesions may heal to some extent as the mesenchymal chondroprogenitor cells can penetrate through the vascularised subchondral bone into the lesion and form cartilage. However, the formed cartilage is mainly fibrous tissue without the functional properties of native hyaline cartilage (Panseri et al. 2012; Puppi et al. 2010). Osteochondral defects are typically formed by trauma or OA leading to structural and functional failures of the bone-cartilage interface which, in turn, leads to severe pain and reduced joint motion (Martin et al. 2007; Castro et al. 2012). As a result, osteochondral defects typically require surgical methods to heal. Currently, defects over the size of 2.5 cm^2 are difficult to heal with the commonly used methods such as joint debridement, microfracture and mosaicplasty. The above-mentioned methods have limited success in, for example, long-term repair. Therefore, tissue engineering, or more precisely interfacial tissue engineering (Castro et al. 2012), would give the best outcome for osteochondral defect repair (Panseri et al. 2012).

The classification of cartilage defects using the most popular system, the Outerbridge Classification System, is represented in Figure 3. The Outerbridge Classification System ranks the different cartilage lesion types into five different grades, where the Grade 0 is normal cartilage, from which point Grade I lesions (not shown in Figure 3) denote swelling and softening of the cartilage. Grade II is a partial thickness chondral defect, the type most often seen clinically, that has a defect diameter of less than 1.5 cm. A Grade III defect is a full thickness chondral defect that has a diameter larger

than 1.5 cm. A Grade IV defect is an osteochondral defect, where the subchondral bone is exposed (Nukavarapu & Dorcemus 2013).

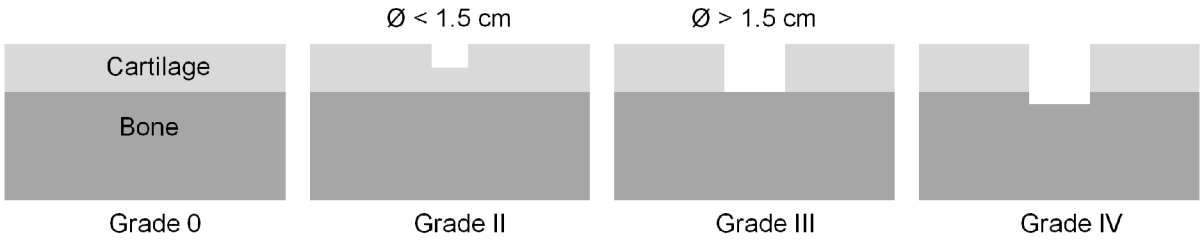

Figure 3. Representative graphs of different classifications of osteochondral defects: the Outerbridge Classification System. Grade 0: normal cartilage, Grade II: partial thickness defect (with a diameter less than 1.5 cm), Grade III: full thickness defect (with a diameter larger than 1.5 cm), and Grade IV: osteochondral defect (adapted from Nukavarapu & Dorcemus 2013).

4.2 Different scaffold strategies for osteochondral tissue engineering

Some of the possible scaffold strategies for osteochondral tissue engineering are represented in Figure 4. The scaffold can contain an independent bone scaffold combined with a cartilage scaffold (4 and 5 in Figure 4), a so-called bi-layered scaffold. The scaffold can be a combination of both parts (1 and 3 in Figure 4), with only one scaffold that can be either homogeneous or heterogeneous. Also, only one scaffold may be used for only one part, for example, for bone (2 in Figure 4) (Nooeaid et al. 2012). In addition, the used materials can vary for different components and the scaffold may contain only one material with one or more compositions. The different layers of combined bone and cartilage scaffolds may also be attached to each other prior to implantation or at the time of implantation (Martin et al. 2007).

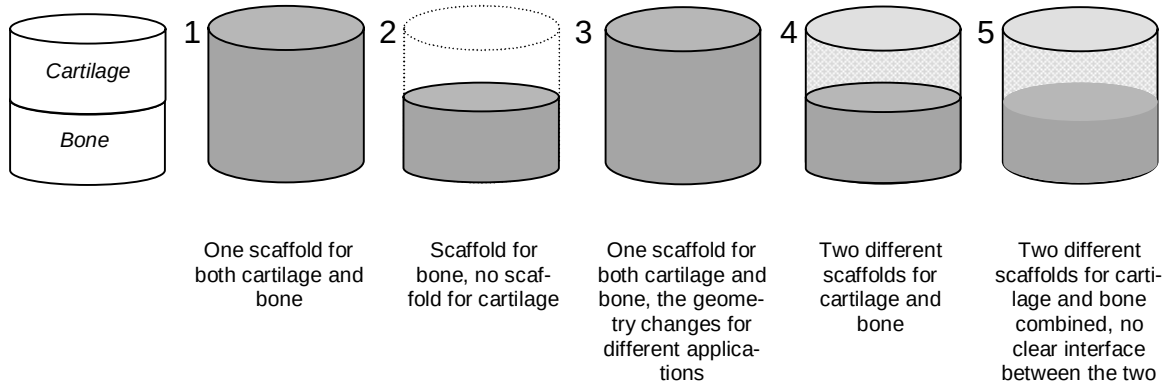

Figure 4. Schematic representations of different scaffold strategies for osteochondral tissue engineering.

In addition to the different scaffold strategies for osteochondral tissue engineering, there are also different strategies for loading cells into the scaffold. The scaffolds may be loaded with a single cell source that has chondrogenic capacity, with two cell sources that have either chondrogenic or osteochenic capacity, with a single cell source that have both chondrogenic and osteochenic differentiation capacity or with no cells (cell-free approach). Furthermore, different cell types such as articular chondrocytes, chondrocytes obtained from non-articular cartilage tissues or mesenchymal progenitor cells can be applied (Martin et al. 2007).

4.3 Current approaches to osteochondral tissue engineering

Though considerable progress has been made, several challenges still remain and so far only a few of the approaches developed have effectively found their way into the clinic. For example, the variable geometry of the 3D articular surface should be changeable in the scaffolds, the proportions between bone and cartilage thickness should be considered, the micro and nanoscale arrangement of cells and ECM should be considered within the tissue and the micromotion at the graft-tissue interface should also be avoided (Panseri et al. 2012).

Since the possibilities for osteochondral tissue engineering includes either cartilage and bone components or a combination of the two, the focus in planning a suitable osteochondral scaffold comprises both tissue type scaffolds as well as combined scaffolds, i.e., osteochondral scaffolds. In the beginning, single-phase scaffolds served as the standard. Since then, bi-layered, also called biphasic scaffolds, have been developed to promote cartilage and bone growth in the individual layers. In addition, the importance of an intermediate layer between the cartilage and bone layers has been realized, and so-called triphasic scaffolds have been developed as a result. However, it has not been demonstrated that the triphasic scaffolds are superior to biphasic scaffolds and, therefore, need further investigation (Shimomura et al. 2014). Current osteochondral tissue engineering strategies are heading in the direction of gradient scaffold development because such a structure would be similar to osteochondral tissue and would establish osteochondral interface formation. However, the optimal fabrication process for graded osteochondral scaffolds has not yet been established and the challenge is how to achieve optimal osteochondral interface formation into the scaffold. When it comes to product development, a scaffold alone strategy (scaffold with no cells or growth factors) is currently being given priority because of regulatory challenges and difficulties (Nukavarapu & Dorcemus 2013).

4.4 Freeze-dried composites for cartilage, bone and osteochondral applications

As the main processing technique discussed in this thesis is freeze-drying, examples of different approaches such as cartilage tissue engineering scaffolds, bone tissue engineering scaffolds and osteochondral tissue engineering scaffolds manufactured with freeze-drying are subsequently reviewed in the next chapters. The focus of these freeze-dried scaffolds is on composite structures as many of the studied scaffolds are a combination of two or more components because many times the use of only one component structure does not contain all the needed properties such as mechanical strength, optimal scaffold geometry, biomimetic properties, optimal resorption rate or bioactivity for the studied applications.

4.4.1 Freeze-dried composites for cartilage tissue engineering

Cartilage tissue engineering relies mostly on the natural components of the native tissue such as collagen and some naturally occurring glycosaminoglycans (GAGs) such as hyaluronic acid (HA) or chondroitin sulphate. Also, another natural polymer, chitosan, is used because of its natural GAG-like properties (Iwasa et al. 2009). Since many of the freeze-dried scaffolds do not have the ability to be used as only one component or one material structure, or without any reinforcement, Table 5 summarizes the freeze-dried composite scaffolds for cartilage tissue engineering. As can be seen in Table 5, natural polymers, such as collagen, are often combined with synthetic polymer components to achieve better mechanical strength for the freeze-dried scaffold. In the case of freeze-dried composite systems for cartilage tissue engineering, the constructs are often achieved by combining a so-called synthetic polymer skeleton with natural components. The skeleton of synthetic polymer is in these cases often some kind of embedded fibres, textile or embedded solid structures (Moutos & Guilak 2008).

Table 5. Freeze-dried composite scaffolds for cartilage tissue engineering.

Used materials	Filler	Processing method	Ref.
Collagen I + PLGA[a]	PLGA knitted mesh (Vicryl)	PLGA knitted mesh and freeze-dried collagen	(Chen et al. 2003; Chen et al. 2004; Dai et al. 2010)
Collagen I + PLGA	PLGA sponge	Collagen freeze-dried into NaCl-particle leached PLGA sponge	(Chen et al. 2004; Sato et al. 2001)
Collagen I + PLGA	PLGA microbeads (Loaded with insulin)	Freeze-drying of collagen solution with PLGA microbeads and ice particulates (as porogen material)	(Nanda et al. 2014)
Collagen I + PLLA[b]	PLLA nanoparticles	Frreze-drying of collagen solution with PLLA nanoparticles	(Xu et al. 2012; Bian et al. 2014)
Collagen I + HA[c] + chitosan		Freeze-drying of collagen + HA + chitosan solution	(Lin et al. 2009)
Collagen I + HA		Freeze-drying of collagen + HA solution	(Tang et al. 2007)
Collagen II + chondroitin sulphate + HA		Freeze-drying of collagen solution and subsequent immersion of collagen scaffolds into chondroitin sulphate and HA solutions with cross-linker	(Ko et al. 2009)
Collagen II + chondroitin sulphate		Freeze-drying of collagen + chondroitin sulphate solution	(Tamaddon et al. 2013)
Recombinant collagen + HAp[d]	Nano-HAp	Freeze-drying of collagen + HAp solution	(Jia et al. 2013)
PCL[e] + HA / chitosan	PCL rapid prototyped porous structure	Freeze-drying of HA or chitosan into the PCL structure	(Schagemann et al. 2010)
PVA[f] + PCL + gelatin		Freeze-drying of a foam-like mixture (formed with high-speed mixing) of PVA + PCL + gelatine solution	(Karkhaneh et al. 2014)
PGA[g] + HA		PGA scaffolds (BioTissue AG, Zurich, Switzerland) immersed with HA and subsequently freeze-dried	(Patrascu et al. 2013)
Poly(L-glutamic acid) + chitosan		Freeze-drying of poly(L-glutamic acid) + chitosan solution	(Zhang et al. 2013)
Silk fibroin + collagen / gelatin		Freeze-drying of silk fibroin, silk-fibroin + collagen or silk-fibroin + gelatin solutions	(Chomchalao et al. 2013)

[a]PLGA = poly(lactide-co-clycolide), [b]PLLA = poly(L-lactic acid), [c]HA = hyaluronic acid, [d]HAp = hydroxyapatite [e]PCL = polycaprolactone, [f]PVA = poly(vinyl alcohol), [g]PGA = polyglycolide

4.4.2 Freeze-dried composites for bone tissue engineering

In bone tissue engineering composites, bioabsorbable and bioactive materials are often combined. The combination of bioabsorbable polymers and bioactive ceramics is often applied. As can be seen in Table 6, there have been several studies about bone tissue engineering composite scaffolds fabricated by freeze-drying. The mostly studied components for these studied scaffolds are natural polymers such as collagen (especially type I, the most common collagen type in bone), chitosan or gelatine, together with some bioactive components such as calcium phosphates (CaP), for example, HAp or tricalcium phosphate (TCP). Because widely used natural polymers such as collagen and chitosan lack the mechanical strength required for load-bearing applications, natural polymer composites with other more mechanically stable components such as CaP or synthetic bioabsorbable polymer components are often used for load-bearing applications (Puppi et al. 2010). As can be seen in Table 6, the used filler for freeze-dried bone tissue engineering composite scaffolds is most often in the form of small particles, powders such as nanoscale HAp or other small particles (< 40 µm). Synthetic matrices, for example PLA and PLGA, are also combined with BaGs for bone tissue engineering. BaGs are thought to buffer the acidic degradation products of the polyesters and prevent catalytic action on the degradation and also the development of adverse tissue reaction. Since the hydroxyl carbonate apatite phase on the bioactive ceramic implant is chemically and structurally equal to the mineral phase of bone, it provides the interfacial bonding between the implant and the surrounding tissue. CaPs such as HAp or TCP and BaGs are considered to be bone bioactive ceramics as they bind the surrounding osseous tissue and enhance bone tissue formation. However, the poor mechanical properties of BaGs, low fracture toughness and mechanical strength, especially in the case of porous structures, limit their use in load-bearing applications (Puppi et al. 2010).

Table 6. Freeze-dried composite scaffolds for bone tissue engineering.

Used materials	Filler	Processing method	Ref.
Collagen I + HAp[a]	HAp (nanoparticles / particles or powder / whiskers / *in situ* formed HAp)	Freeze-drying of collagen solution and with HAp / *in situ* precipitation of HAp after freeze-drying of collagen / freeze-drying of collagen and subsequent immersion of the collagen scaffolds into HAp solution (and freeze-drying again)	(Sionkowska & Kozłowska 2010; Al-Munajjed et al. 2009; Ciardelli et al. 2010; Cunniffe et al. 2010; Shen et al. 2011; Hoyer et al. 2012; Kane & Roeder 2012)
Collagen I + chitosan / PVA[b] + HAp	HAp	Freeze-drying of collagen + chitosan / polyvinyl alcohol solution with HAp	(Nitzsche et al. 2010)
Collagen I + PLCL[c] + HAp	HAp	Freeze-drying of the collagen + PLCL solution with HAp and NaCl particles followed by porogen leaching	(Akkouch et al. 2011)
Collagen I + CaP[d]	CaP (sodium ammonium hydrogen phosphate: $NaNH_4HPO_4$ and calcium chloride: $CaCl_2$)	Freeze-drying of collagen solution and subsequent immersion of the collagen scaffolds into $NaNH_4HPO_4$ and $CaCl_2$ solutions to form CaP coating	(Al-Munajjed & O'Brien 2009)
Collagen I + BaG[e] (+ PS[f]) / TCP[g]	BaG / TCP	Freeze-drying of collagen (+PS) solution with BaG / TCP	(Oprita et al. 2008)
Collagen I / PGA[h]	PGA non-woven	Freeze-drying of collagen solution into PGA non-woven	(Hosseinkhani et al. 2006)
Collagen I + BPC[i] + HCA[j]	BCP (HAp and TCP particles)	Sintered BCP scaffold immersed in collagen solution and freeze-dried. Subsequently the scaffolds were biomineralized *in vitro* with supersaturated calsification solution (SCS)	(Yang et al. 2005)
Collagen I + HA[k] + PS + BaG	BaG	Freeze-drying of collagen + HA + PS solution with BaG particles	(Wang et al. 2006; Xie et al. 2008)
Chitosan + HAp (+ nano-silver)	HAp	Freeze-drying of chitosan solution with HAp (and subsequently soaking the scaffolds in aqueous silver nitrate solution to enrich the scaffold surface with silver)	(Zhang et al. 2012)
Chitosan + CMC[l] / collagen + HAp	HAp	Freeze-drying of chitosan + CMC /collagen solution with HAp	(Jiang et al. 2008; Liuyun et al. 2009)
Chitosan + carbon nanotube (+ HAp)	Carbonnanotubes (+ HAp)	Freeze-drying of chitosan solution with carbon nanotubes (+HAp)	(Venkatesan et al. 2012)
Chitosan + HAp + nano-copper-zinc / amylopectin / chondroitin sulphate	HAp + Cu-Zn alloy nanoparticles / amylopectin / chondroitin sulphate	Freeze-drying of chitosan solution with HAp + nano-copper-sinc / amylopectin / chondroitin sulphate	(Tripathi et al. 2012)
Chitosan + alginate + HAp		Freeze-drying of chitosan + alginate solution and *in situ* co-precipitation of HAp (with H_3PO_4 and $Ca(OH)_2$)	(Jin et al. 2012)
Chitosan (+ gelatine) + BaG / TCP	BaG / TCP	Freeze-drying of chitosan (+gelatine) solution with BaG / TCP particles	(Zhang & Zhang 2001)
Chitosan + CaP	HAp+TCP macroporous block	Freeze-drying of chitosan solution inside the macroporous CaP block	(Zhang & Zhang 2002; Zhang et al. 2003)
Chitosan + silica + zirconia	Silicon dioxide and zirconia	Freeze-drying of chitosan solution with silicon dioxide and zirconia powders	(Pattnaik et al. 2011)

Table 6 continues.

Used materials	Filler	Processing method	Ref.
Chitosan + CaP	CaP	Freeze-drying of chitosan solution with CaP precursor ($CaCl_2$ and NaH_2PO_4)	(Tanase et al. 2011)
Chitosan + carbonate apatite	Carbonate apatite particles	Freeze-drying of chitosan solution with carbonate apatite particles after thermal drying	(Shen et al. 2007)
Chitosan + PLGA + HAp	HAp powder	Freeze-drying of chitosan + HAp solution and subsequently adding PLGA on the scaffolds and freeze-dried	(Endogan Tanir et al. 2014)
Chitosan + collagen + PVA + BaG	PVA + BaG composite powder	Freeze-thawing + freeze-drying of chitosan + collagen solution with PVA + BaG composite powder	(Pon-On et al. 2014)
Chitin + gelatine + HAp	HAp	Freeze-drying of carboxymethyl chitin + gelatine solution with nano-HAp	(Sagar et al. 2012)
Chitin + chitosan + TiO_2[m]	TiO_2 nanoneedles	Freeze-drying of chitin + chitosan solution with TiO_2-nanoneedles	(Jayakumar et al. 2011)
Chitin + HAp	HAp	Freeze-drying of chitin solution with HAp	(Kumar et al. 2011)
Gelatin (+ gellan gum) + HAp	HAp	Freeze-drying of gelatine (+ gellan gum) solution with HAp	(Kim et al. 2005)
Gelatin + TCP / HAp + fibrin + rhBMP-2[n] / montmorillonite + cellulose	TCP / HAp + rhBMP-2 + fibrin glue / montmorillonite	Freeze-drying of gelatine solution with TCP / HAp + rhBMP-2 + fibrin / montmorillonite particles	(Panzavolta et al. 2009)
Gelatin + HAp	HAp	Freeze-drying of gelatine + HAp solution	(Panzavolta et al. 2013)
Gelatin + HA + alginate		Freeze-drying of gelatine + HA + alginate solution	(Singh et al. 2014)
CaP + silk	CaP + silk	Freeze-drying of silk water solution with CaP + silk powder	(Zhang et al. 2010)
Carboxy methyl cellulose + HAp	HAp powder	Freeze-drying of carboxy methyl cellulose, immersing of scaffolds into HAp solution and freeze-drying	(Pasqui et al. 2014)
PLGA[o] + HAp	HAp	Freeze-drying of PLGA solution with HAp and salt particles followed by dissolution of the salt particles	(Aboudzadeh et al. 2010)
PLGA + HAp + rhBMP-2 / PDLLA[p] + BaG / pHEMA[q] + HAp / PLGA + BaG / PHBV[r] + HAp	HAp / BaG, rhBMP-2	Freeze-drying of polymer solution with HAp / BaG (and rhBMP-2)	(Miki et al. 2000)

[a]HAp = hydroxyapatite, [b]PVA = polyvinyl alcohol, [c]PLCL = poly(lactide-co-caprolactone), [d]CaP = calsium phosphate, [e]BaG = bioactive glass, [f]PS = phosphatidylserine [g]TCP = tricalcium phosphate, [h]PGA = polyglycolide, [i]BPC = biphasic calcium phosphate, [j]HCA = hydroxyl-carbonate-apatite, [k]HA = hyaluronic acid, [l]CMC = carboxymethyl cellulose, [m]TiO_2 = titanium oxide [n]rhBMP-2 = recombinant human bone morphogenetic protein, [o]PLGA = poly(lactide-co-clycolide), [p]PDLLA = poly(D,L)lactide, [q]pHEMA = poly(2-hydroxyethyl methacrylate), [r]PHBV = poly(hydroxybutyrate-co-hydroxyvalerate)

4.4.3 Freeze-dried composites for osteochondral tissue engineering

The complexity of osteochondral lesions also affects the osteochondral tissue engineering scaffold geometry. The unique structure of the combined tissues, bone and cartilage, as well as the proportions of bone and cartilage thickness makes it difficult to define the optimal osteochondral scaffold geometry (Panseri et al. 2012). Different freeze-dried composite scaffolds studied for osteochondral tissue engineering are listed in Table 7. The scaffolds used for osteochondral tissue engineering can roughly be divided into two categories: one component scaffold for both regions and two different components for cartilage and bone tissues. The one component scaffolds can also be divided into scaffolds with homogenous regions and scaffolds with heterogeneous regions (Martin et al. 2007). As Table 7 indicates, a variety of different freeze-dried scaffolds have been studied for osteochondral tissue engineering as the components used and the scaffold geometry vary a lot. Even though, no clear trend in Table 7 exists for manufacturing the different layers for osteochondral scaffolds, collagen, the main component in both tissues, seems to be the most studied material for the application. However, the trend in osteochondral tissue engineering seems to be towards bilayered scaffolds and a gradient scaffold structure. More and more freeze-dried osteochondral composite scaffolds have been developed during the past few years. Therefore, it can be concluded that freeze-drying has been found to be an applicable way to produce different kinds of multilayered scaffolds for tissue engineering of osteochondral lesions.

Table 7. Freeze-dried composite scaffolds for osteochondral tissue engineering.

Used materials	Filler	Processing method	Ref.
Collagen I + GAG[a] (chondroitin sulfate)	Calsium salts (CaP, calciumhydroxide)	Freeze-drying of collagen + GAG-solution with calcium salts in a solution of phosphoric acid	(Harley et al. 2010b)
Collagen I / collagen II + GAG (chondroitin sulfate)	Different collagen type I or II + GAG solutions in different layers	Freeze-drying of collagen type I + GAG and collagen type II + GAG-solutions sequentially in one mould	(Harley et al. 2010a)
Collagen I + HAp[b]	Different blend ratios of collagen + HAp in different layers	Combining the different blend layers on top of a Mylar sheet and finally freeze-drying	(Kon et al. 2010)
Collagen I + HAp	HAp paste	Freeze-drying of collagen or collagen + HAp solutions for two different scaffolds to be combined for two layered scaffold	(Zhou et al. 2011)
Collagen I + collagen II + HAp + HA[c]	HAp powder	Combining of different layers with step-by-step freeze-drying. Bone layer: Collagen I + HAp. Intermediate layer: Collagen I + collagen II + HAp. Cartilage layer: Collagen I + collagen II + HA	(Levingstone et al. 2014)
Collagen I + PLGA[d]	PLGA knitted mesh (Vicryl)	PLGA knitted mesh and freeze-dried collagen	(Chen et al. 2006)
Collagen + CaP[e]	Calsium phosphate formation onto the collagen matrix	Freeze-dried collagen soaked in calcium solution for CaP crystallisation onto the collagen matrix	(Yaylaoglu et al. 1999)
Collagen II + chitosan + PCL[f]		Layered scaffolds with different ratios of components in layers. Chitosan-PCL copolymers blended with collagen II manufactured with combinatorial processing of adjustable temperature gradients, collimated photothermal heating and freeze-drying	(Zhu et al. 2014)
Chitosan + gelatine / chitosan + gelatine + HAp	HAp powder, TGF-β[g] and BMP-2[h]	Freeze-drying of chitosan + gelatine solution and subsequently loaded with TGF-β for cartilage layer. Freeze-drying of chitosan + gelatine + HAp and subsequently loaded with BMP-2 for bone layer	(Chen et al. 2011)
BaG[i] + chitosan / alginate / gelatine or sucrose	Electrospun chitosan membranes, BaG (Bioglass®)-based substrate	Bottom layer: BaG substrate fabricated by foam replica dipped into chitosan or alginate or gelatine or sucrose and freeze-dried. Top layer: electrospun chitosan	(Liverani et al. 2012)
BaG + chitosan + PCL	BaG (Bioglass®) scaffold manufactured by foam-replication method	Porous BaG scaffolds immersed into chitosan + PCL solution and freeze-dried. Second layer manufactured by applying chitosan + PCL solution on top of BaG scaffold and freeze-dried	(Yao et al. 2014)
Gelatin + BaG	BaG (bioresorbable phosphate glass) particles	Freeze-drying of gelatine solution with BaG particles	(Gentile et al. 2012b)
PLLA[j] + ACP[k]	ACP powder (+ bFGF[l])	Freeze-drying of PLLA solution with ACP powder and subsequently impregnating the scaffolds in PBS+bFGF	(Huang et al. 2007)

[a]GAG = glycosaminoglycan, [b]HAp= hydroxyapatite, [c]HA = hyaluronic acid, [d]PLGA = poly(lactide-co-clycolide), [e]CaP = calsium phosphate, [f]PCL = polycaprolactone, [g]TGF-β = transforming growth factor- β [h]BMP-2 = bone morphogenic protein-2 [i]BaG = bioactive glass, [j]PLLA = poly(L-lactic acid), [k]ACP = amorphous calcium phosphate, [l]bFGF = fibroblast growth factor

5 Aims of the study

The primary aim of this thesis was to find optimal ways to manufacture cartilage and osteochondral tissue engineering scaffolds using freeze-drying. To overcome the high demands of osteochondral lesions, two types of scaffolds are studied based to the origin of the polymer applied. The studied natural polymer-based scaffolds are aimed for cartilage tissue engineering and synthetic polymer-based scaffolds for bone or osteochondral tissue engineering. Therefore, the more detailed aims of the current study are divided into two categories: aims of the natural polymer-based scaffolds and aims of the synthetic polymer-based scaffolds.

The aims of the thesis were to find answers to the following questions:

Natural polymer-based scaffolds for cartilage tissue engineering:

1. How to manufacture freeze-dried collagen scaffolds and what is the best way to cross-link freeze-dried collagen scaffolds? (Publication I)
2. Does the blending of collagen with chitosan improve the properties of freeze-dried collagen scaffolds? (Publication IV)
3. Does PLA fibre-reinforcement improve the properties of freeze-dried natural polymer-based scaffolds? (Publication IV)
4. Are the manufactured natural polymer-based scaffolds suitable for cell seeding? (Publication IV)

Synthetic polymer-based scaffolds for bone or osteochondral tissue engineering:

1. How to manufacture freeze-dried synthetic polymer-based scaffolds? (Publications II, III, V)
2. Is there a difference between the used filler particles, TCPp and BGp, or between the filler particle concentrations in PLA70 composites? (Publications II, III)
3. Do BG fibres improve the properties of PLGA scaffolds? (Publication V)
4. Are the manufactured synthetic polymer-based composite scaffolds suitable for cell seeding? (Publication II)

6 Materials and methods

6.1 Materials

The materials, reagents and their suppliers used in this work are presented in Table 8. The used collagens (COLI) were pepsin-solubilized bovine dermal collagens dissolved in 0.01 M HCl with collagen concentration of 3.0 mg/ml. The collagen supplier and the product name of the used collagen changed by the time the second batch of collagen was purchased, although the product remained the same. The commercial synthetic polymers Poly(L/D,L)lactide 70/30 (PLA 70) and Poly(L/D)lactide 96/4 (PLA 96) were both medical grade, highly purified polymers with a residual monomer content of <0.5%. The Poly(D,L-lactide-co-glycolide) 70/30 (PLGA1 and PLGA2) with a rac-lactide-to-glycolide ratio of 70:30 were synthesized by ring-opening polymerization. The bioactive glass fibres (BGf1 and BGf2 in Table 8) were glass fibres coated with polycaprolactone (PCL).

Table 8. The used materials and reagents, and their suppliers.

Material/Reagent	Supplier	Publication
Natural polymers		
Bovine dermal Collagen type I (COLI)* VITROGEN® (3.0 mg/ml in 0.01 M HCl)	Nutagon B V, The Netherlands	I
Bovine dermal Collagen type I (COLI)* PureCol™ (3.0 mg/ml in 0.01 M HCl)	Nutagon B V, The Netherlands	I, IV
Medical grade chitosan (CHI) Protasan UP B 90/500 (deasetylation degree of 90%, molecular weight of 460,000 g/mol)	FMC Biopolymer d/b/a NovaMatrix, Norway	IV
Synthetic polymers		
Poly(L/D,L)lactide 70/30 (PLA 70) (inherent viscosity of 3.1 dl/g)	PURAC Biochem B V, The Netherlands	II, III
Poly(L/D)lactide 96/4 (PLA 96) (inherent viscosity of 2.2 dl/g)	PURAC Biochem B V, The Netherlands	IV
Poly(D,L-lactide-co-glycolide) 70/30 (PLGA1) (molecular weight of 76 300 g/mol)	Åbo Akademi, Finland	V
Poly(D,L-lactide-co-glycolide) 70/30 (PLGA2) (molecular weight of 48 300 g/mol)	Åbo Akademi, Finland	V
Bioceramics and bioactive glasses		
β-TCP (TCP) Beta Whitlockite (porous particles size of 75–106 µm)	Plasma Biotal Ltd, UK	III
Bioactive glass (BG) BaG0127 (5% Na_2O, 7.5% K_2O, 3% MgO, 25% CaO and 59.5% SiO_2, particle size of 75–125 µm)	Åbo Akademi, Finland	II
Bioactive glass (BGf1) (11.9% Na_2O, 13.3% CaO, 4.4% MgO, 0.3% Al_2O_3, 0.9% B_2O_3, 0.6% P_2O_5 and 68.7% SiO_2, fibre diameter of 13 µm)	Vivoxid Ltd., Finland	V
Bioactive glass (BGf2) (12.5% Na_2O, 9.3% CaO, 7.2% MgO, 1.8% B_2O_3, 0.6% P_2O_5 and 68.6% SiO_2, fibre diameter of 13 µm)	Vivoxid Ltd., Finland	V
Reagents		
1-ethyl-3-(3-dimethylaminopropyl)carbodiimide hydrochloride (EDC)	Sigma-Aldrich, Finland	I
N-Hydroxysuccinimide (NHS)	Sigma-Aldrich, Finland	IV
1,4-dioxane	Sigma-Aldrich, Finland	II, III

* Same product, the supplier and the name of the product had changed when purchasing the second batch

6.2 Methods

6.2.1 Fabrication of freeze-dried scaffolds

Fabrication of plain and blend solutions of natural polymers (I, IV)

Collagen fibril formation was carried out using the method previously described by Williams et al. 1978 (Williams et al. 1978) with some modifications. The collagen-HCl solution was mixed with fibrillogenesis buffer (0.2M NaH_2PO_4, pH 11.2) at a ratio of 1:10. The pH of the solution was adjusted to 7.20 and the solution was incubated at room temperature (RT) for 6 h. The cross-linker, EDC, was added into the solution, if used prior to freeze-drying. This was followed by incubation of the collagen solution at RT overnight. The collagen solution manufactured had an initial concen-

tration of 0.3 wt%. Higher collagen concentrations were achieved by centrifuging and then concentrating the solution. Using this method, concentrations from 0.5 to 2.0 wt% were achieved. The chitosan solution was manufactured by dissolving the chitosan in an acetic acid solution at a ratio of 1:1 (w/v) with chitosan concentrations of 0.5 or 1.0 wt%. For collagen-chitosan blends, the initial collagen and chitosan solutions were mixed at ratios of 1:1 or 2:1 (v/v), respectively.

Fabrication of synthetic polymer solutions (II, III, V)

PLA solutions were manufactured by dissolving the polymer in 1,4-dioxane. The solutions were stirred vigorously overnight to form a uniform slurry. The used polymer concentrations were 2.0 or 3.0 wt%, for PLA70 and 3.0 or 5.0 wt% for PLGA1 and PLGA2.

Fabrication of polylactide and bioactive glass mesh (IV, V)

The PLA96 was melt-spun into multi-filament fibres (16-ply, with the average diameter of a single fibre ~20 µm) using a Gimac microextruder (Gimac, Gastronno, Italy) with a screw diameter of 12 mm. The bioactive glass fibres, BGf1 and BGf2 (with a diameter of a single fibre 13 µm), were used as received. To manufacture the carded mesh, PLA96, BGf1 or BGf2 fibres were cut into staple fibres at a length of ~10 cm and carded into mesh manually by feeding a standard number of fibres to the drum carder (Louët Elite Drum Carder, Louët, The Netherlands).

Fabrication of different scaffold types (I-V)

The abbreviations used for the different scaffold types, the materials used (matrix and filler) and the number of components, possible cross-linking method and the related publications are listed in the table presented in Abbreviations. A more detailed table with the different scaffold types, the materials used (matrix and filler) and the number of components, cross-linking method, the type of mould used in the processing (the material used for the mould and the size of the mould), possible sterilization method, abbreviations for the different scaffold types, as well as the related publications are presented in Appendix I.

All of the scaffolds were manufactured by freeze-drying the manufactured solutions by freezing at -30 °C for 24 h prior to freeze-drying for 24 h. Schematic diagrams of the fabrication process of natural polymer-based scaffolds as well as the synthetic polymer-based scaffolds are presented in Appendix II.

For scaffolds containing collagen (Publications I and IV), EDC or EDC+NHS cross-linking was performed to improve the stability of the scaffolds. When cross-linked with EDC prior to freeze-drying, the cross-linker was added into the collagen solution after the first incubation at RT for 6 h and followed by incubation at RT overnight. When cross-linked post freeze-drying, the freeze-dried scaffolds were immersed in 95% ethanol either with 1 mM or 10 mM EDC, or 14 mM EDC + 6 mM NHS in the solution. In the case of the 1 mM or 10 mM EDC solution, the incubation time for

cross-linking was 24 h at RT. With the 14 mM EDC + 6 mM NHS solution, the incubation time was 4 h at RT. After cross-linking, the scaffolds were withdrawn from the cross-linking solution and carefully washed several times with deionized water and freeze-dried again using the same freezing method at −30 °C for 24 h prior to freeze-drying for 24 h.

To stabilize the structure of the plain chitosan scaffolds (Publication IV), the freeze-dried scaffolds were neutralized with 99.5% and 70% ethanol steps for 30 minutes in each. After that, the chitosan scaffolds were washed several times with deionized water and freeze-dried again, as described earlier.

All of the manufactured scaffolds were held under vacuum at RT for a minimum of 48 h prior to any characterization or sterilization of the synthetic polymer-based scaffolds with 25 kGy gamma irradiation.

The structure of the natural polymer-based hybrids, collagen+PLA96, chitosan+PLA96 and collagen+chitosan+PLA96 (Publication IV) was a so-called sandwich structure with the PLA96 fibrous mesh laid at the bottom and at the top of the scaffold. In the PLA70+TCP or PLA70+BG composites (Publications II and III), the structure of the scaffolds was heterogeneous with the filler particles at the bottom of the scaffold structure. The structure in the PLGA1/BGf1 and PLGA2/BGf2 composites (Publication V) was homogenous with BG fibrous mesh acting as a skeleton inside the polymer matrix.

6.2.2 Scaffold microstructure analysis (I-V)

Scanning electron microscopy (SEM) was used to characterize the microstructure of the scaffolds. SEM imaging with a JEOL T100 scanning electron microscope (JEOL Ltd, Tokyo, Japan) was performed for scaffolds sputtered with gold prior to analysis (Publications I and V). SEM imaging with an FEI Quanta 250 Field Emission Gun (Electron Microscope Unit, Institute of Biotechnology, Helsinki, Finland) was performed for platinum coated scaffolds (Publication IV). An environmental scanning electron microscopy (ESEM; Philips XL30 ESEM-TMP, Amsterdam, The Netherlands) was used to study the microstructure of the scaffolds in wet conditions (Publications II and III) as well as the cell morphology (Publication II). Pore sizes were determined from the SEM images using Image J software.

MicroCT analysis to study the microstructure of the scaffolds was carried out with two different pieces of equipment: a MicroCT scanner (SkyScan 1172, SkyScan, Kontich, Belgium) with tube voltage and voxel size of 40 kV and 30.2 × 30.2 × 30.2 μm^3, respectively (Publication IV), or with MicroXCT-400 (Carl Zeiss X-ray Microscopy, Inc., Pleasanton, USA) with tube voltage and voxel size of 40 kV and 2.2 × 2.2 × 2.2 μm^3, respectively (Publication V). A Fiji (Schindelin et al. 2012) with a BoneJ (Doube et al. 2010) plugin was used to determine the pore structure of the scaffolds

(porosity, pore size, material thickness and pore size distribution). No filters were used in the microCT analyses.

6.2.3 Contact angle measurements (V)

The contact angle (CA) of the dry scaffolds was examined with a Theta optical tensiometer (Biolin Scientific, Västra Frölunda, Sweden) device (Publication V). The measurements were done with deionized water, phosphate buffered saline solution (PBS) and with bovine blood (commercially available) (n=6).

6.2.4 *In vitro* studies (III, V)

In vitro hydrolytic degradation of synthetic polymer-based scaffolds was conducted in PBS, prepared as described by Shah et al. 1992 (Shah et al. 1992), with standard volume (according to International Standard, ISO 15814, 1999 (Implants for surgery - copolymers and blends based on polylactide - in vitro degradation testing 1999)) of 10 ml. The pH of the hydrolysis solution was measured weekly using a Mettler Toledo MP225 pH meter (Mettler-Toledo GmbH, Schwerzenbach, Switzerland). The buffer solution was changed fortnightly or weekly if its pH exceeded the given limits (7.35–7.45). The degradation studies were timed at weeks 0, 2, 4, 8, 16 and 26 for plain PLA70 and PLA70+TCP scaffolds (Publication III), and at weeks 0, 2, 4, 6, 8 and 10 for plain PLGA and PLGA+BGf scaffolds (Publication V). Samples each half the size of the original freeze-dried scaffolds were used (n=6) with an initial sample weight of approximately 5 mg or 15 mg for PLA70 and PLGA-based samples, respectively.

6.2.5 Weight change (I, III, IV, V)

The weight change of scaffolds during hydrolysis (Publications III and V) was determined by the following Equation 1:

$$\text{Weight change (\%)} = [(W_e - W_b)/W_b] \times 100\%, \quad (1)$$

where W_e is the measured weight after immersion in PBS (wet or dry, depending if measuring the water intake or the overall weight change) and W_b is the initial dry weight of the scaffold. When determining the weight change during hydrolysis, the scaffolds were rinsed with deionized water and gently dried with tissue paper, dried in a fume hood for 2 days, and then one week in a vacuum at RT before the dry weighing.

The ability of the natural polymer-based scaffolds to bind water was determined by using the same equation of weight change. The scaffolds were immersed in PBS in a volume of 3 ml for 1 h at RT (Publication I, n=2) or in 5 ml for 24 h at 37 °C (Publication IV, n=6). The overall ability of the scaffold to bind water (the material itself with the pore system) was measured by removing the scaffold from the PBS without dripping (Publications I and IV). Also, the ability of the scaffold itself

(no excess water inside the pore system) to bind water was measured after drying the scaffolds between filter papers to remove the water inside the pore system of the scaffold (Publication IV).

6.2.6 Thermal properties (I, III, V)

A differential scanning calorimeter (DSC, Q1000, TA Instruments, New Castle, DE, USA) was used to determine the collagen denaturation temperatures (T_d) in order to evaluate the efficiency and extent of collagen (Publication I). The T_d values were evaluated as a maximum value of an endothermic peak, while heating the sample from 5 to 140 °C with a heating rate of 20 °C/min. The sample size used was approximately 1–2 mg. For synthetic polymer-based scaffolds, a DSC was used to determine the glass transition temperature (T_g) (Publication V). The results are from the second heating scan using the following procedure: heat to 200 °C, 20 °C/min, cool to 0 °C, 50 °C/min, and heat to 200 °C, 20 °C/min. The sample size used was approximately 5 mg. All samples were measured in standard aluminium pans under a dry N_2 atmosphere (n=2).

Thermogravimetric analysis (TGA) with a Q500 (TA Instruments, New Castle, DE, USA) device was used for analytic measurement of the component ratios of synthetic polymer and inorganic filler in the composite scaffolds. The method used was Hi-Res-Dynamic and samples were heated to 640 °C (Publication III) or to 800 °C (Publication V). The sample size was approximately 2 mg (Publication III) or 10 mg (Publication V) (n=2).

6.2.7 Inherent viscosity measurements (III)

The inherent viscosity (i.v.) of the synthetic polymer-based scaffolds was measured with a Lauda PVS viscometer (Lauda DR. R. Wobster GmbH, KG, Königshofen, Germany) (Publication III). Samples were prepared by dissolving the polymer in 1 mg/ml chloroform. An Ubbelohde capillary viscometer type 0c (Schott-Geräte, Mainz, Germany) was used to determine the viscosity. Viscosity measurements were run for plain polymer scaffolds (n=2).

6.2.8 Gel permeation chromatography (V)

The determination of the molecular weight of the polymer component in synthetic polymer-based scaffolds (Publication V) was performed using gel permeation chromatography (GPC). The measurements were carried out with an LC-10ATVP HPLC-pump (Shimadzu Corporation, Kyoto, Japan), an AM GPC Gel 10 µm Linear colon (Mentor, Ohio, USA) and a Sedex 85 light scattering detector (Sedere SA, Alfortville, France) at 40 °C at a flow rate of 1 ml/min using tetrahydrofuran as a solvent. Polystyrene standards from Polymer Standard Service were used for calibration. The samples were filtered with 0.22 µm polytetrafluoroethylene (PTFE) filters before analysis. The GPC analysis was conducted as an average of parallel samples, as the remaining average mass of the studied scaffolds was too low for individual parallel measurements.

6.2.9 Compression testing (IV)

Compression tests for dry and wet natural polymer-based scaffolds (Publication IV) were done with Loyd LR30K mechanical tester (Loyd Instruments Ltd, Hampshire, UK). To test wet scaffolds, the scaffolds were immersed in PBS for 24 h at 37 °C. Scaffolds were compressed at a rate of 0.5 mm/min and a cell load of 1 kN. The corresponding compressive modulus was determined from the linear elastic region (from 7 to 9% strain), and the compressive stiffness values were determined (n=6).

6.2.10 Cell studies (II, IV)

The viability, distribution, proliferation, and osteogenic differentiation of adipose stem cells (ASCs) were studied with synthetic polymer-based scaffolds (Publication II). The study was conducted in collaboration with Regea Institute for Regenerative Medicine (currently Regea Cell and Tissue Center, University of Tampere / BioMediTech, Tampere, Finland) in accordance with the Ethics Committee of the Pirkanmaa Hospital District, Tampere, Finland. The ASCs were isolated from adipose tissue samples taken from six donors (mean age = 44 ± 7 years) and the tissue samples were received from the Department of Gastroenterology and Alimentary Tract Surgery, Tampere University Hospital. The adipose tissue was digested with collagenase type I (1.5 mg/ml; Invitrogen, Paisley, UK), and the ASCs were expanded in T-75 polystyrene flasks. After the primary culture in T-75 flasks, the ASCs were harvested and analyzed by a fluorescence-activated cell sorter (FACSAria; BD Biosciences, Erembodegem, Belgium). Three to four patient samples were pooled together for each experiment to yield enough cells. The scaffolds were pretreated with maintenance medium for 48 h at 37 °C. The bottom surface of the scaffolds was seeded with 350 000 cells in a 0.175 ml drop, and the cells were allowed to attach to the scaffolds for 3 h at 37 °C in 5% carbon dioxide before additional medium was added. Cell seeding for up to two weeks was performed. Cell attachment and viability were studied by Live/Dead staining. Cell morphology was evaluated with ESEM, and cell proliferation and quantitative analysis of alkaline phosphatase (ALP) activity was measured. Statistical analysis was performed with SPSS, version 13. The experiments were repeated three times.

The viability and attachment of adult bovine chondrocytes were studied with the natural polymer-based scaffolds (Publication IV). These cell studies were conducted in collaboration with the Department of Orthopaedics and Traumatology, University of Helsinki and Helsinki University Central Hospital, Helsinki, Finland. One million adult bovine primary chondrocytes isolated from the femoral condyle of the knee of 5–6 month-old male cows (*Bos Taurus*) were seeded into the 0.5 cm^2 scaffold by pipetting. First, 50 µl of cell culture medium containing 500 000 cells were pipetted on top of the scaffold. After 5 min of incubation at RT, the scaffolds were turned around and another 50 µl of cell culture medium containing 500 000 cells were pipetted on the other side of the scaffold. The scaffolds were cultured in the common proliferation medium DMEM/F12 (21331-020 Gibco, Invitrogen, USA) at 37 °C in 5% CO_2 for up to one week. The chondrocytes were fixed and

imaged at the Light Microscope Unit, Institute of Biotechnology, Helsinki with a Leica TCS SP5II HCS A confocal microscope using 10x or 20x air objectives. For the imaging of the cross-section, the scaffolds were cut in half with a scalpel and the cross-section was imaged at an approximate depth of 150 µm.

6.2.11 Statistical analysis (II, V)

Majority of the data are presented as mean ± standard deviation. In Publication II, the effects on the DNA content and ALP activity between the TCP and BG composite material were compared using a one-way ANOVA, after checking for normal distribution and homogeneity of variance. *Post hoc* tests were performed to detect significant differences between groups. The significance level of $p < 0.05$ was considered significant. In Publication V the contact angle data was analysed with the Mann-Whitney test. The significance level of $p \leq 0.05$ was used.

Table 9 lists all the characterization methods for different freeze-dried natural and synthetic polymer-based scaffolds as well as the related publications.

Table 9. Characterization methods applied for different freeze-dried natural and synthetic polymer-based scaffolds.

Scaffold	Characterization method									Publication
	SEM/ ESEM/ µCT	CA	*In vitro*	Weight change	DSC/ TGA	i.v.	GPC	Compression testing	Cell studies	
Natural polymer-based scaffolds										
Col0.3NoE	SEM	-	-	Yes	DSC	-	-	-	-	I
Col0.3(E)	SEM	-	-	Yes	DSC	-	-	-	-	I
Col0.3E	SEM	-	-	Yes	DSC	-	-	-	-	I
Col0.5NoE	SEM	-	-	Yes	DSC	-	-	-	-	I
Col0.5(E)	SEM	-	-	Yes	DSC	-	-	-	-	I
Col0.5E	SEM	-	-	Yes	DSC	-	-	-	-	I
Col1.0NoE	SEM/µCT	-	-	Yes	DSC	-	-	Yes	Yes	I
Col1.0(E)	SEM	-	-	Yes	DSC	-	-	-	-	I
Col1.0E	SEM	-	-	Yes	DSC	-	-	-	-	I
Col	SEM/µCT	-	-	Yes	-	-	-	Yes	Yes	IV
Col2.0NoE	SEM	-	-	Yes	DSC	-	-	-	-	I
Col2.0(E)	SEM	-	-	Yes	DSC	-	-	-	-	I
Col2.0E	SEM/µCT	-	-	Yes	DSC	-	-	-	-	I
Chi	SEM/µCT	-	-	Yes	-	-	-	Yes	Yes	IV
C1C1	SEM/µCT	-	-	Yes	-	-	-	Yes	Yes	IV
C2C1	SEM/µCT	-	-	Yes	-	-	-	Yes	Yes	IV
ColPLA	SEM/µCT	-	-	Yes	-	-	-	Yes	Yes	IV
ChiPLA	SEM/µCT	-	-	Yes	-	-	-	Yes	Yes	IV
C1C1PLA	SEM/µCT	-	-	Yes	-	-	-	Yes	Yes	IV
C2C1PLA	SEM/µCT	-	-	Yes	-	-	-	Yes	Yes	IV
Synthetic polymer-based scaffolds										
PLA2	ESEM	-	Yes	Yes	TGA	Yes	-	-	Yes	II, III
PLA3	ESEM	-	Yes	Yes	TGA	Yes	-	-	-	III
PLA2TCP5	ESEM	-	Yes	Yes	TGA	Yes	-	-	-	III
PLA2TCP10	ESEM	-	Yes	Yes	TGA	Yes	-	-	Yes	II, III
PLA2TCP20	ESEM	-	Yes	Yes	TGA	Yes	-	-	Yes	II, III
PLA3TCP5	ESEM	-	Yes	Yes	TGA	Yes	-	-	-	III
PLA3TCP10	ESEM	-	Yes	Yes	TGA	Yes	-	-	-	III
PLA3TCP20	ESEM	-	Yes	Yes	TGA	Yes	-	-	-	III
PLA2BG10	ESEM	-	-	-	-	-	-	-	Yes	II
PLA2BG20	ESEM	-	-	-	-	-	-	-	Yes	II
PLGA1	SEM/µCT	Yes	Yes	Yes	DSC/TGA	-	GPC	-	-	V
PLGA2	SEM/µCT	Yes	Yes	Yes	DSC/TGA	-	GPC	-	-	V
PLGA1BG1	SEM/µCT	Yes	Yes	Yes	DSC/TGA	-	GPC	-	-	V
PLGA2BG2	SEM/µCT	Yes	Yes	Yes	DSC/TGA	-	GPC	-	-	V

7 Results

The study was divided into natural polymer-based freeze-dried scaffolds aimed for cartilage tissue engineering and synthetic polymer based freeze-dried scaffolds aimed for bone or osteochondral tissue engineering. The different scaffold types studied are shown in Table 10. The more specific material compositions and characteristic of the scaffolds are shown in Appendix I and the schematic diagrams of the fabrication processes of the different scaffolds are shown in Appendix II.

Table 10. The different scaffold types and their compositions.

Scaffold type	Scaffold composition	Publication
Natural polymer-based scaffolds		
Collagen	Freeze-dried collagen scaffold	I, IV
Chitosan	Freeze-dried chitosan scaffold	IV
Collagen+Chitosan	Freeze-dried collagen+chitosan blend scaffold	IV
Collagen+PLA96	Freeze-dried collagen scaffold with PLA96 mesh	IV
Chitosan+PLA96	Freeze-dried chitosan scaffold with PLA96 mesh	IV
Collagen+Chitosan+PLA96	Freeze-dried collagen+chitosan blend scaffold with PLA96 mesh	IV
Synthetic polymer-based scaffolds		
PLA70	Freeze-dried PLA70 scaffold	II, III
PLA70+TCP	Freeze-dried PLA70 scaffold with TCP particles	II, III
PLA70+BG	Freeze-dried PLA70 scaffold with BG particles	II
PLGA	Freeze-dried PLGA scaffold	V
PLGA+BGf	Freeze-dried PLGA scaffold with BG mesh	V

7.1 Characterization of freeze-dried natural polymer-based scaffolds

7.1.1 Cross-linking of natural polymer-based scaffolds containing collagen

The effect of cross-linking time on freeze-dried collagen scaffolds was studied in Publication I. The difference in cross-linking time, cross-linking used prior or post freeze-drying, was found to have an effect on the cross-linking ability of collagen scaffolds. The denaturation temperature (T_d) indicating the cross-linking degree of collagen can be determined with DSC (Duan & Sheardown 2005; Friess & Lee 1996). The T_d of the studied collagen scaffolds varied mainly because of the collagen concentration, as the scaffolds with lower collagen concentration (0.3 and 0.5 wt%) showed higher T_d values when cross-linked post freeze-drying (Figure 5A). The water uptake abilities of the scaffolds cross-linked post freeze-drying (with 1 or 10 mM EDC) were much higher (Figure 5B) indicating improved wettability abilities of the scaffolds cross-linked post freeze-drying. Reference scaffolds for 2.0 wt% collagen scaffolds with no cross-linking were not manufactured as it was

shown in preliminary tests that scaffolds with high collagen concentration do need cross-linking to hold their structure and to be suitable for tissue engineering applications.

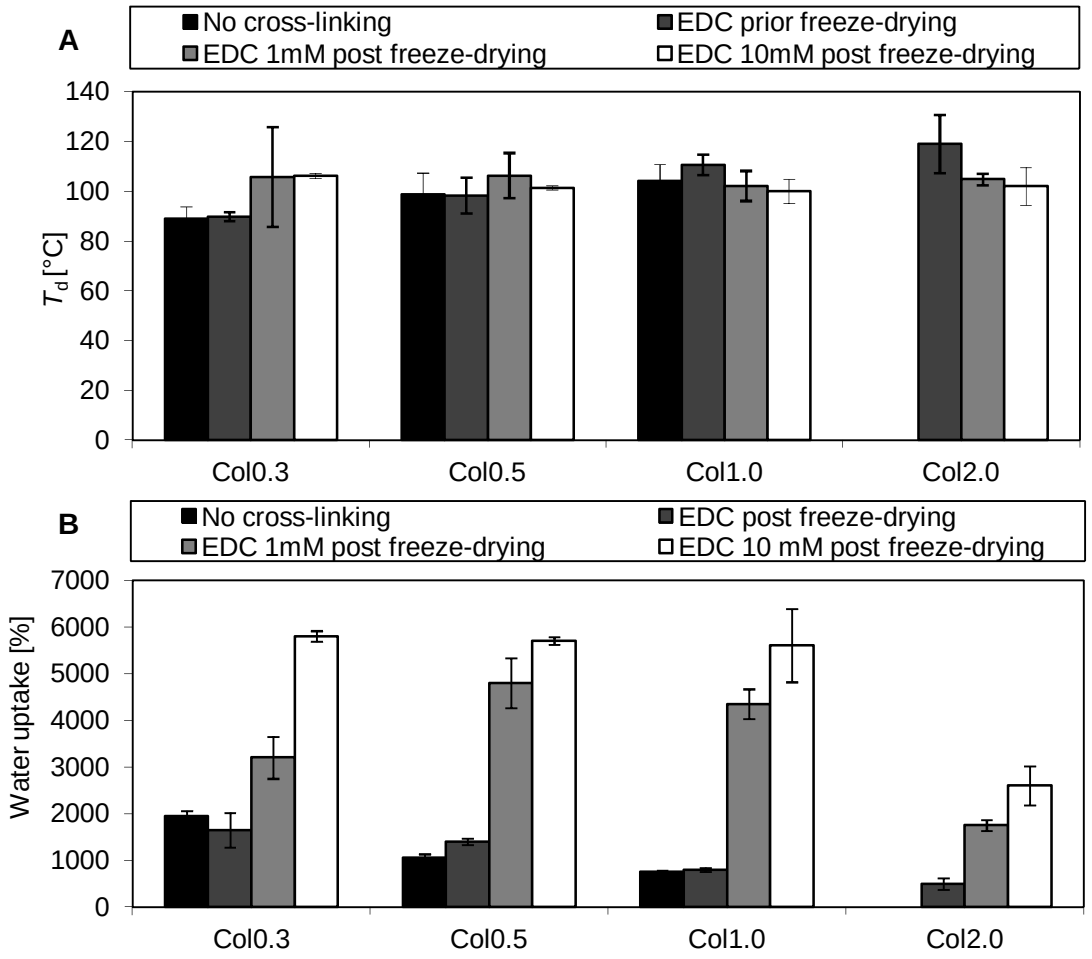

Figure 5. A) Denaturation temperatures (T_d) and B) water uptake of the collagen scaffolds indicating the degree of cross-linking and wettability abilities of the scaffolds using different cross-linking methods.

The lower wettability characteristics of collagen scaffolds cross-linked prior to freeze-drying was most likely due to the shrinking of the scaffolds and the losing of their initial shape (visual characterization of the scaffolds, data not shown). This also indicates that the cross-linking with EDC prior to freeze-drying is not an effective way to cross-link these collagen scaffolds even though the T_d values of those scaffolds are relatively at the same level than the corresponding values of scaffolds cross-linked post freeze-drying.

The average pore sizes of the collagen scaffolds cross-linked with EDC prior to freeze-drying was 96–115 µm with all collagen concentrations. The cross-linking with EDC post freeze-drying lowered the pore sizes of most of the collagen scaffolds (Table 11), which was due to shrinking of the scaffolds during the cross-linking procedure. When cross-linking collagen scaffolds with EDC post freeze-drying, a noticeable difference was noticed between scaffolds with a lower collagen concentration (0.3–0.5 wt%) with a lower amount of EDC (EDC 1 mM). The shrinkage of the pores was

over 20% compared with the pore sizes of scaffolds cross-linked with EDC prior to freeze-drying. For the scaffolds with the lowest collagen concentration (0.3 wt%), the shrinking of the scaffolds was also high when cross-linking with a higher amount of EDC (EDC 10 mM). With a higher collagen concentration (1.0 and 2.0 wt%), the pore sizes varied maximally only 7% compared with the scaffolds cross-linked prior to freeze-drying. Therefore, no major difference was observed between the different cross-linking methods of those scaffolds.

Table 11. The effect of the cross-linking method on the pore size (mean ± SD) of the scaffolds using different concentrations of collagen. The high shrinkage of pore sizes compared with the initial pore structure (scaffolds cross-linked with EDC prior to freeze-drying) is marked in *red*.

Scaffold	***Cross-linking method / pore size***		
	EDC prior freeze-drying/ [µm]	**EDC 1 mM post freeze-drying/ [µm]**	**EDC 10 mM post freeze-drying/ [µm]**
Col0.3	115 ± 42	48 ± 12	80 ± 35
Col0.5	96 ± 28	76 ± 22	86 ± 10
Col1.0	106 ± 34	98 ± 21	99 ± 36
Col2.0	103 ± 24	105 ± 37	98 ± 28

7.1.2 Structure of the natural polymer-based scaffolds

The natural polymer-based scaffolds were studied in Publications I and IV. The structure of the scaffolds in Publication I was plain freeze-dried collagen. The structure of the scaffolds in Publication IV was a hybrid with freeze-dried collagen/chitosan (collagen, chitosan or collgan+chitosan blend) polymer matrix combined with PLA96 fibrous mesh. Also, plain collagen, chitosan and collagen+chitosan scaffolds were used as reference in the Publication IV. The structure of the hybrids in Publication IV was so-called sandwich structure with PLA96 fibrous mesh at the bottom and at the top of the scaffold. The microstructure of all freeze-dried natural polymer-based scaffolds (Publications I and IV) was highly similar. The overall structure of the freeze-dried component in the natural-based scaffolds was highly porous (Figure 6).

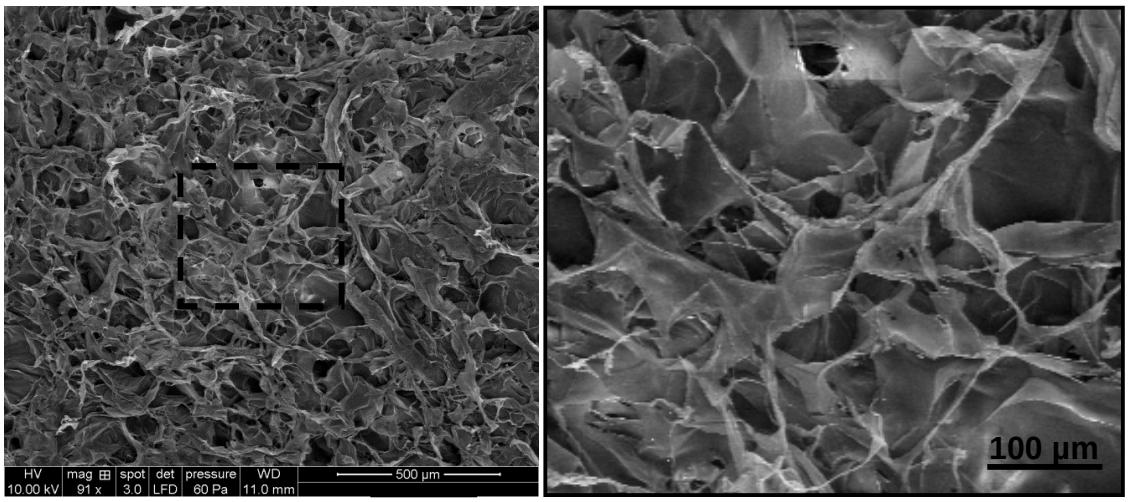

Figure 6. SEM image of the porous structure of the freeze-dried collagen scaffold (Col) on the left, and on the right the magnification of the area pointed out from the original image on the left (Scale bars 500 µm and 100 µm, respectively).

For all freeze-dried scaffolds (Publications I-V), the skin formation on top of the scaffolds could be noticed as a result of the freeze-drying process (Figure 7).

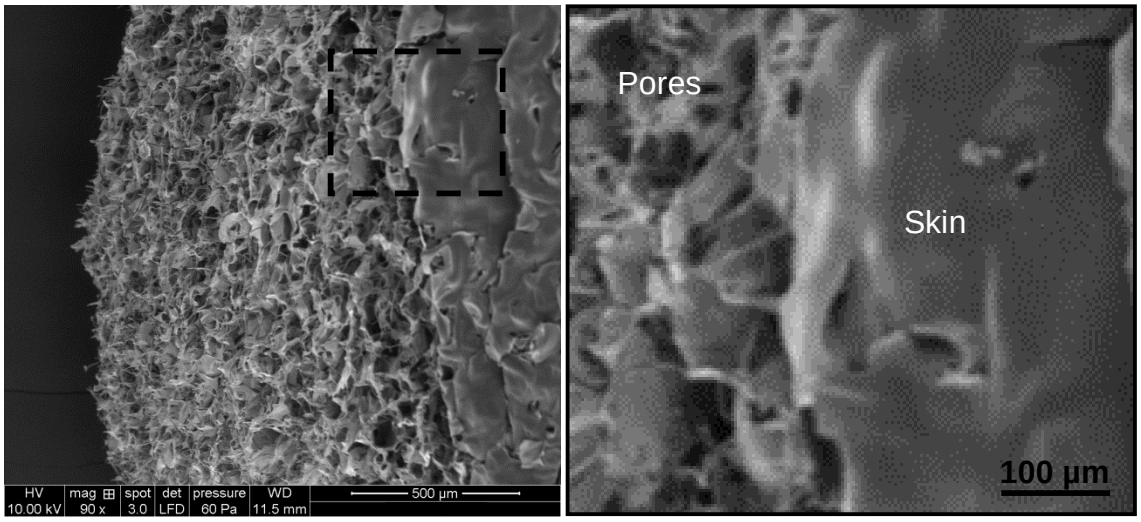

Figure 7. SEM image from the side of the freeze-dried chitosan scaffold (Chi) on the left, indicating the overall porous structure of the scaffold and the skin on top of the scaffold. On the right, magnification of the area pointed out from the original image on the left (Scale bars 500 µm and 100 µm, respectively).

The 3D reconstructions of microCT images (Figure 8) show the highly porous structure of different natural polymer-based scaffolds. The PLA carded mesh was well attached to the matrix polymer, collagen, chitosan or collagen+chitosan blend and the matrix polymer filled the PLA carded mesh thoroughly.

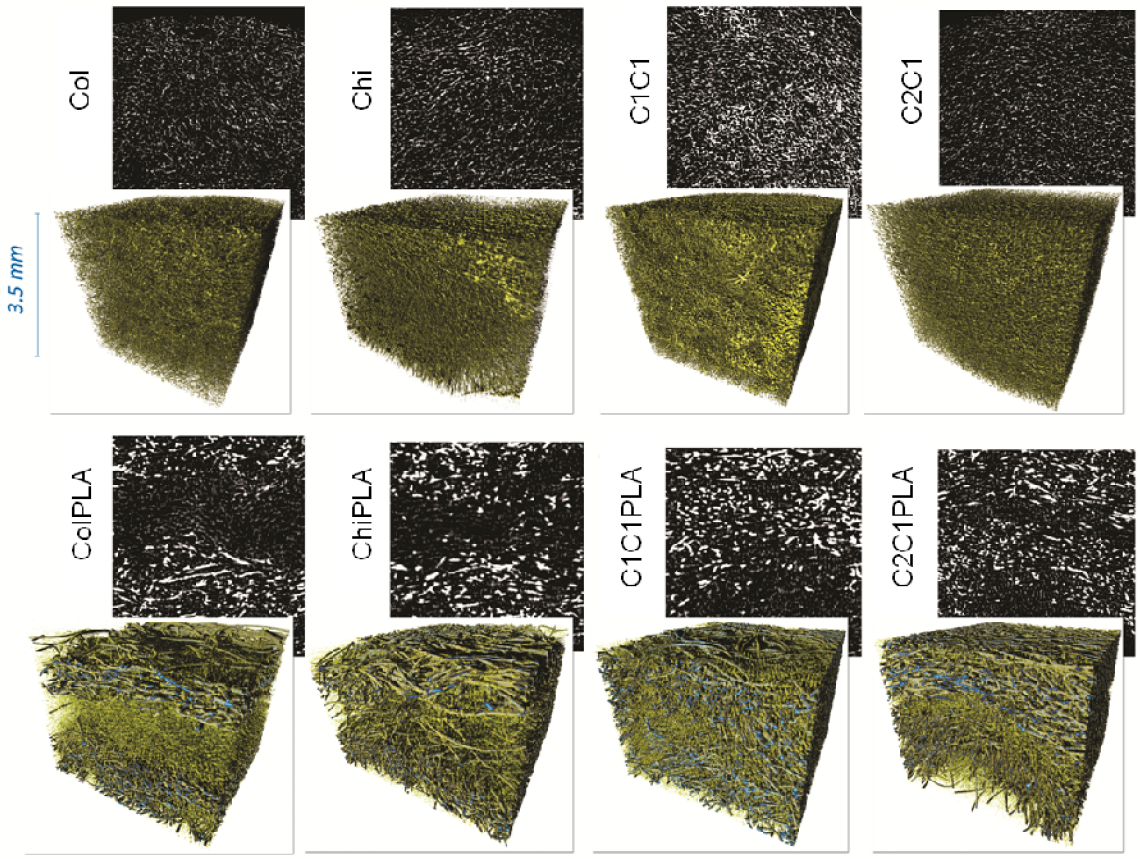

Figure 8. Cross-sectional views and 3D reconstructions of microCT images of different natural polymer-based scaffolds. Natural polymer component in *green* and PLA in *blue*.

The porosity in different freeze-dried natural polymer-based scaffolds was over 85% for all scaffolds (Publication IV), except for the collagen+chitosan (C1C1) scaffolds for which the porosity was only 66% (Table 12). The lower porosity for C1C1 scaffolds was, however, due to the shrinkage of the scaffolds during processing, as the neutralization procedure was found to be inadequate (Publication IV). The pore structure was highly interconnected as there were no difference between the total porosity and the open porosity values.

Table 12. Porosity values of different freeze-dried natural based polymer scaffolds (microCT data).

Scaffold	**Col**	**Chi**	**C1C1**	**C2C1**	**ColPLA**	**ChiPLA**	**C1C1PLA**	**C2C1PLA**
Total porosity [%]	86	89	66	87	93	88	85	88
Open porosity [%]	86	89	66	87	93	88	85	88

7.1.3 Wettability of the natural polymer-based scaffolds

The wettability of the freeze-dried natural polymer-based scaffolds was relatively high (Figure 9). The water uptake was the highest for plain collagen scaffolds and, therefore, the higher amount of collagen in the collagen+chitosan blends as well as in the hybrids increased the water uptake of the scaffolds. The water uptake was much higher for the whole scaffold (scaffold and pore system)

when the water was also inside the pores of the scaffolds than for the scaffolds with no excess water inside the pores (scaffold only). Chitosan in the scaffolds lowered the water uptake ability of the scaffolds to a great extent, which was due to the shrinking of the scaffold in wet conditions.

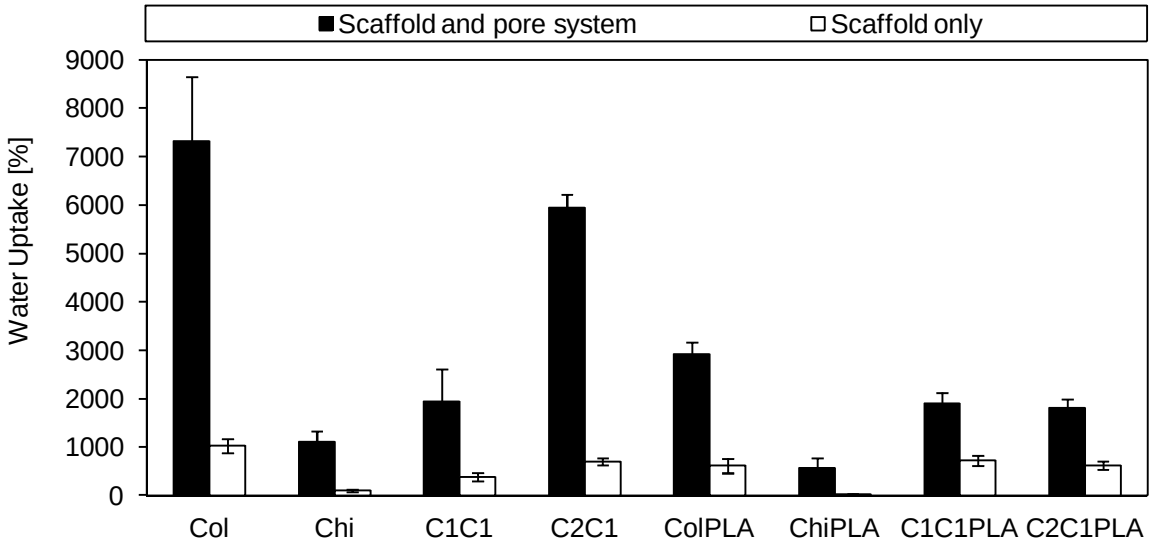

Figure 9. Water uptake of the different freeze-dried natural polymer-based scaffolds for the scaffold and pore system (whole scaffold, also the water inside the pores) and for scaffold only (no excess water inside the pore system).

7.1.4 Compression properties of the natural polymer-based scaffolds

The compressive modulus and compressive stiffness values, of the different freeze-dried natural based scaffolds are shown in Figure 10. Over 50% higher compressive stiffness values were detected for dry hybrid scaffolds compared with the corresponding plain scaffolds. In wet conditions, the compressive stiffness was over 70% higher for hybrid scaffolds compared with the corresponding plain scaffolds, with the exception of the C1C1 scaffolds that had much higher compressive stiffness than the other plain scaffolds. The compressive modulus of dry hybrid scaffolds was much lower than the corresponding plain scaffolds, though the difference between wet hybrid and plain scaffolds was more moderate. The collagen component in the scaffolds showed good recovery to their original shape after immersing the scaffold in PBS for 1 h after compression testing. Therefore, the plain collagen scaffolds (Col) and the ColPLA scaffolds had the best ability of all the scaffolds to recover to their original shape.

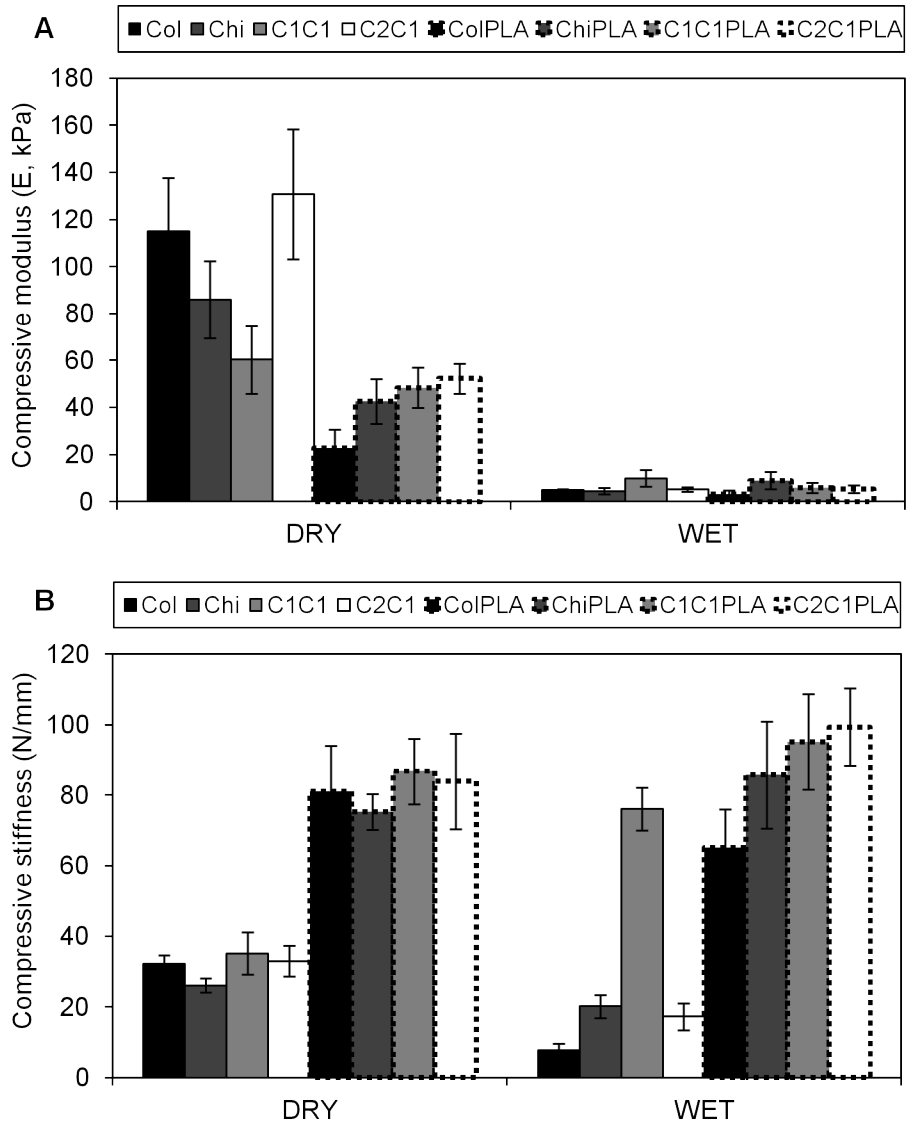

Figure 10. Compressive modulus and compressive stiffness (mean ± SD) of different freeze-dried natural polymer-based scaffolds in dry and wet conditions.

As described by Harley et al. (Harley et al. 2007), elastomeric foam compression curves were noticed for all of the freeze-dried natural polymer-based scaffolds. The initial elastic region, a middle collapse plateau region, and final densification of the material could be distinguished from the graphs (Figure 11). The compressive stress–strain curves of dry scaffolds rose steadily after the linear elastic region until the point of 75% strain that occurred after the densification. The compressive stress values stayed at a relatively low level with the wet scaffolds until 60 to 70% of strain. The hybrids showed the highest compressive stress values when wet after the point of 70% of strain, except for the C1C1 scaffolds which had much higher compressive stress values than the other plain scaffolds in wet conditions.

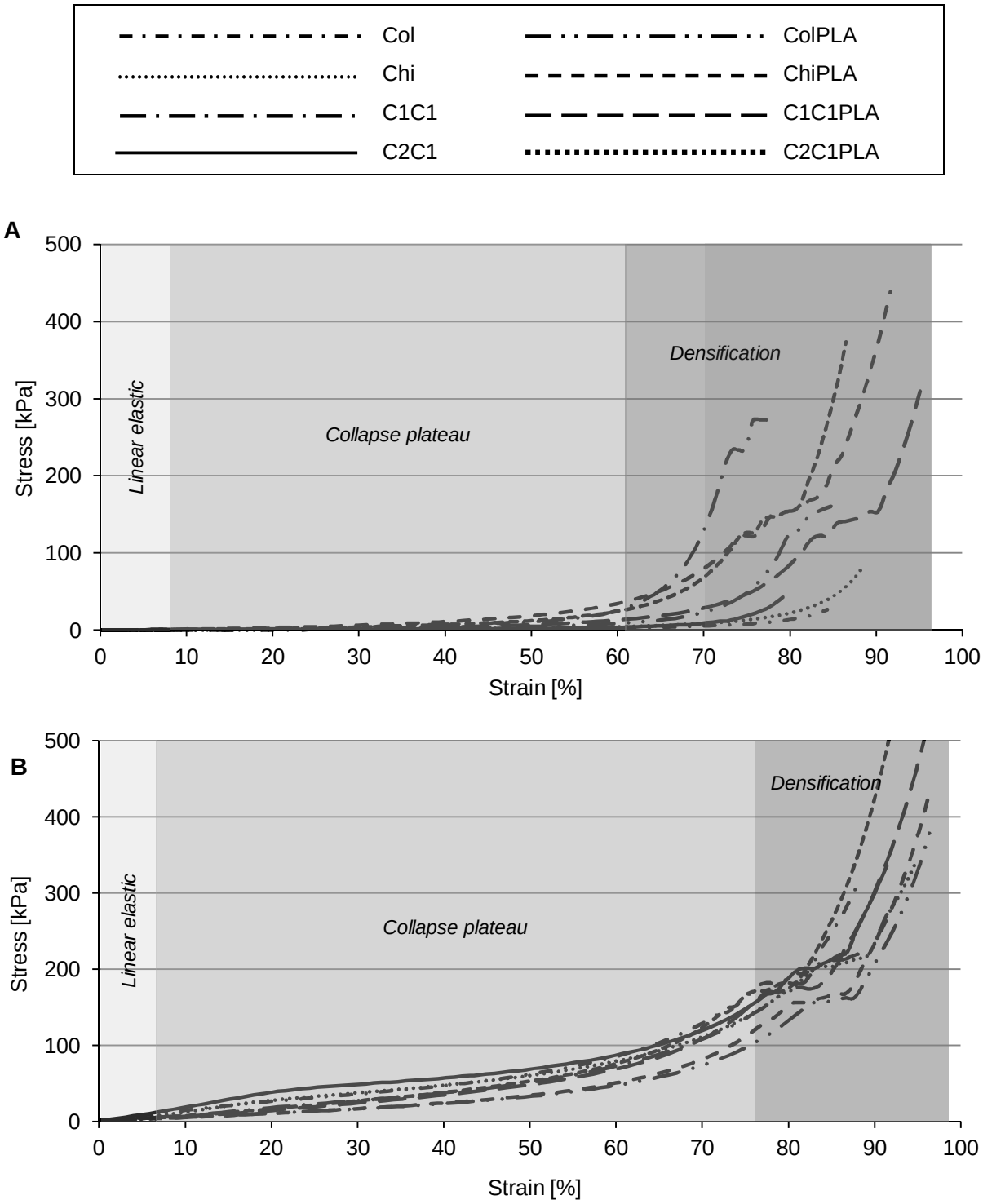

Figure 11. Compressive stress–strain curves for A) dry and B) wet freeze-dried natural polymer-based scaffolds indicating linear elastic, collapse plateau, and densification regimes.

7.2 Characterization of freeze-dried synthetic polymer-based scaffolds

7.2.1 Structure of the synthetic polymer-based scaffolds

The synthetic polymer-based scaffolds were studied in Publications II, III and V. The structure of the scaffolds in Publications II and III was heterogeneous, with TCP or BG particles at the bottom of the freeze-dried scaffold. The structure of the scaffolds in Publication V was homogenous with BG fibrous mesh inside the polymer matrix. As noticed with freeze-dried natural polymer-based scaffolds (Figure 7), the synthetic polymer-based scaffolds also suffered from skin formation on top of the top surface of the scaffold as a result of the freeze-drying process (Figure 12).

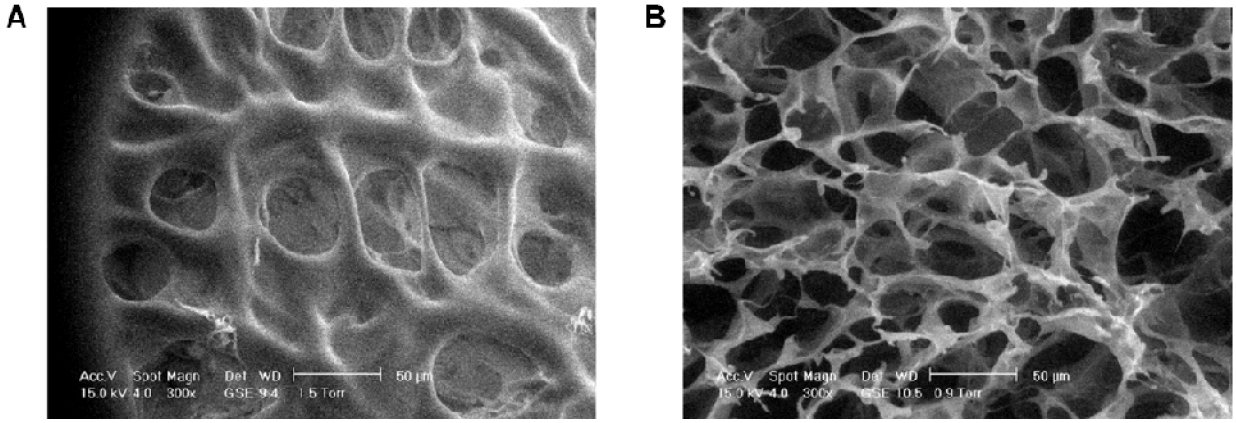

Figure 12. ESEM images of the A) dense top surface (with skin formation), and B) porous bottom surface of freeze-dried PLA70 (PLA2) scaffold (Scale bars 50 µm).

Scaffolds with PLA70/30 as matrix polymer

Figure 13 shows the representative ESEM image of the overall cross-sectional view of the PLA70 scaffolds with TCP particles. The structure of the PLA70 scaffolds containing BG particles was highly similar as well. As can be seen from the image of the overall structure of the freeze-dried PLA3TCP10 scaffold, the skin surface formed during the freeze-drying process is very thin showing almost no clear denser surface in the top of the scaffold (on the right in the image) (Figure 13). Figure 13 also shows the layered structure of the PLA70 scaffolds containing either TCP or BG where the filler particles are laid down at the bottom of the scaffold and the rest of the structure is a porous PLA70 matrix.

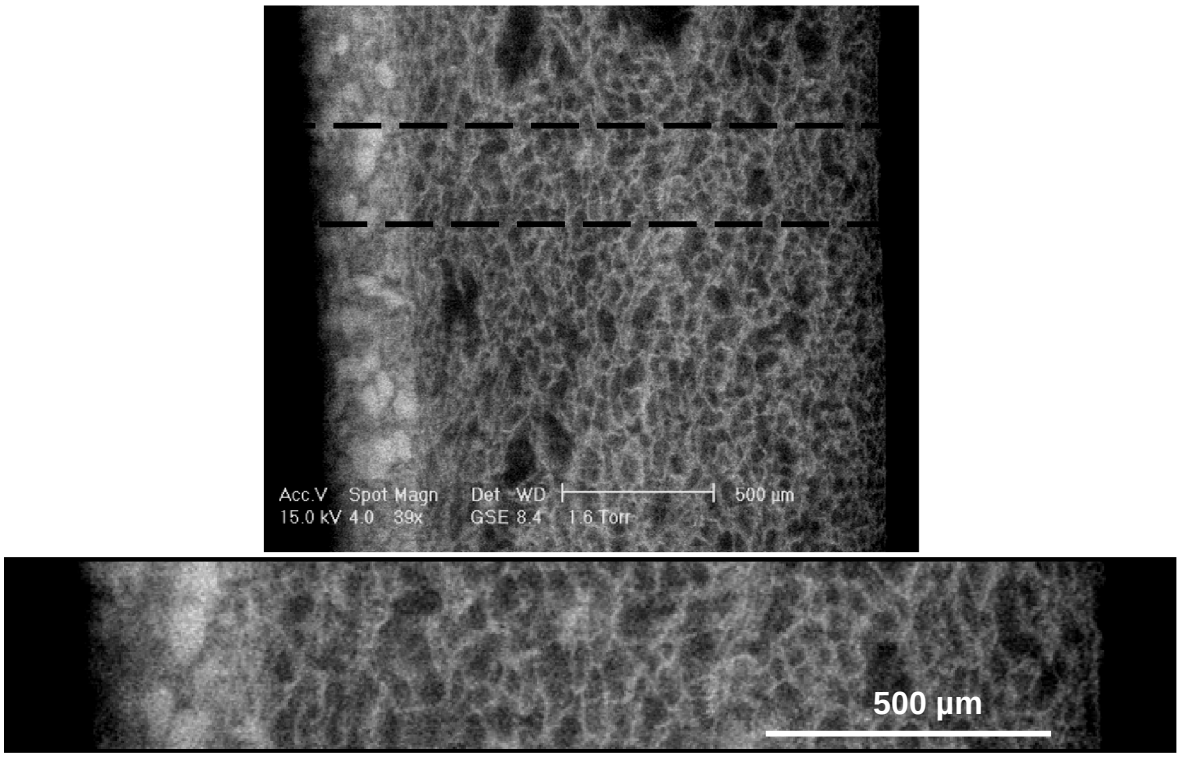

Figure 13. ESEM image of the cross-section of a freeze-dried PLA70 (PLA3TCP10) scaffold showing the overall structure of the scaffold (top image). Magnification of the area pointed out from the original image on top (lower image). On the right hand side, the top surface of the scaffold and the bottom surface with most of the TCP particles on the left hand side (Scale bars 500 µm).

The filler particles in the PLA scaffolds had good connectivity to the surrounding matrix polymer as seen in Figure 14A and B.

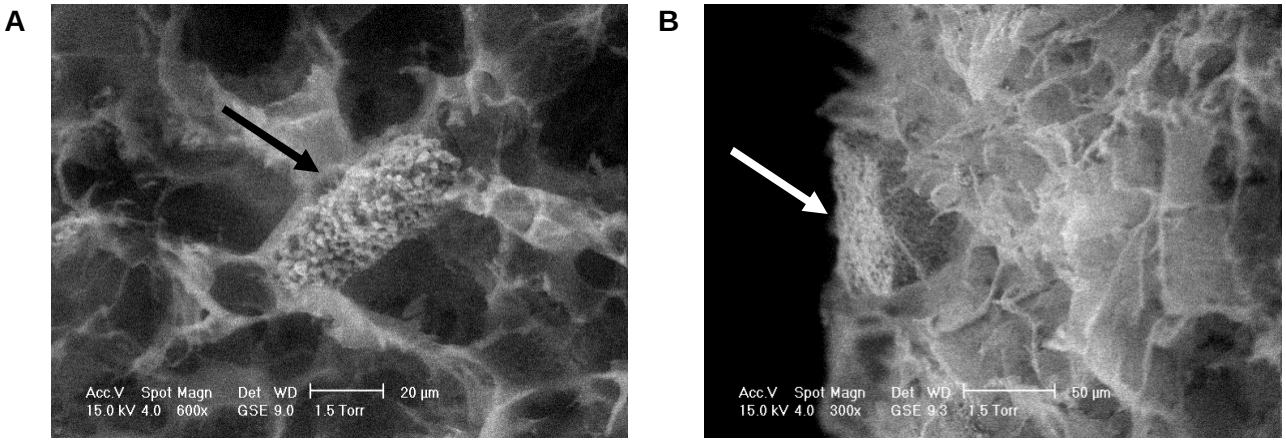

Figure 14. ESEM images of a freeze-dried PLA70+TCP (PLA2TCP5) scaffold A) from the bottom of the scaffold, and B) from the side of the scaffold, showing the good interconnection of the TCP particle in the PLA matrix (Scale bars 20 and 50 µm, respectively). The arrows indicate the TCP particle in the images.

The highly porous structure of the TCP particles is represented in Figure 15. The porous surface of the porous TCP particles was retained during the processing and could be seen even after 2 weeks in hydrolysis.

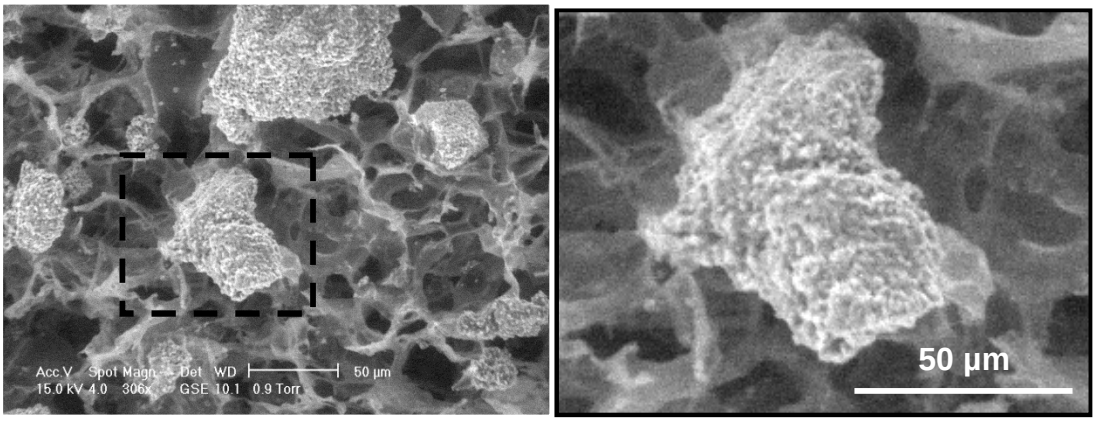

Figure 15. On the left, ESEM image of a freeze-dried PLA70+TCP (PLA2TCP20) scaffold after 2 weeks in hydrolysis, showing the highly porous structure of the TCP particle. On the right, magnification of the area pointed out from the original image on the left (Scale bars 50 µm).

The processing of freeze-dried scaffolds with relatively large filler particles was challenging. Therefore, the content of used filler particles (marked as desired TCP content in Table 13) in the processing did not always lead to the same content of filler particles (marked as measured TCP content in Table 13) in the manufactured scaffolds (Table 13A and B). Table 13 indicates that with higher contents of particles (over 5 wt% of particles) the measured particle content was between 5 wt% and 10 wt% smaller compared with the desired contents of 15 wt% and 30 wt%, respectively. Therefore, with a higher content of filler particles in the solution, it is more difficult to achieve the desired content of filler particles for the scaffolds. This same phenomenon was noticed for PLA70 scaffolds with BG as filler particles (data not shown).

Table 13. The content of different components (matrix: PLA70 and filler: TCP) in A) 2wt% PLA70+TCP and B) 3wt% PLA70+TCP scaffolds.

(A) **Scaffold**	**2 wt% PLA (wt%)**	**TCP content: desired/measured[a] (wt%)**	**(B)** **Scaffold**	**3 wt% PLA (wt%)**	**TCP content: desired/measured[a] (wt%)**
PLA2	100	0/0	*PLA3*	100	0/0
PLA2TCP5	95	5/5	*PLA3TCP5*	95	5/5
PLA2TCP10	85	15/10	*PLA3TCP10*	85	15/10
PLA2TCP20	70	30/20	*PLA3TCP20*	70	30/20

[a] by thermogravimetric analysis (TGA)

The pore size distribution of the PLA70+TCP scaffolds was from 20 to 80 µm, and the mean pore size was around 50 µm, measured from the ESEM images (data not shown). As can be seen in Figure 13, a few larger macropores could be detected. The TCP particles in the composites or the PLA70 concentration (2 or 3 wt%) did not affect the pore size of the scaffolds.

Scaffolds with PLGA as matrix polymer

The porous structure of the PLGA and PLGA+BGf scaffolds are shown in SEM images in Figure 16 and in microCT images in Figure 17. The overall structure of the matrix polymer, PLGA, is

highly porous in all of the scaffolds. Good interconnection of fibres, BGf, in the matrix polymer was noticed for both, PLGA1BG1 and PLGA2BG2 composites.

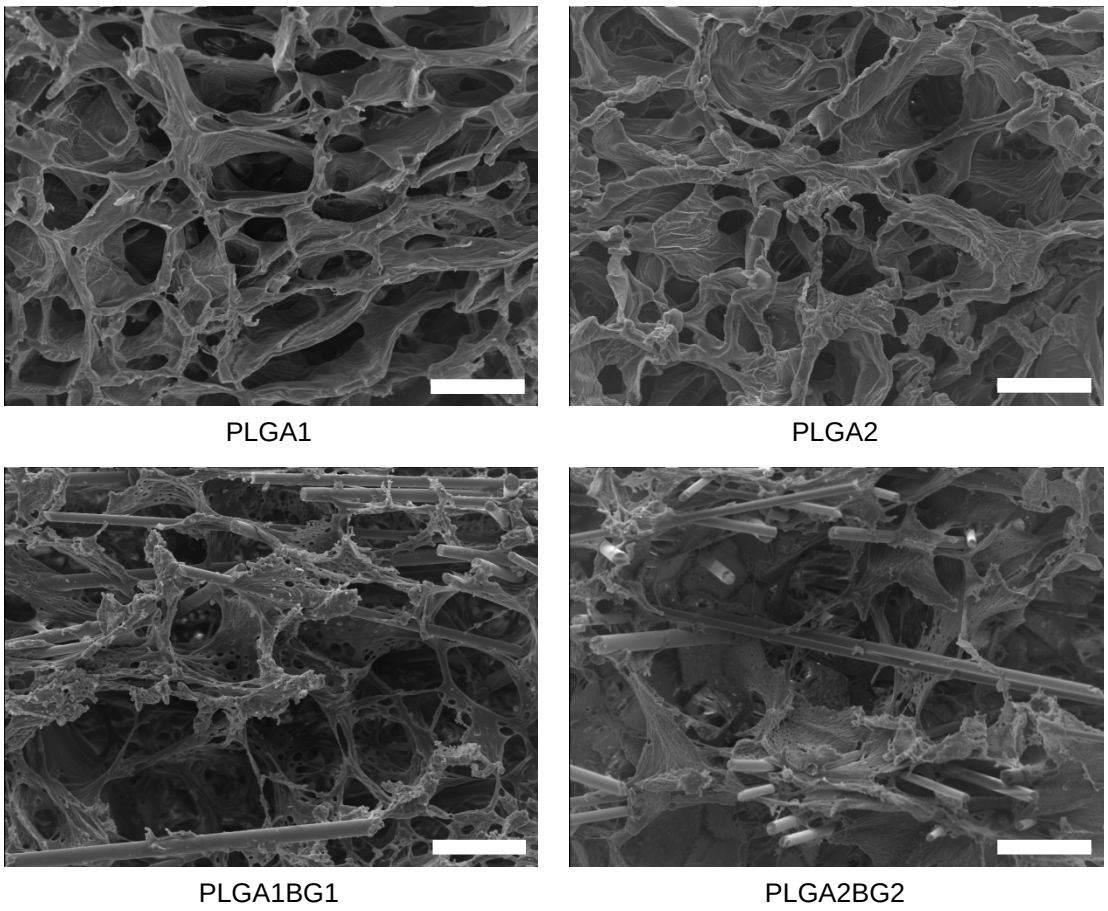

Figure 16. SEM images of the structure of the different PLGA and PLGA+BGf scaffolds (Scale bars 100 μm).

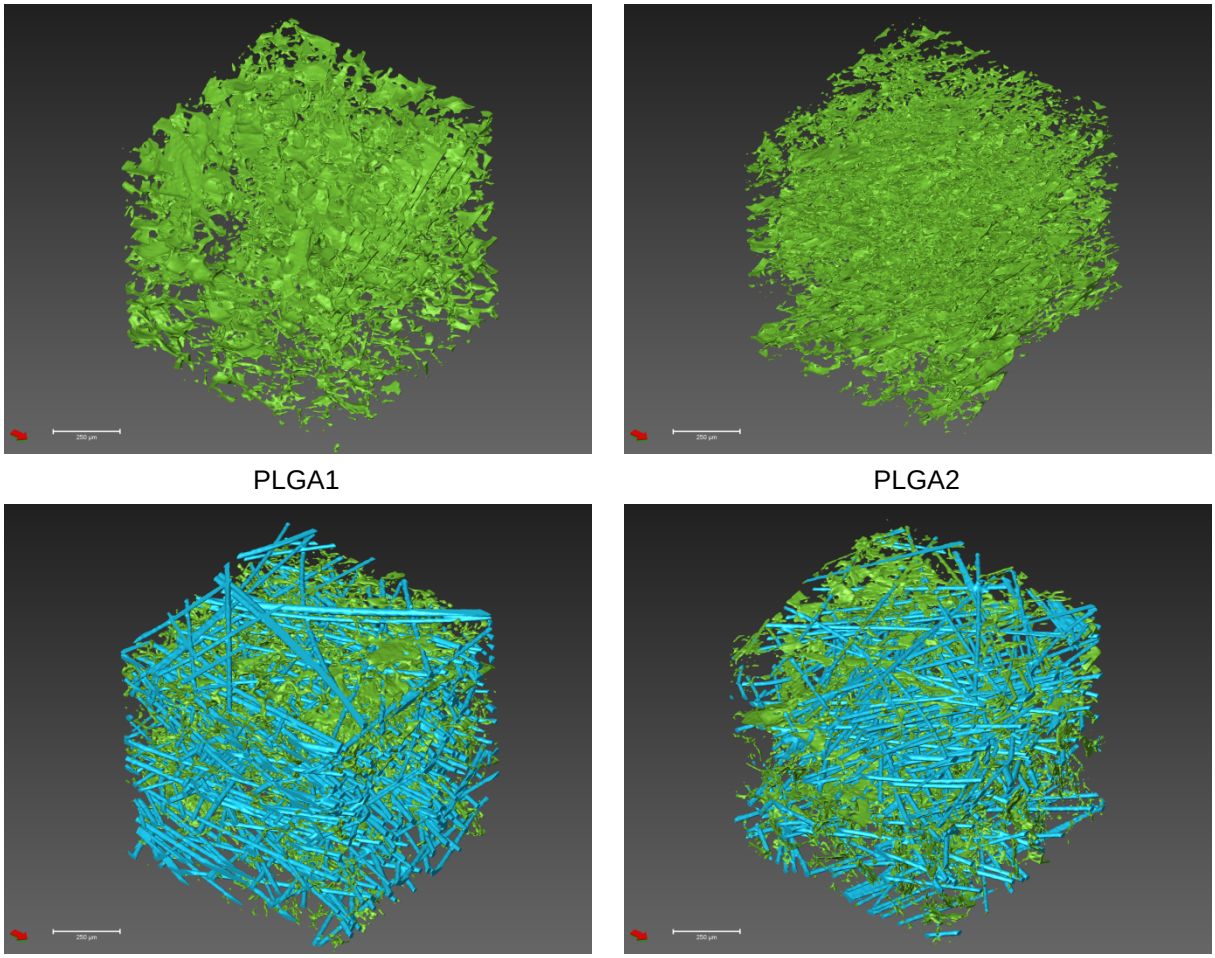

Figure 17. 3D reconstructions of microCT images of different PLGA and PLGA+BGf scaffolds. PLGA in *green* and BGf in *blue* (Scale bars 250 µm).

High porosity values, porosity over 93% for all the PLGA and PLGA+BGf scaffolds were detected by microCT analysis (Table 14). Higher material thickness was noticed in composite, PLGA+BGf, scaffolds when compared with the plain PLGA scaffolds. The mean pore sizes varied in a range from 49 to 77 µm, and the maximum pore sizes from 105 to 251 µm. The highest porosity, mean pore size and maximum pore size, were detected for the PLGA2BG2 scaffold. Furthermore, the PLGA2BG2 scaffold also showed broader pore size distribution (Figure 18) and a higher number of pores over the size of 100 µm compared with the other PLGA or PLGA1BG1 scaffolds.

Table 14. Porosity, material thickness, and pore size of different PLGA and PLGA+BGf scaffolds analysed by microCT.

Scaffold	Porosity [%]	Material thickness [µm]	Material thickness max. [µm]	Pore size [µm]	Pore size max. [µm]
PLGA1	93	9 ± 3	24	69 ± 24	173
PLGA2	93	7 ± 2	18	49 ± 13	105
PLGA1BG1	93	13 ± 5	30	53 ± 18	118
PLGA2BG2	96	8 ± 3	20	77 ± 34	251

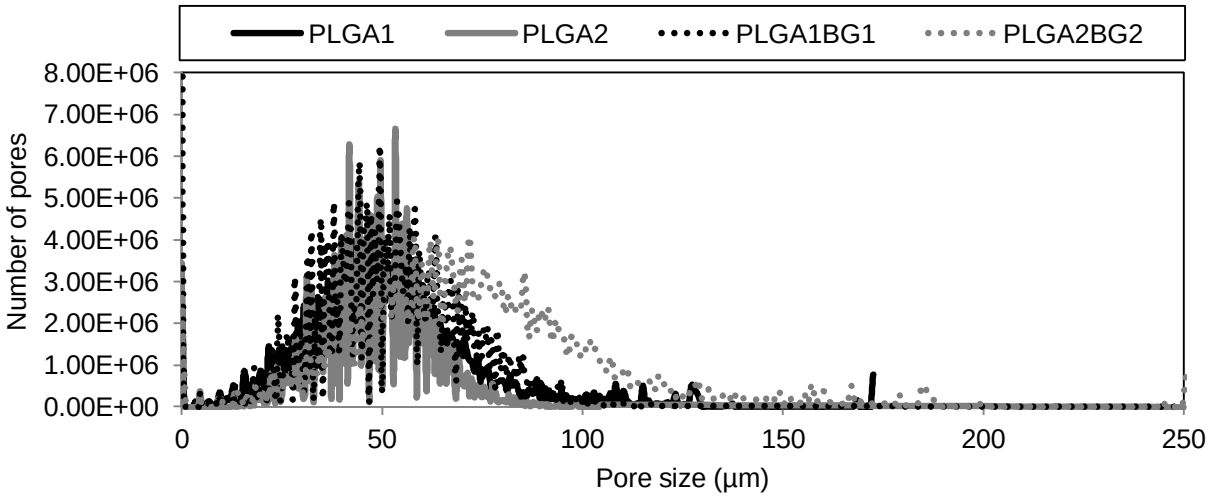

Figure 18. Pore size distribution of different PLGA and PLGA+BGf scaffolds analysed by microCT.

The majority of the scaffolds comprise open pores, as the total porosity and open porosity graphs show (Figure 19). Open pore structure also indicates an interconnected pore structure. The PLGA1 and PLGA2BG2 scaffolds also showed a considerable number of open pores at sizes even exceeding 100 µm.

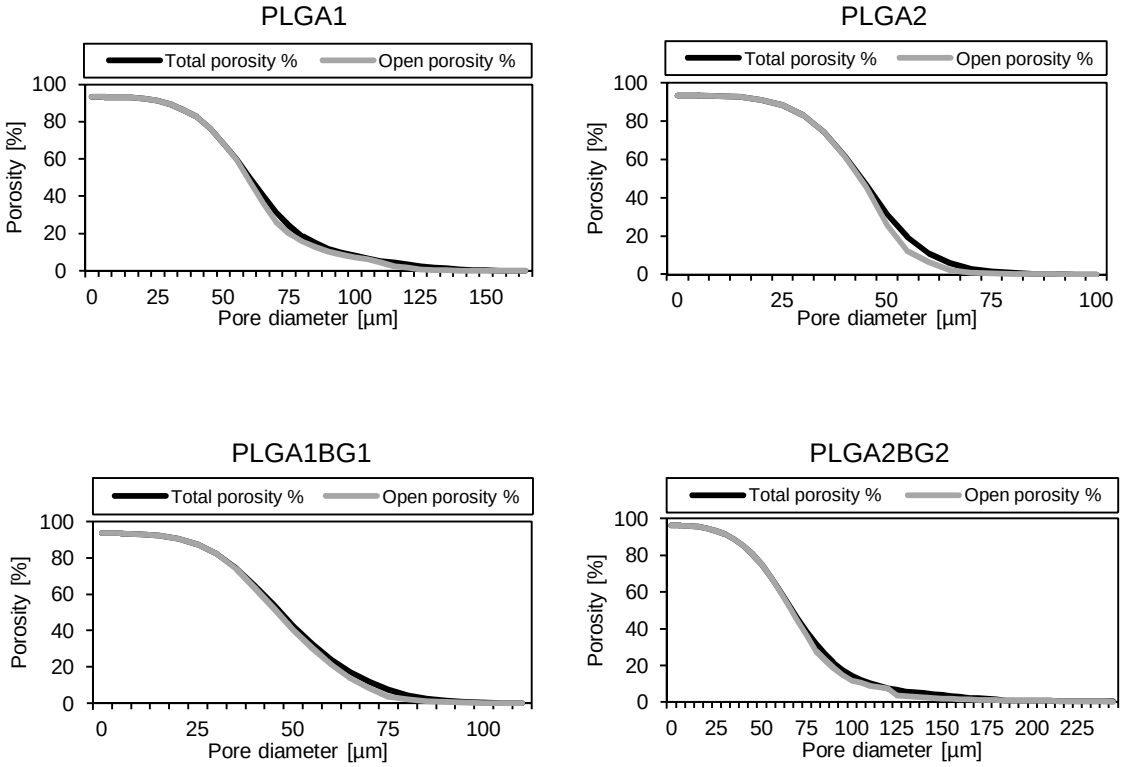

Figure 19. Total porosity and open porosity graphs of different PLGA and PLGA+BGf scaffolds analysed by microCT.

7.2.2 Wettability of the synthetic polymer-based scaffolds

Scaffolds with PLGA as matrix polymer

The contact angle measurements were done for PLGA and PLGA+BGf scaffolds to analyze the hydrophobisity of the scaffolds (Figure 20). The contact angle values of the different scaffolds varied from 92 to 118°, and only some variation was noticed between different scaffold compositions or between different fluids. The PLGA1 scaffolds showed significant difference in water with respect to PLGA1BG1 ($p < 0.05$), PLGA2 ($p = 0.05$) and PLGA2BG2 ($p < 0.05$) scaffolds. PLGA1 showed relatively significant difference with respect to PLGA2BG2 ($p = 0.055$) scaffolds in blood. No significant difference in contact angle values was detected between different scaffolds when measured in PBS.

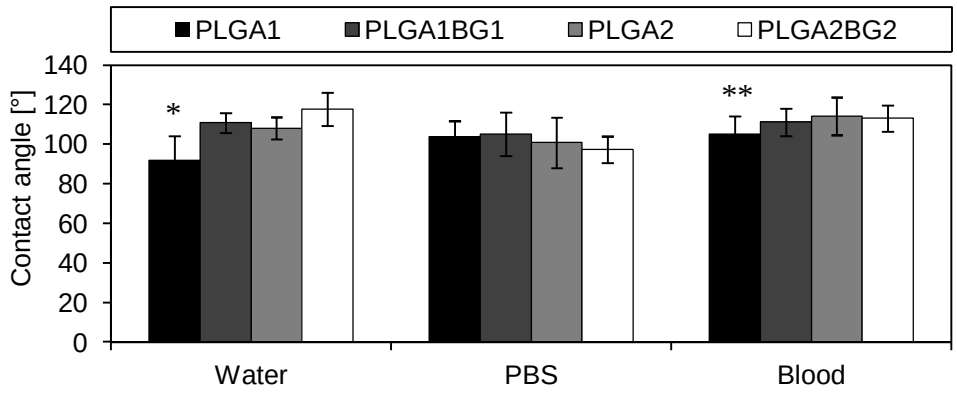

Figure 20. Contact angle results in water, PBS and bovine blood for different dry PLGA+BG scaffolds. *$p \leq 0.05$ with respect to PLGA1BG1, PLGA2 and PLGA2BG2. **$p = 0.055$ with respect to PLGA2BG2.

The wettability of the PLGA and PLGA+BGf scaffolds was measured as water uptake of the scaffolds during 10-week hydrolysis (Figure 21). All the scaffolds had a constant water absorption rate during the hydrolysis until week 8. The PLGA+BGf composites had higher water absorption than the corresponding plain PLGA scaffolds during the first weeks in hydrolysis. After week 4, the water absorption gradually increased with the plain PLGA scaffolds, and the plain PLGA1 had the highest water absorption at the end of the hydrolysis in week 10.

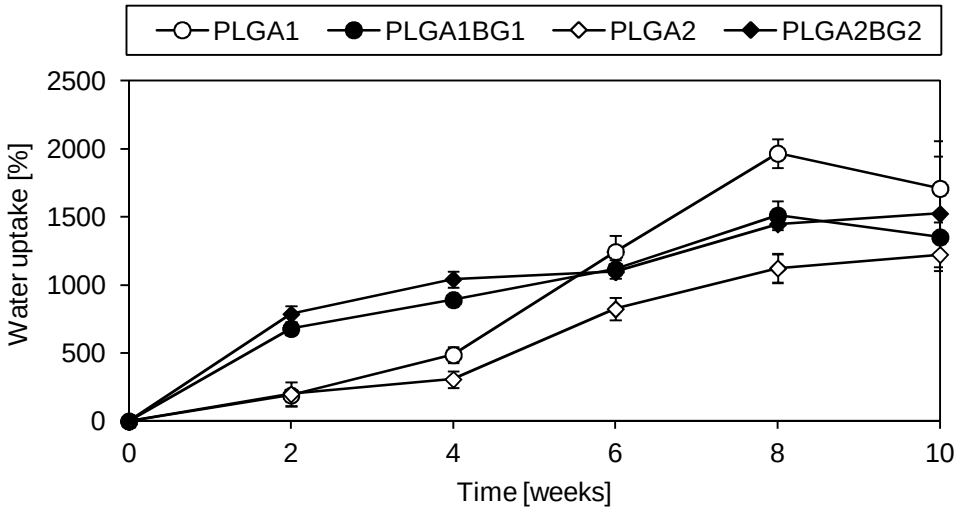

Figure 21. Water uptake of the different PLGA and PLGA+BGf scaffolds during the hydrolysis (10 weeks).

7.2.3 *In vitro* hydrolytic degradation of the synthetic polymer-based scaffolds

In vitro degradation tests of synthetic polymer-based scaffolds were done for PLA70+TCP and PLGA+BGf scaffolds for 26 and 10 weeks, respectively. The pH of the buffer, PBS, stayed within the given limits (7.35–7.45) with the scaffolds with PLA70 as the matrix polymer. The pH of the buffer with the scaffolds with PLGA as the matrix polymer, on the other hand, showed lower pH

values with plain PLGA scaffolds. The buffering effect of BGf was noticed in the PLGA+BGf scaffolds, as the BGf was shown to buffer the acidic degradation products of PLGA in the composites (PLGA1BG1 and PLGA2BG2).

Scaffolds with PLA70/30 as matrix polymer

The porous structure of plain PLA70 and PLA70+TCP composite scaffolds remained relatively stable during the 26 weeks in hydrolysis (Figure 22). In addition, the scaffolds with 2 wt% of PLA70 showed only little or no visual difference in the appearance of the scaffolds during the 26 weeks of hydrolysis. During the hydrolysis, only the edges of the pores became smoother and more visible. This was caused by a minor degradation of the scaffolds. The TCP particles did not change in appearance after the 26 weeks of hydrolysis.

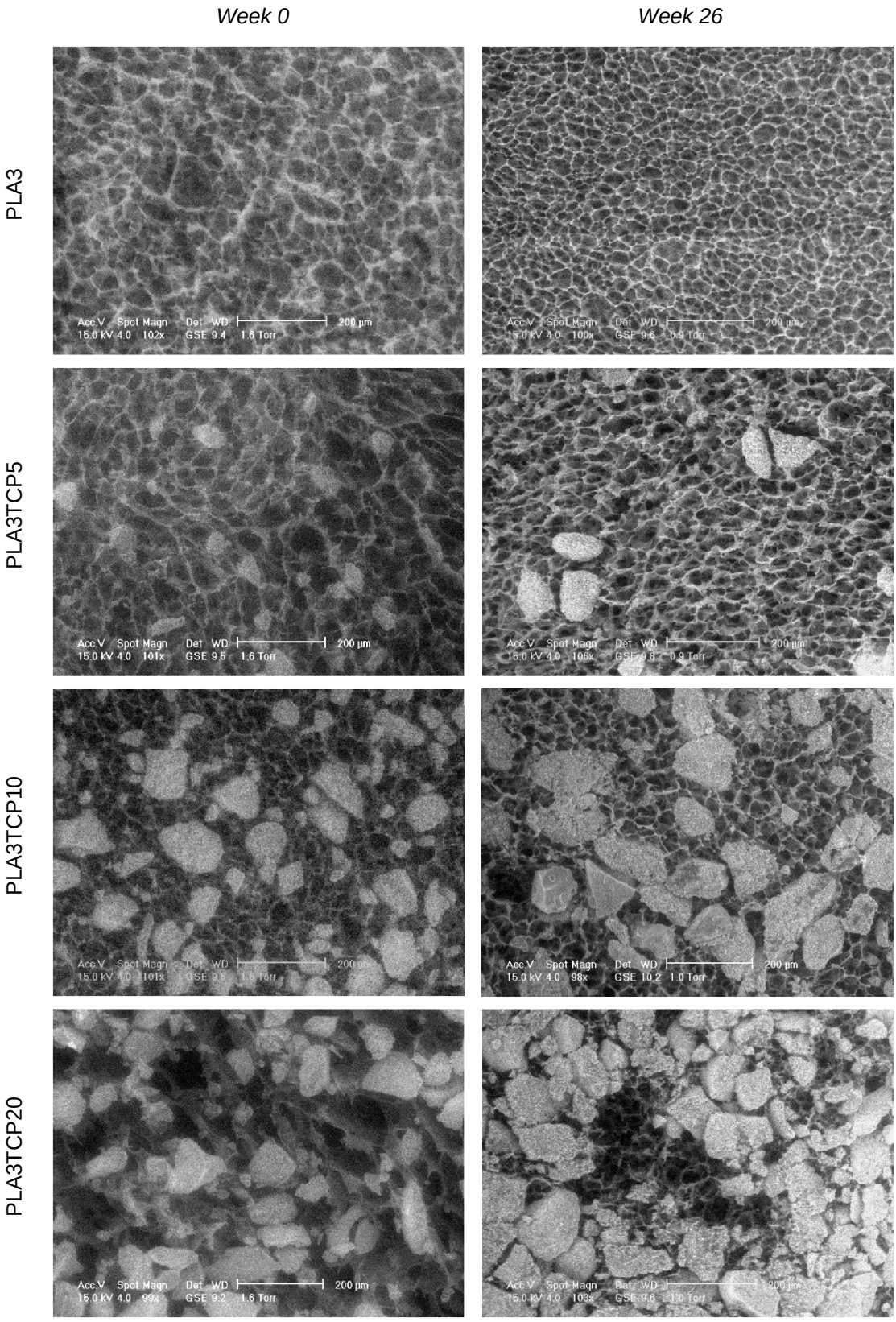

Figure 22. ESEM images of freeze-dried PLA70+TCP (with 3 wt% PLA) composite scaffolds from the porous bottom surface before hydrolysis at week 0 and at the end of the hydrolysis at week 26 (Scale bars 200 µm).

Only partial degradation was noticed for the PLA70+TCP scaffolds during 26 weeks in hydrolysis. The weight change of the scaffolds during the 26 weeks in hydrolysis and after week 4, between weeks 8 and 16, all the scaffolds showed an increase in weight, a maximum increase of 5% (Figure 23). After week 8 for most of the scaffolds and after week 16 for all of the scaffolds, a steady decrease in weight was seen until the end of the hydrolysis. Overall weight loss after the 26 weeks in hydrolysis was maximally 5% in all of the scaffolds.

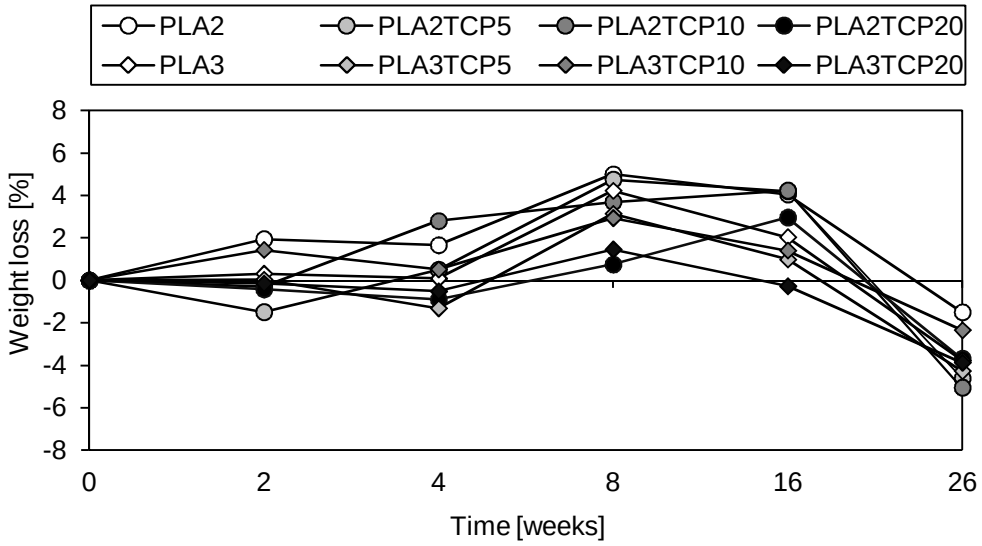

Figure 23. Weight loss of the PLA70+TCP scaffolds during hydrolysis.

The i.v. value of the PLA70 raw material was 3.1 dl/g. The i.v. values of the PLA70+TCP scaffolds decreased by 22% and 25% during the processing for the PLA2 and PLA3 scaffolds, respectively (Figure 24). The solvent, 1,4-dioxane, was shown to lower the i.v. values of PLA70 because the i.v. of the polymer decreased significantly after the polymer was dissolved in the solvent. After processing, the i.v. values decreased from 2.4 to 1.2 dl/g and 2.3 to 1.3 dl/g for the PLA2 and PLA3 scaffolds after 26 weeks in hydrolysis.

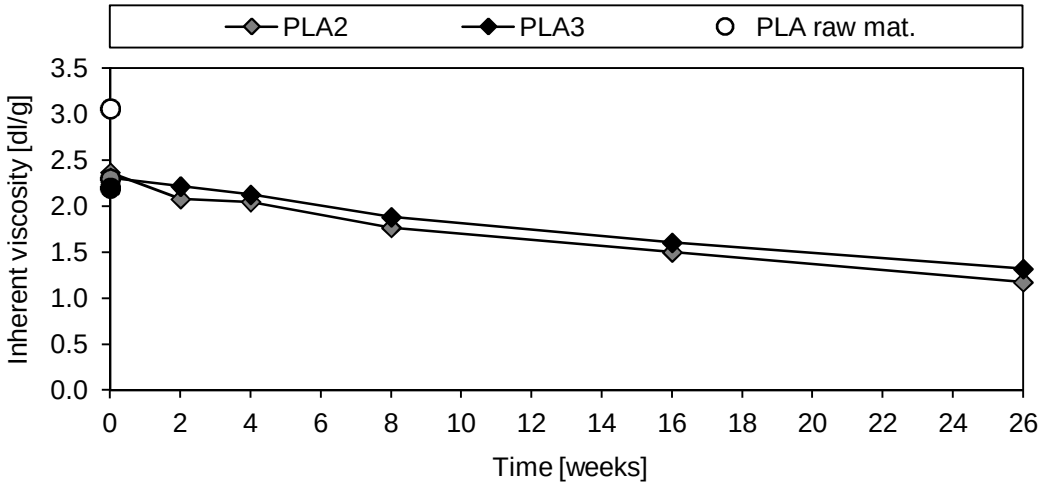

Figure 24. Inherent viscosity values of PLA2 and PLA3 scaffolds during hydrolysis, PLA raw material and 2 wt% and 3 wt% PLA70 solutions in 1,4-dioxane.

The thermal stability of the plain PLA70 and PLA70+TCP composite scaffolds was shown to be improved after the processing, at week 0, compared with the thermal properties of the raw material (Figure 25). After two (scaffolds containing 20 wt% of TCP) to four weeks (scaffolds with ≤ 10 wt% of TCP) in hydrolysis, the thermal stability was shown to decrease again and the lowest thermal stability values were detected at the end of the hydrolysis, at week 26, for all scaffolds.

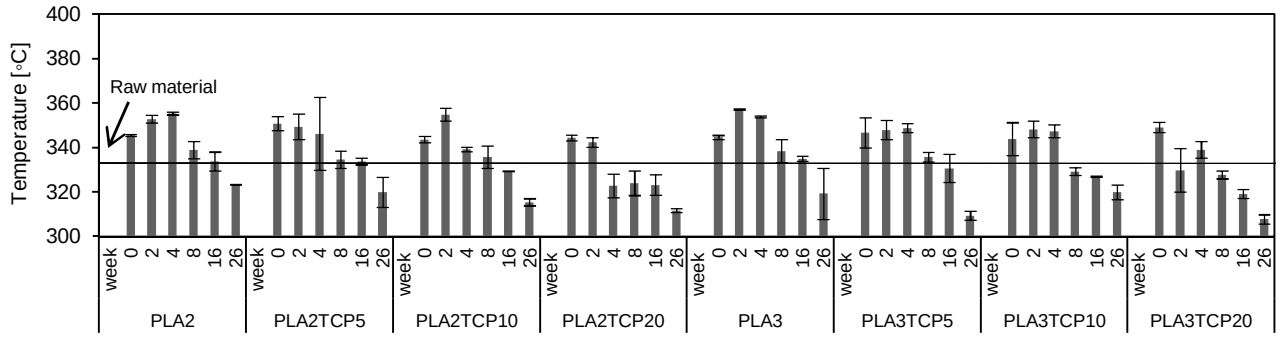

Figure 25. Peak maximum values of the first derivate curve measured with TGA indicating the thermal stability of the scaffolds.

Scaffolds with PLGA as matrix polymer

The difference in the porous structure of plain PLGA compared to the composite structure of PLGA+BGf varied greatly during the 10 weeks in hydrolysis. The plain PLGA scaffolds suffered from severe shrinking and twisting already after 2 weeks in hydrolysis and the porous structure of the scaffolds was partially lost (PLGA1 scaffolds) or completely lost (PLGA2 scaffolds), as seen in Figure 26. The composite scaffolds retained their initial structure better and the porous structure of the PLGA matrix was still visible after 2 weeks in hydrolysis.

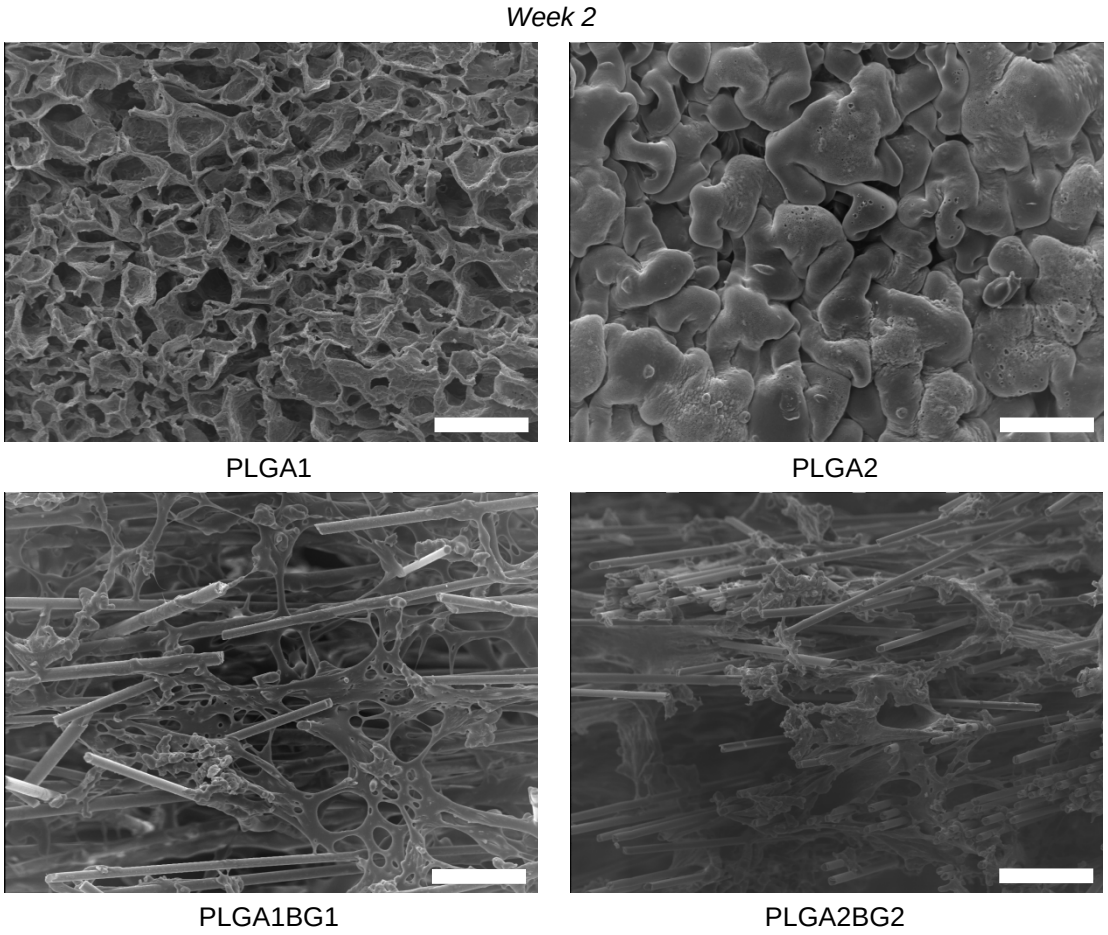

Figure 26. SEM images of plain PLGA and PLGA+BGf composite scaffolds after 2 weeks in hydrolysis (Scale bars 100 µm).

The BGf in PLGA+BGf composites stabilised the structure of the composites during the whole hydrolysis time, 10 weeks, and the open porous structure could still be observed (Figure 27). The porous structure of the plain PLGA1 scaffold was lost after 10 weeks in hydrolysis. This was expected because the porous structure was already partially lost in the PLGA1 scaffolds after 2 weeks in hydrolysis (Figure 26).

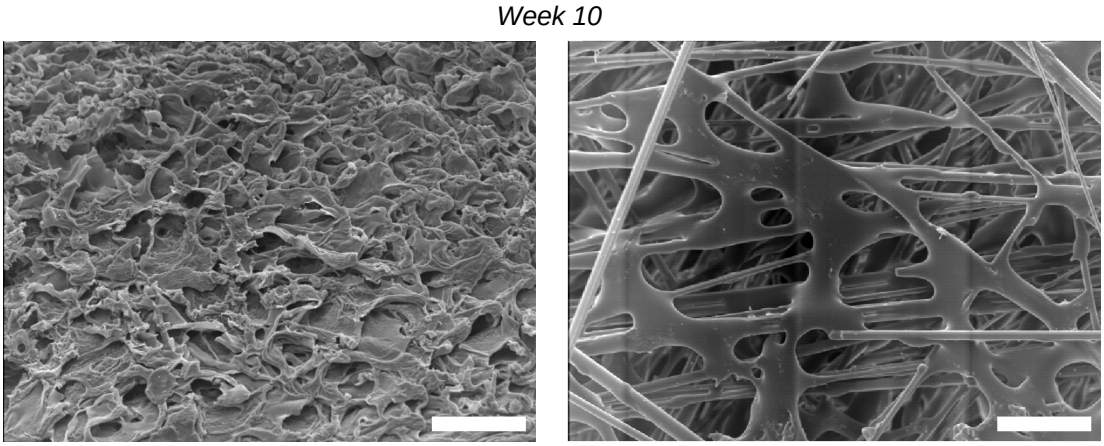

Figure 27. SEM images of plain PLGA scaffold (PLGA1) and PLGA+BGf composite scaffold (PLGA1BG1) after 10 weeks in hydrolysis (Scale bars 100 µm).

The M_w and M_n of the PLGA decreased constantly during the hydrolysis (Figure 28). The highest drop in the molecular weight values was detected after processing and sterilization of the scaffolds. PLGA1 scaffolds with the highest initial molecular weight lost their molecular weight more severely after the processing and sterilization, and the M_n of PLGA1 decreased to the same level as PLGA2. At the beginning of the hydrolysis, during the first two weeks, the M_n stayed relatively constant, after which the M_n started to decrease gradually. The trend in the decrease of molecular weights (M_w and M_n) was similar for all scaffolds.

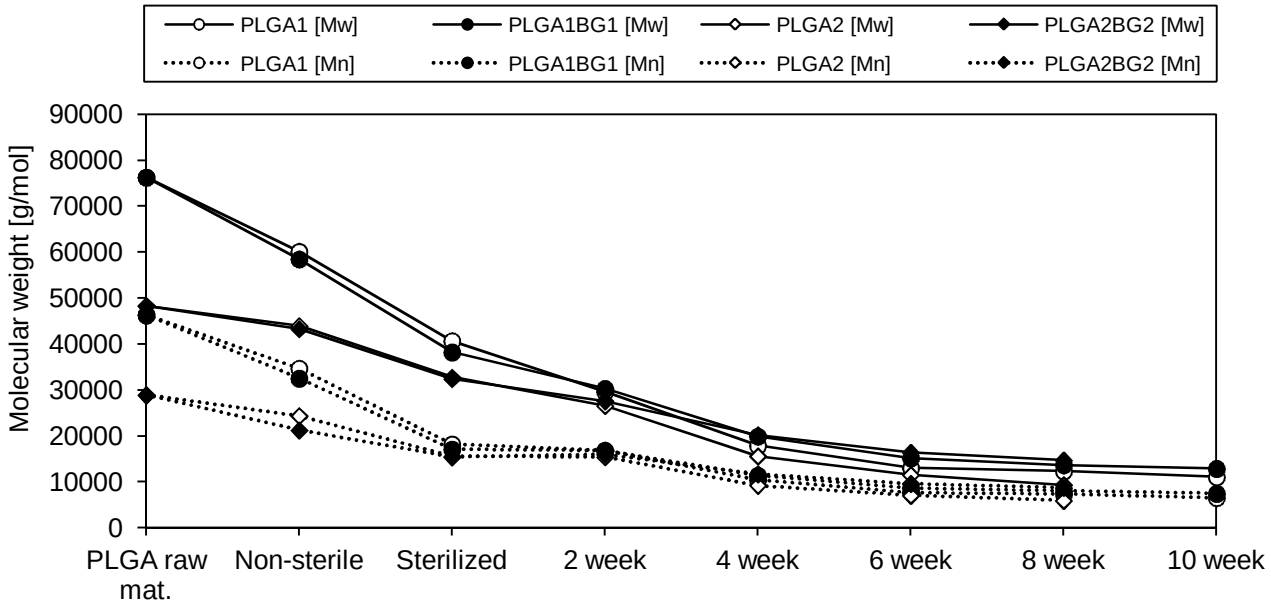

Figure 28. Molecular weight change of PLGA+BGf scaffolds during hydrolysis.

The core-accelerated bulk degradation process by chain scission of ester bonds for poly(α-hydroxyesters) can be described by a first order law (Pitt et al. 1981). More specifically, the M_n decrease during ester hydrolysis can be modelled by Equation 2 as follows:

$$\frac{1}{M_n} = \frac{1}{M_n^0} \times e^{kt} \quad (2)$$

or in its linearized form (Equation 3):

$$ln\left(\frac{M_n}{M_n^0}\right) = -kt \quad (3)$$

where M_n (g/mol) is the number average molar mass of the polymer at any time point, M_n^0 is the initial number average molar mass (g/mol), k is the ester hydrolysis rate constant (per day) and t is the degradation time (day). Assuming that the above model is also applicable to composite degradation, the values of $\ln(M_n/M_n^0)$ as a function of t can be described by a linear function. Both the plain PLGA scaffolds and the PLGA+BG composites showed M_n decrease according to the first order law during hydrolysis, with straight lines with good fits indicating core accelerated bulk degradation (Figure 29).

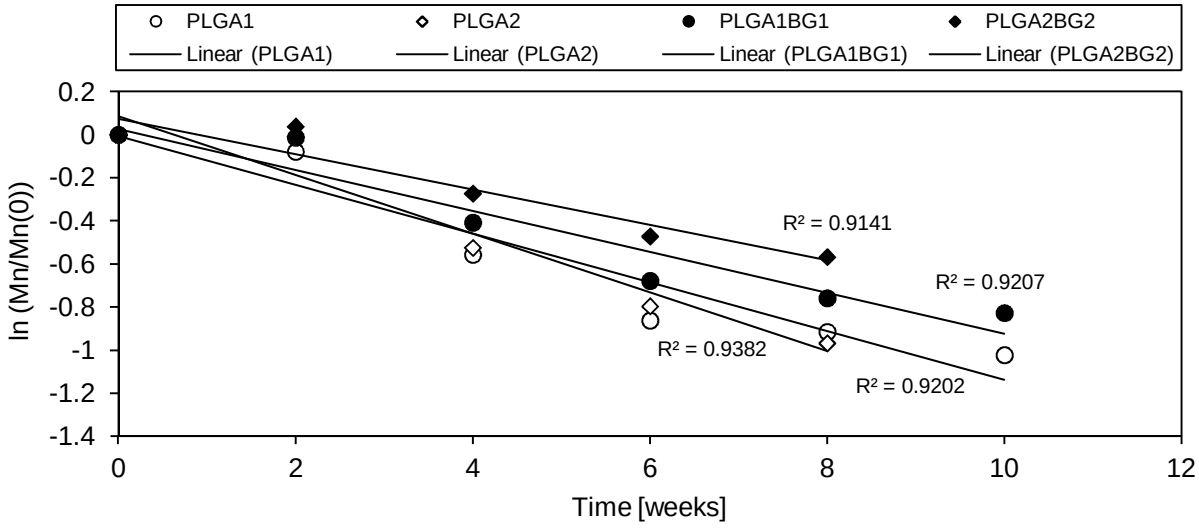

Figure 29. Fitting the number average molecular weight decrease of PLGA+BGf composites during ester hydrolysis according to the first order law.

The trend in weight loss of the scaffold with PLGA1 as the matrix polymer was constant during the hydrolysis, though the loss in plain PLGA1 scaffold was higher than in the corresponding composite scaffold, PLGA1BG1 (Figure 30). The trend in weight loss of the scaffold with PLGA2 as the matrix polymer was not that straightforward. Though, it is very likely that the results at week 2 for the PLGABG2 and at week 4 for the PLGA2 and the PLGA2BG2 scaffolds are incorrect due to an error in scale. At the end of the hydrolysis (at week 10), the overall weight loss of the scaffolds was 63, 59, 41 and 63% for PLGA1, PLGA2, PLGA1BG1 and PLGA2BG2 scaffolds, respectively.

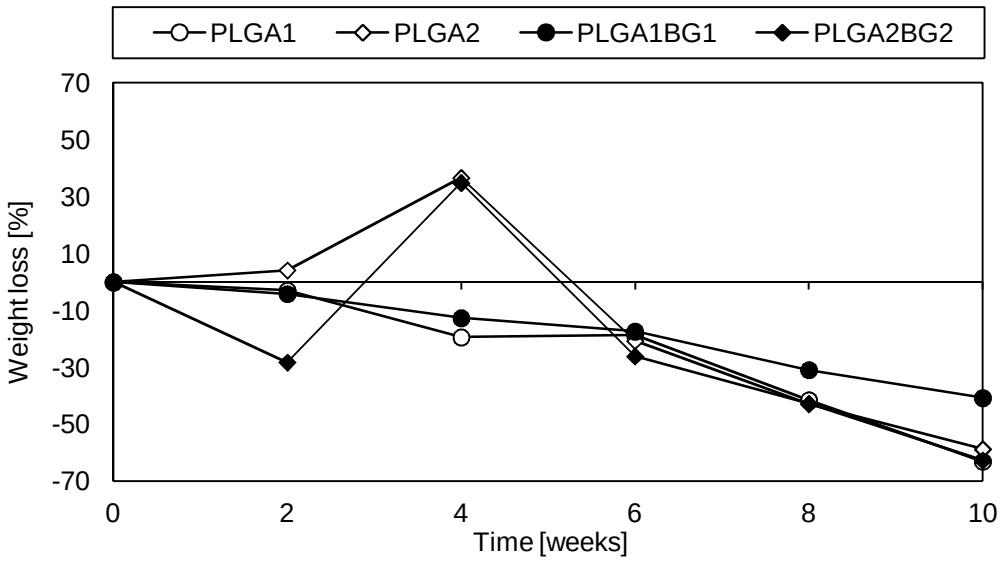

Figure 30. Weight loss of the PLGA+BG scaffolds during hydrolysis.

The T_g values of the PLGA+BGf scaffolds decreased the most after the processing (from 51.9 to 42.0 °C for PLGA1) and sterilization (from 47.3 to 37.5 °C for PLGA2) (Figure 31). After 2 weeks in hydrolysis, the T_g of plain PLGA scaffolds (PLGA1 and PLGA2) increased, and after that the T_g remained relatively constant during the hydrolysis.

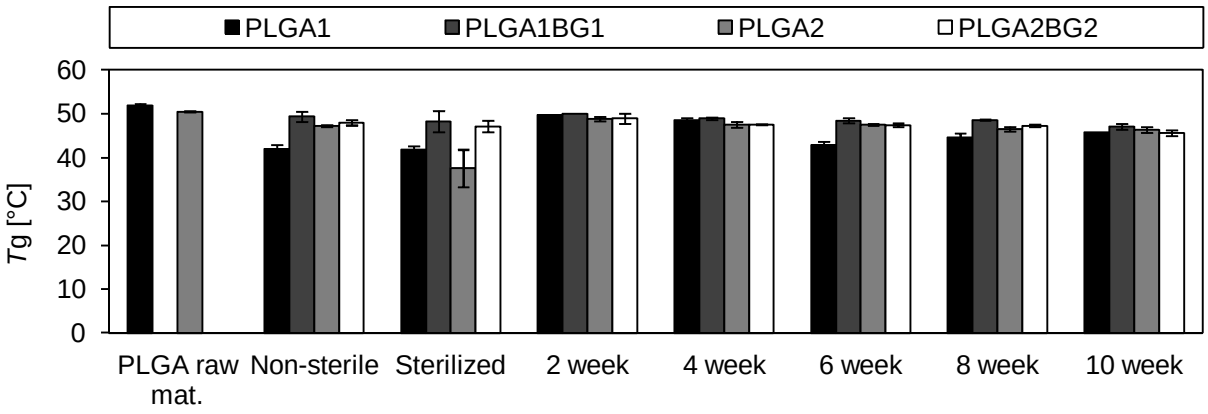

Figure 31. Glass transition temperatures of PLGA+BGf scaffolds during hydrolysis.

The BG content in PLGA+BGf scaffolds was 50.7±5.2% and 41.9±3.0% in the PLGA1BG1 and PLGA2BG2 composites, respectively (Figure 32). The difference in BGf content between parallel samples was moderate, 5.2 and 3.0 for PLGA1BG1 and PLGA2BG2 composites, respectively. No major change in the BGf content in PLGA+BGf composites was noticed during the hydrolysis of 10 weeks.

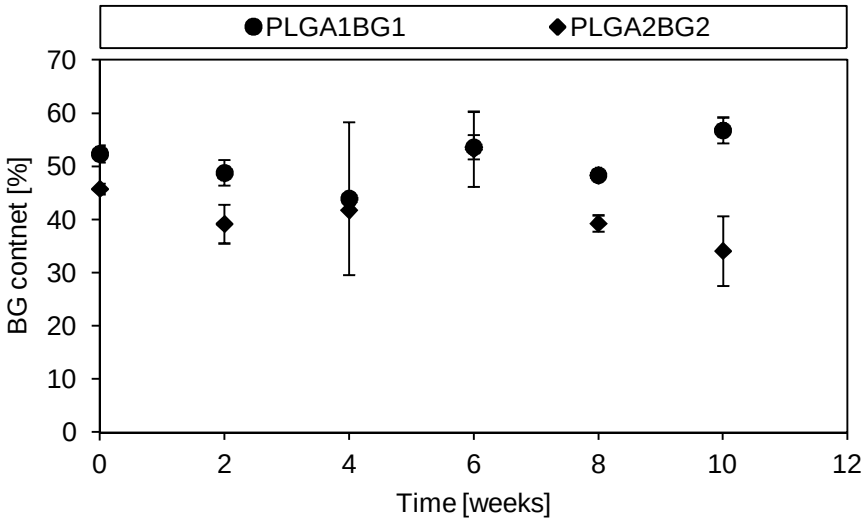

Figure 32. BG content of different PLGA+BGf composite scaffolds during hydrolysis.

7.3 The feasibility of the freeze-dried scaffolds for tissue engineering applications

7.3.1 Cellular responses to the natural polymer-based scaffolds

Chondrocytes were seeded into the natural polymer-based scaffolds for one week and the viability and distribution was analysed in Publication IV. Cells were evenly distributed on the surfaces of the scaffolds and were viable after one week of culture. The cells were well attached to the freeze-dried collagen and chitosan networks as well as the PLA96 fibres (Figure 33).

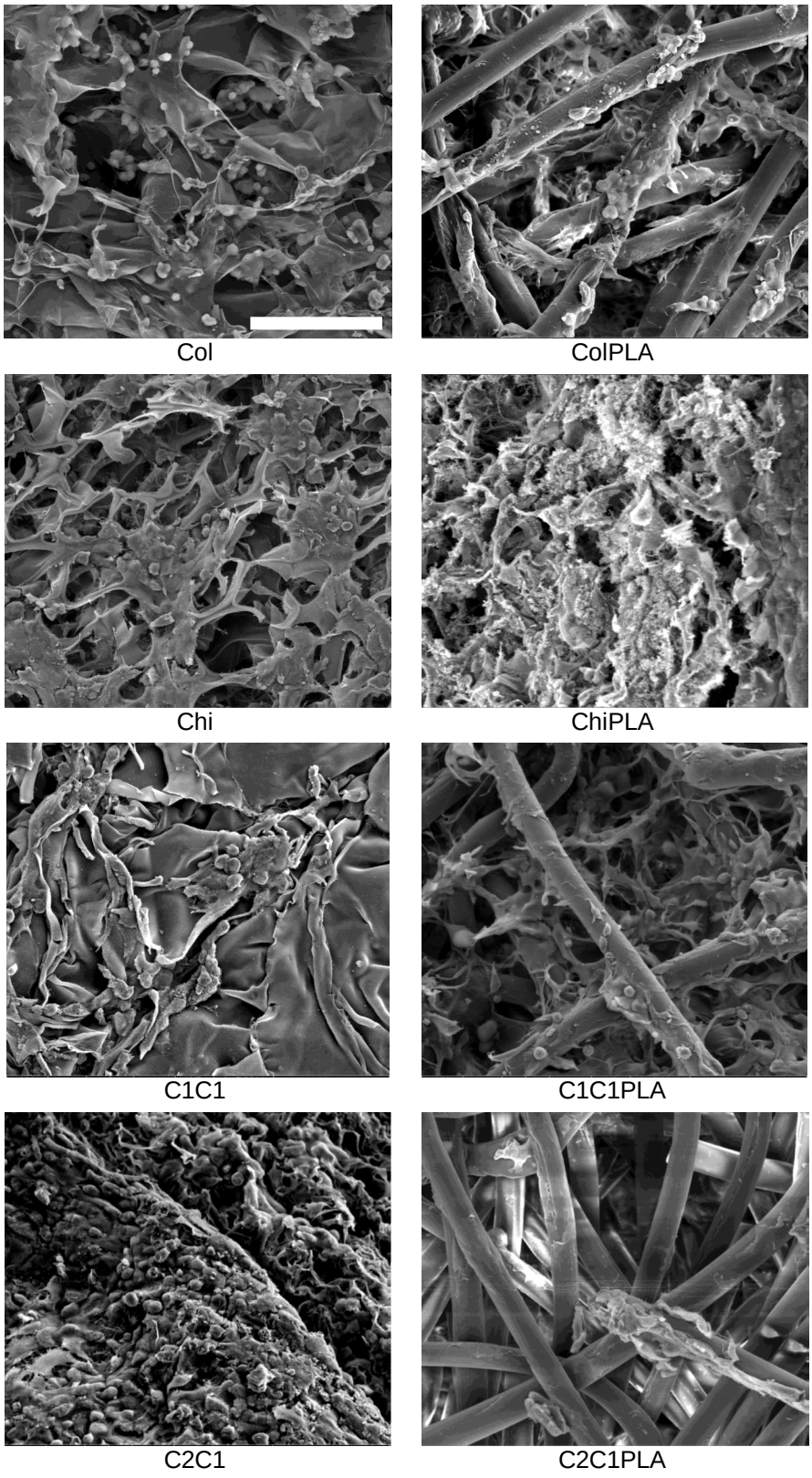

Figure 33. SEM images of natural polymer-based scaffolds containing bovine chondrocytes after one week in culture (Scale bar 100 µm).

The seeded chondrocytes expressed collagen type II in the cytoplasm, indicating that the cells had retained chondrogenic phenotype in the scaffolds (Figure 34). High variation in the penetration of the cells was detected between the different scaffolds. Most of the cells remained at the top surface

of the scaffolds where the cells were pipetted while seeding. In ColPLA and C2C1PLA scaffolds the penetration of the cells was good and the cells were detected throughout the scaffold. In ChiPLA and C1C1PLA scaffolds some penetration was detected. In plain scaffolds (Col, Chi, C1C1 and C2C1), the penetration of the cells was weak.

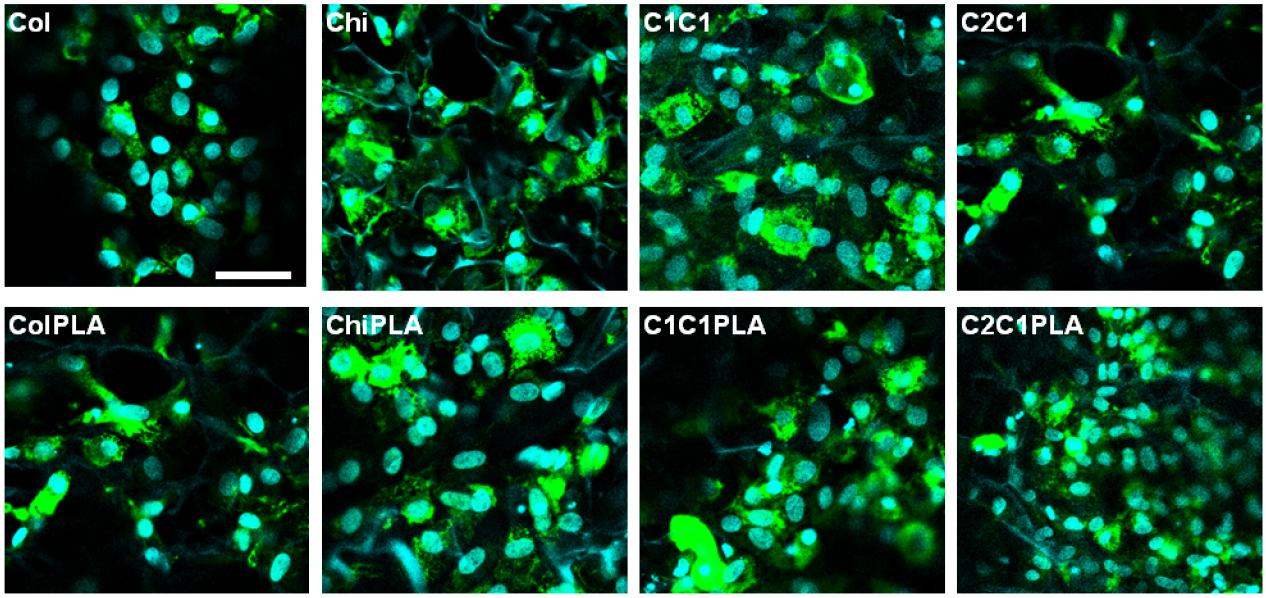

Figure 34. Evenly distributed and viable chondrocytes show collagen II expression in the natural polymer-based scaffolds after one week in culture. Collagen II in *green*, nuclei of the cells in *blue* (Scale bar 50 µm).

7.3.2 Cellular responses to the synthetic polymer-based scaffold

Cell attachment and growth was studied on PLA70+TCP and PLA70+BG composite scaffolds (2 wt% PLA70 + 10 or 20 wt% filler) and for plain PLA70 scaffold (PLA2) (Publication II). The number of viable cells was observed at 3 h and 2 weeks time points (2 weeks time point is shown in Figure 35). After 2 weeks, the number of cells had increased (compared with the 3 h time point), observed by Live/Dead staining. The cells were only attached close to the cell seeding area, in the region close to the surface in all of the scaffolds after the 3 h time period. After 2 weeks, the cells had spread inside the scaffolds. However, the cell density was the highest in the region close to the surface. Only a few cells were found on the dense top surface of the scaffolds. In the PLA2TCP20 scaffolds, the cells were spread more evenly, but in the other scaffolds the cells had formed cluster structures between the pores in the scaffold structure in the region close to the surface.

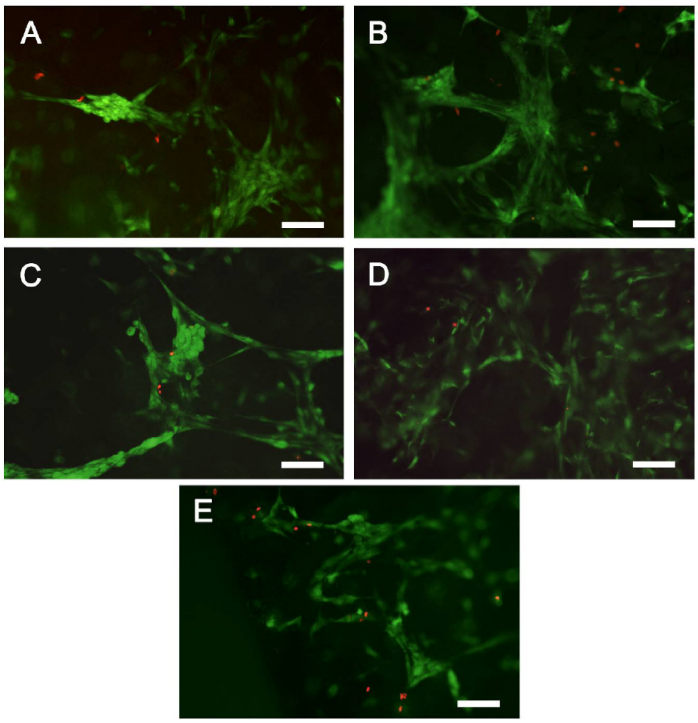

Figure 35. Representative images of viable (*green fluorescence*) and dead (*red fluorescence*) ASCs attached to A) PLA2BG10, B) PLA2BG20, C) PLA2TCP10, D) PLA2TCP20, composite scaffolds, and E) plain PLA2, after 2 weeks in culture (Scale bars 200 µm).

The cell morphology and spreading was examined with ESEM and SEM imaging after the 2 week time period (Figures 36 and 37). The filler particles, TCP or BGp, were not found to affect the morphology of the cells. During the culturing period of 2 weeks, the ASCs started to colonize the scaffolds without forming a homogenous monolayer. The ASCs were found to form bridges between the filler particles, TCP and BGp, in the composite scaffolds. The ASCs were seen to stretch and to form projections on the porous surface of the scaffolds, as seen in SEM images on the right in Figure 37.

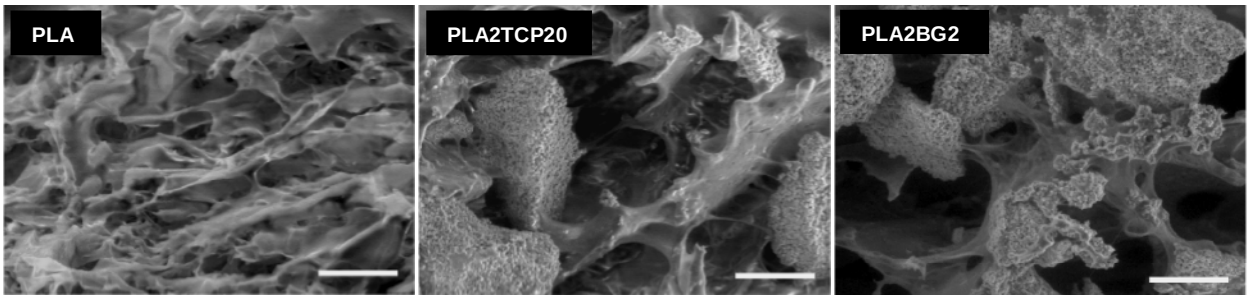

Figure 36. ESEM images of ASCs on the PLA2, PLA2TCP20 and PLA2BG20 scaffolds (Scale bars 50 µm).

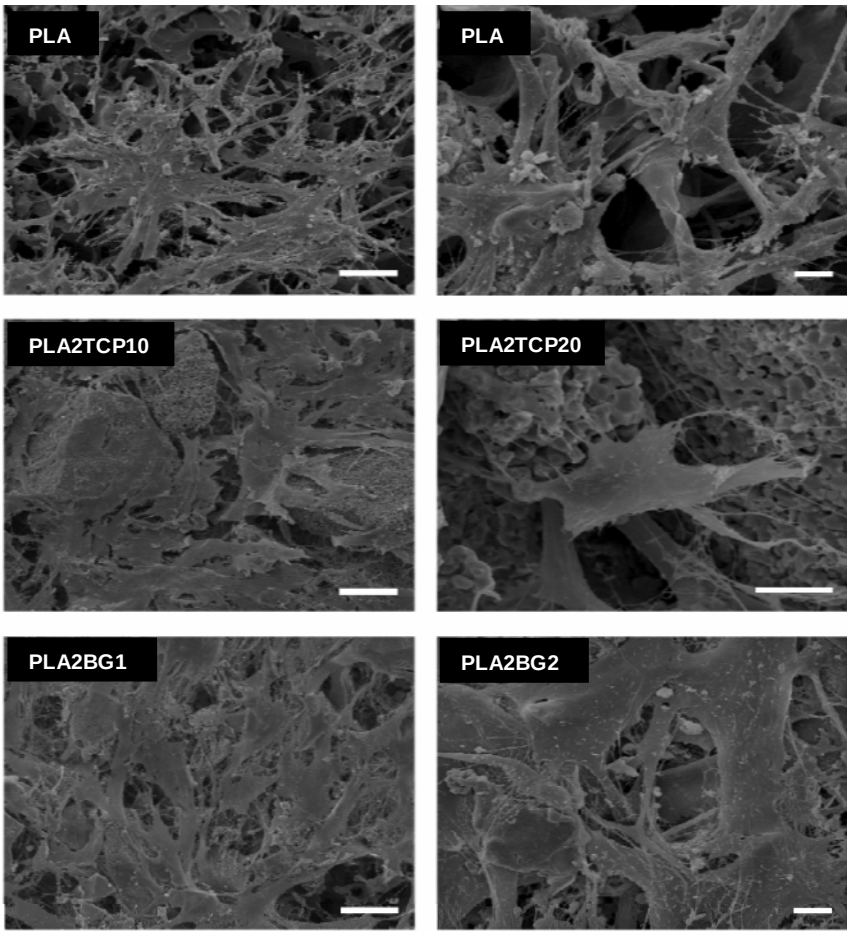

Figure 37. SEM images of ASCs on the PLA2, PLA2TCP10 and PLA2BG10 scaffolds on the left (Scale bars 50 µm), and on the PLA2, PLA2TCP20 and PLA2BG20 scaffolds on the right (Scale bars 10 µm).

The cell number in the scaffolds was assessed by measuring the total DNA content (Figure 38A). After 2 weeks, the cell number was significantly higher in scaffolds with TCP filler than with the other scaffolds. The DNA content was significantly lower in scaffolds with BGp filler than with the other scaffolds. No considerable difference was noticed between the two filler ratios of TCP, 10 and 20 wt%. The early differentiation of ASCs into an osteogenic pathway was evaluated by quantitative measurement of ALP activity in the scaffolds (Figure 38B). The same magnitude of relative ALP activity was detected for PLA2TCP10 and PLA2TCP20 scaffolds. However, the PLA2TCP10 scaffolds had significantly higher magnitude compared with the other scaffolds. The relative ALP activity of ASCs cultured on PLA2BG10, PLA2BG20 and PLA2 scaffolds was comparable after 2 weeks of culture. This was due to the lower cell number in PLA2BG10 and PLA2BG20 scaffolds compared with PLA2 scaffolds.

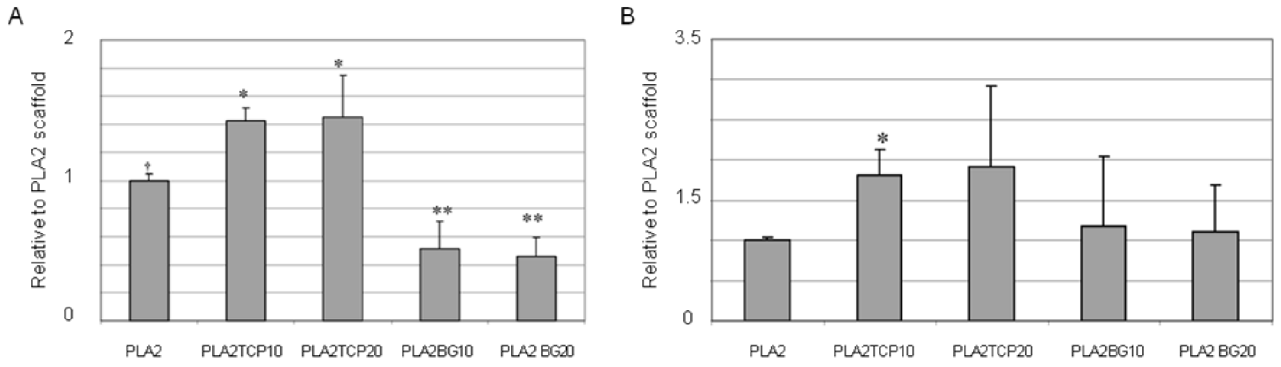

Figure 38. Relative A) DNA content and B) ALP activity of PLA70+TCP and PLA70+BG composite scaffolds cultured with ASCs for 2 weeks. Results are expressed as mean + SD relative DNA content or ALP activity in three experiments ($n = 4$). *$p < 0.005$ with respect to PLA2, PLA2BG10 and PLA2BG20; **$p < 0.005$ with respect to PLA2, PLA2TCP10 and PLA2TCP20; $^{\dagger}p < 0.005$ with respect to PLA2TCP10 and PLA2TCP20, and PLA2BG10 and PLA2BG20.

The culturing period was also found to have an effect on ASC proliferation. The relative DNA content was not increased when cells were cultured on scaffolds with BGp as a filler for 2 weeks compared to 1 week (data not shown). The DNA content increased for plain PLA2 scaffolds and the scaffolds with TCP as a filler when ASCs were cultured on scaffolds at 2 weeks. However, no significant difference was noticed between weeks 1 and 2. The ALP activity of ASCs cultured on plain PLA2 scaffolds or scaffolds with BGp as a filler produced two times higher levels, but a significant increase was only seen at the 2-week time point when ASCs were cultured on PLA2TCP20 scaffolds. The ALP activity of ASCs cultured on PLA2TCP10 scaffolds was also three times higher at the 2-week time point than at the 1-week time point.

8 Discussion

There are several different approaches that can be used for osteochondral tissue engineering (Nukavarapu & Dorcemus 2013; Martin et al. 2007), categorised briefly into one component or two component scaffolds. The one-component scaffold can be manufactured with one or more components in one scaffold with a homogenous or heterogeneous structure. The two-component scaffold is manufactured from separate cartilage and bone components and the different layers can be combined during processing or at the time of implantation. Numerous studies are trying to solve the tissue engineering challenges of cartilage, bone and osteochondral lesions (Panseri et al. 2012; Hutmacher 2000; Castro et al. 2012; Puppi et al. 2010). Nevertheless, no optimal way to heal cartilage, bone, or osteochondral trauma exists and, therefore, the study is still ongoing. Publications II and III are mainly focused on osteochondral tissue engineering applications. Publication IV focuses on cartilage tissue engineering, and Publication V focuses on bone or osteochondral tissue engineering applications.

Natural polymers are widely studied materials in the field of tissue engineering because of their high biocompatibility, biodegradability, and the ability to mimic certain aspects of native ECM, and thus facilitate cell adhesion, migration, differentiation, and ECM deposition (Panseri et al. 2012). Collagen is a structural protein in native articular cartilage, and chitosan, a natural polysaccharide (Iwasa et al. 2009), possesses a similar structure to naturally present GAGs found in articular cartilage (Kim et al. 2008; Francis Suh & Matthew 2000). Therefore, the natural polymers, collagen and chitosan, are studied in this thesis in order to best meet the characteristics of native cartilage tissue (Publication IV). However, the poor mechanical properties of natural polymer scaffolds, when used as highly porous structures, need to be overcome. Therefore, hybridisation with a fibrous network of synthetic polymer with PLA96/4 used as the reinforcing component was studied in this thesis.

Synthetic polymers were selected as a matrix component for the studied bone or osteochondral tissue engineering scaffolds (Publications II, III, and V) as they possess better mechanical properties (compared with natural polymer scaffolds) and their degradation rate can be altered more accurately (Panseri et al. 2012). Also, the preliminary cell studies with ASCs showed improved properties for freeze-dried PLA70 scaffolds compared with freeze-dried collagen type I scaffolds (data not shown). Therefore, PLA70 was selected for the bone tissue engineering scaffolds (Publications II and III). For synthetic polymer-based composites, bioceramics and bioactive glasses were selected to obtain more osteoconductive properties for the synthetic scaffolds designed for bone or osteochondral tissue engineering applications.

8.1 Cross-linking of collagen

Untreated collagen has a fast degradation rate and low mechanical strength and, therefore, cross-linking is a conventional way to improve the properties of collagen scaffolds. Either chemical or physical cross-linking can be used as a method to cross-link collagen. From the chemical methods glutaraldehyde (GA) is the most traditional agent used in the treatment of porous collagen scaffolds (Lee et al. 2001; Friess 1998). However, GA is potentially cytotoxic and it can cause excessive cross-linking. As a result, several alternatives have been reported and EDC is widely studied for the cross-linking of collagen (Park et al. 2002; Powell & Boyce 2006; Duan & Sheardown 2005; Lee et al. 2001). EDC facilitates the formation of amide bonds between carboxylic and amino groups on the collagen molecules without becoming a part of the actual linkage (Park et al. 2002; Powell & Boyce 2006; Duan & Sheardown 2005; Friess 1998).

To determine the effectiveness of different cross-linking methods (Publication I), DSC was used to measure the T_d values of collagen scaffolds with different cross-linking methods. Higher T_d indicates higher degree of cross-linking in collagen scaffolds (Duan & Sheardown 2005; Miles et al. 2005). In Publication I, the cross-linking with EDC post freeze-drying was found to be a more applicable method to be used for freeze-dried collagen scaffolds. As the differences in T_d values of the different collagen scaffolds were moderate, the improved wettability characteristics in scaffolds that were cross-linked post freeze-drying indicates that the scaffold structure can be improved by cross-linking the collagen scaffolds with EDC post freeze-drying. Also, higher wettability was achieved with 10 mM EDC cross-linking than with 1 mM EDC. Therefore, a higher amount of EDC in the cross-linking solution leads to improved scaffold properties.

The scaffolds cross-linked with EDC prior to freeze-drying suffered from inferior dimensional stability in wet conditions. The use of a higher amount of EDC for cross-linking could solve this problem. However, even though EDC is a zero-length cross-linker and does not stay as a part of the linkage, it is an irritant and should be leached out from the system. Therefore, higher amounts of the used cross-linker prior to freeze-drying could pose the risk that not all EDC is actually leaching out of the scaffold. That is why cross-linking with EDC post freeze-drying should be a more secure way to use EDC as it is possible to rinse the scaffolds carefully after the cross-linking to ensure no excess cross-linker remains in the system (Park et al. 2002).

The post freeze-drying method of cross-linking with EDC is also preferred because with higher collagen concentrations there is almost no change (no shrinking of the porous structure of the scaffolds) in the pore sizes of the scaffolds when cross-linking scaffolds with higher collagen concentrations (1.0–2.0 wt%) with either 1 mM or 10 mM EDC. To enhance the cross-linking of collagen scaffolds, even higher amounts of EDC (14 mM) together with NHS (6 mM) were used to improve the cross-linking ability of EDC (Publication IV). The combination of EDC+NHS is a widely used method to

cross-link collagen scaffolds (Pieper et al. 2002; Yang 2012; Cao & Xu 2008) and was, therefore, selected as a cross-linking method for the collagen-based scaffolds in Publication IV.

8.2 The effect of the freeze-drying parameters on the structure of the scaffolds

When fabricating porous scaffolds for tissue engineering by freeze-drying, there are many factors that can be altered that affect the structure of the scaffold (Franks 1998). The concentration of the polymer solution and the freezing temperature affects the pore size. A higher amount of polymer leads to lower pore sizes and smaller pores are formed in lower freezing temperature (Madihally & Matthew 1999). The size of the pores in collagen scaffolds was found to get smaller when a higher than 0.3 wt% collagen concentration was used. However, the concentration of 2 or 3 wt% PLA70 in the PLA70+TCP scaffolds had no effect on the pore sizes of the scaffolds. This was probably due to the relatively low concentration of PLA70 in the scaffolds and the difference would become more visible with higher polymer concentrations. The freezing temperature was the same for all the scaffolds (–30 °C), since at that temperature the porous structure was found to be fairly optimal. Attempts at using lower freezing temperatures were tested as preliminary tests (data not shown), but by lowering the freezing temperature lower pore sizes were detected. The filler particles, TCP or BGp, or the filler fibres, PLA96 or BGf, in the composites did not have an effect on the pore sizes of the scaffolds.

By using unidirectional freezing, the overall porous structure and its orientation can be altered as the pore structure of the freeze-dried scaffolds mirrors the ice-crystal morphology after freezing (Schoof et al. 2001). To achieve unidirectional freezing, some of the parts around the mould are first insulated and then the freezing takes place in the direction in which direction the pores are formed. Unidirectional freezing was used for the plain collagen scaffolds in Publication I where the PS moulds were insulated from the sides and from the top of the moulds. In this way, the freezing starts mainly from the bottom of the sample and leads to a more homogenised pore structure distribution. The mould used for the other natural polymer-based scaffolds (as well as for other scaffolds with a synthetic polymer-based structure) was a PTFE mould with a high amount of mould material (PTFE) in the sides as well as at the bottom of the samples (Publications II, III, IV, and V). These PTFE moulds were found to work in a very similar way to the PS moulds together with the insulator around the mould. The structures of the scaffolds manufactured with PTFE moulds were found to be highly homogenous as well.

8.3 Freeze-drying as a method to manufacture composite and hybrid scaffolds

Natural polymer-based scaffolds manufactured by freeze-drying often lack the required mechanical strength needed for cartilage and bone tissue engineering. The highly porous structure of the matrix polymer can be reinforced by using a filler (Chen et al. 2002; Li et al. 2014). Filler components are often used to enhance other properties of scaffolds as well, for example, the osteoconductive properties of bone tissue engineering scaffolds (Maquet et al. 2004; Miki et al. 2000; Roether et al. 2002; Boccaccini & Maquet 2003). Filler particles were added into the porous freeze-dried polymer component in Publications II and III to enhance the osteoconductivity of the scaffolds studied for bone and osteochondral tissue engineering. The interconnection of the filler particles, TCP and BGp, were found to be good and the matrix polymer PLA70 surrounded the particles. Fibrous structures have also been used to reinforce the tissue engineering scaffolds (Chen et al. 2004; Dai et al. 2010; Sato et al. 2001). By using two or more different processing methods, an even more complex structure that combines two 3D structures into one scaffold can be achieved. Freeze-drying can be used for matrix polymer processing (into a highly porous 3D matrix), and the processing of polymer or bioactive glass into fibres and, subsequently, the processing of the fibres into a 3D fibrous mesh (as a filler component). These two components, two 3D structures (highly porous matrix and fibrous mesh as filler) may then be combined into one scaffold. The method of combining two different 3D structures, a freeze-dried matrix and a fibrous filler component, was studied in Publications IV and V. The interconnection of fibres with the matrix polymer was good for both types of scaffolds, the natural polymer-based scaffolds with PLA96 fibres and the synthetic polymer-based scaffold with PLGA as the matrix polymer and BGf fibres as a filler.

To manufacture a layered osteochondral structure into the PLA70+TCP scaffolds, relatively large TCP particles were used to ensure the formation of a particle-rich area at the bottom of the scaffolds. These relatively large particles were immersed thoroughly into the polymer solution during processing, and before the freezing step the solution was held in the moulds to ensure that the TCP particles sank to the bottom of the scaffold structure. According to a study (Bohner & Baumgart 2004), the optimum radius for bone substitute particles should be in the range of 100–200 µm. In this range, the particle size is small enough to provide a large surface area and still large enough for bone ingrowth. The study also showed that with CaP bone substitutes with no macropores, small particles should be present to increase their resorption rate. By using large but porous TCP particles in Publications II and III, the positive effect of larger particles with a high surface area was also achieved. Larger particles could also be favourable since small particles (size of 2.2 µm) have been found to cause inflammation *in vivo*. Apparently, this inflammation is caused by small, slowly resorbable particles concentrating in the surrounding tissues (Heidemann et al. 2001).

8.4 Porous structure of the freeze-dried scaffolds

A highly porous, interconnected and open pore structure is needed for tissue engineering scaffolds to ensure tissue ingrowth and the flow transport of nutrients and metabolic waste. For example, the porosity of natural bone is in the range of 50–90% porosity, depending on the type of the bone (Stevens et al. 2008). The freeze-dried porous structure was highly similar in all of the freeze-dried scaffolds. A highly porous structure with high porosity and interconnected pores was detected in all natural polymer-based scaffolds (Publication IV) as well as in all synthetic polymer-based scaffolds (Publications III and V). The C1C1 scaffolds, with 50% of chitosan, were, however, an exception with a much lower porosity of only 66%. Therefore, it was assumed that the scaffolds containing chitosan suffered from shrinking as a result of inadequate neutralisation during processing, although the neutralisation process was evaluated in preliminary studies (data not shown). While cross-linking with EDC+NHS, the inadequate neutralization of the chitosan component led to the collapse of the initial porous structure of the blend scaffold. Therefore, the C1C1 scaffold with higher amounts of chitosan (compared with C2C1 scaffolds) suffered from shrinking more extensively. This is also the reason why the plain chitosan scaffold (Chi) showed superior porosity values, as those scaffolds were not cross-linked after the first freeze-drying step, as was the case with the other scaffolds with collagen in the blend structure. The shrinking of C1C1 scaffolds was also visible in the mechanical tests where the wet C1C1 scaffolds showed higher stiffness values than other plain natural polymer scaffolds, a phenomenon due to a denser scaffold structure.

The pore structure of natural polymer-based scaffolds, as well as of PLGA+BGf scaffolds was also shown to be open as detected by microCT studies. The interconnectivity of pores was also verified for natural polymer-based scaffolds and for PLGA+BGf as synthetic polymer-based scaffolds. The optimal pore size for cartilage (Griffon et al. 2006) and bone (Hulbert et al. 1970; Freyman et al. 2001; Hench & Polak 2002) tissue engineering scaffolds has been reported to be in the range of 70–120 µm and ~100 µm, respectively. However, in the study of Itälä et al. (Itälä et al. 2001), pore sizes of 50–125 µm in porous titanium structures led to the formation of secondary osteonal structures. Therefore, the optimal pore size range for osteogenic scaffolds might only be slightly higher when compared with the chondrogenic scaffolds. The pore size of the studied natural polymer-based scaffolds was for the optimally manufactured scaffolds (with a collagen concentration of 0.5–1.0 wt% and cross-linking with EDC post freeze-drying with 10 mM EDC solution) ~100 µm. The pore size range of the PLA70+TCP scaffolds was 20–80 µm, with a mean pore size of ~50 µm. The pore size range of the PLGA+BGf scaffolds was around 50–80 µm, with maximum pore sizes in the range of 100–250 µm. Therefore, the pore size of the natural polymer-based scaffolds fits well to the limits given for an optimal cartilage (as well as bone) tissue engineering scaffold. The pore sizes of the synthetic polymer-based scaffolds are not the most optimal for bone tissue engineering and are slightly smaller than the preferred pore sizes. However, there are also larger pores (as well as macropores) that could help cell migration into scaffolds. Also, the synthetic polymer-based scaf-

folds would fit in the requirements for cartilage tissue engineering scaffolds if used for osteochondral applications.

Skin formation was noticed on top of the freeze-dried scaffolds even though the overall structure of the freeze-dried scaffolds was highly porous. The skin formation was due to the freeze-drying process where the sublimation of the solvent occurs from the top surface. If it is not possible to control the temperature during freeze-drying, the polymer matrix will not be rigid enough to resist the interfacial tension caused by solvent evaporation. As a result, the porous structure will collapse and a dense skin layer will form on the scaffold (Ho et al. 2004). With an increase in polymer concentration, the skin surface becomes even denser. However, this enables the formation of two different functional surfaces into the scaffold. The formed skin surface could maintain transplanted cells inside the scaffold, while fluids, nutrients, and oxygen could diffuse through the porous surface (Boccaccini et al. 2005).

8.5 Wettability of the freeze-dried scaffolds

The surface of the tissue engineering scaffold is the first component that comes into contact with biological fluids. Therefore, for successful cell seeding the tissue engineering scaffold should contain a highly porous structure as well as optimal wettability, indicating hydrophilic properties. High wettability, however, does not necessarily lead to a more biocompatible scaffold, as even moderately wettable surfaces can result in enhanced biocompatibility. Therefore, the ideal balance of hydrophobic and hydrophilic surfaces still needs to be optimized (Menzies & Jones 2010).

The wettability of natural polymer-based scaffolds was tested in Publications I and IV. The natural polymer-based scaffolds possessed high water uptake ability. The wettability of the plain collagen scaffolds was the highest. Improved water uptake was also noticed for the other plain natural polymer scaffolds with increasing collagen amount. The higher the collagen amount the higher the water uptake. For hybrids, the best water uptake was in the scaffolds with only collagen as a natural polymer component. However, the wettability of collagen+chitosan+PLA96 hybrids was relatively high as well when compared with the ColPLA scaffolds. Chitosan scaffolds had the lowest wettability because of the shrinking in wet conditions caused by inadequate neutralization during the processing.

The wettability of the synthetic polymer-based scaffolds, PLGA+BGf, was studied in Publication V. The contact angle measurements revealed the highly hydrophobic nature of the PLGA and PLGA+BGf scaffolds. Material with contact angle values over 80° is considered hydrophobic (Menzies & Jones 2010), and the contact angle of the studied scaffolds varied in a range of 92 to 118°. The inhomogeneous highly porous structure of the freeze-dried scaffolds could have also affected the results. It was noticed that the parallel contact angle results varied highly, more than 5°

between the two measuring points of each droplet, the contact angle measured from right and from left in the same droplet. This indicates highly uneven surface structure of the scaffolds. That was why the standard deviation in the contact angle results was high in almost all the scaffolds. No significant change was noticed between the contact angle values of different scaffolds measured in PBS. The contact angle measured with water, less viscous liquid than PBS or blood, on the other hand showed significantly lower contact angle value for PLGA1 with respect to PLGA1BG1, PLGA2 and PLGA2BG2. As well, the PLGA1 showed relatively significant difference with respect to PLGA2BG2 in blood. Interestingly, the contact angle of the parallel composites, PLGA1BG1 and PLGA2BG2 was higher than the corresponding plain scaffolds, PLGA1 and PLGA2. This must be due to the structure of the composites, where the BGf fibres are embedded inside the PLGA matrix and do not enhance the initial wetting of the scaffolds. This result is also noticed as a higher material thickness of PLGA+BGf composites in microCT studies. Therefore, it might be that the BG fibres in the composites make the surface of the scaffolds even denser than the plain PLGA scaffolds. As well, the PLGA2 showed higher contact angle values than PLGA1 measured in water, indicating that PLGA1 would be less hydrophobic than the other studied scaffolds. However, these values were measured without pre-wetting of the scaffolds. Pre-wetting is known to enhance the wettability of otherwise highly hydrophobic synthetic polymer scaffolds. Therefore, the structure of the scaffolds should be optimised in order to have improved hydrophilicity with BGf. Another option is to use surfactants that are shown to enhance the hydrophilicity of polyester-based porous scaffolds (Sun et al. 2014). However, the BGf in the composites was seen to improve the wettability of the scaffolds *in vitro* when the PLGA+BGf composites possessed a higher water uptake in the first weeks in hydrolysis.

8.6 Compression properties of the freeze-dried scaffolds

The stiffness of the scaffold influences the mechanical environment of the cells, which in turn can influence cell differentiation and tissue growth (Kock et al. 2012). The compressive modulus of native cartilage varies between the different layers of cartilage, from 0.079 MPa (superficial layer) to 5.7 GPa (subchondral bone) (Castro et al. 2012). The compressive modulus of the studied natural polymer-based scaffolds was in the range of the native cartilage modulus values with dry scaffolds. However, the compressive modulus of the wet scaffolds was relatively low, only 3–10 kPa. The wet properties of the scaffolds could be more comparable to the properties of the scaffolds in *in vivo* conditions. The optimal mechanical properties for plain cartilage tissue engineering scaffolds are not known and the optimal properties of a scaffold may not be an exact copy of the native tissue (Kock et al. 2012) because the cellular microenvironment changes during tissue development *in vivo* and the mechanical properties of the scaffolds are found to improve when compared with *in vitro* cultivation (Pulkkinen et al. 2010). Also, the structure of the studied hybrids was a so-called sandwich structure with only the natural polymer component in the middle of the structure. It was

assumed that the compressive modulus values of the hybrid scaffolds were the compressive modulus of the natural polymer components in the middle of the scaffold, being the softer component in the hybrids. Therefore, it can be assumed that the compressive modulus values of the hybrids, with PLA96 carded mesh, would be improved if the structure of the scaffold was homogenous with the PLA96 carded mesh throughout the matrix. Nevertheless, the compressive stiffness of the hybrids was improved by the PLA96 carded mesh, and an improvement of over 70% for wet scaffolds was noticed. This improvement indicated that hybridisation with PLA96 fibres is an applicable way to improve the compressive properties of the studied natural polymer-based scaffolds. The structure of the hybrid scaffold should still, however, be optimised. The collagen component in the hybrids was also found to improve the ability of the scaffolds to recover their original shape after the compression loading (data not shown). The ability to recover shape is also an important property because it enables the scaffold to work properly in a load-bearing surrounding in cartilage. This is an important property of a functional cartilage tissue engineering scaffold because the liquid and nutrition exchange of the tissue is implemented in the avascular tissue by this phenomenon (Ge et al. 2012). This phenomenon was verified in the compressive stress–strain curves of the wet scaffolds, where it can be seen that no densification in the ColPLA hybrid scaffold was detected before the compression of 70%. This indicates that no plastic deformation yet exists.

The compressive properties of synthetic polymer scaffolds (Publication II, III, and V) were not tested because the scaffolds were fairly thin, only about 2 mm in height, and the compression testing machine was not able to compress samples that thin with adequate accuracy. However, it can be assumed that the compressive properties of the PLA70 scaffolds with TCP or BGp as filler particles (Publications II and III) were not enhanced, or not at least from the porous polymer side of the scaffolds, as the filler particles were inhomogeneously in the scaffolds. The BGf fibres in the PLGA+BGf scaffolds (Publication V) could have improved the properties of the composite scaffolds, compared to plain PLGA scaffolds, since the structure of those composites was homogenous. However, those scaffolds were also too thin for adequate accuracy measurements. All of the studied synthetic polymer-based scaffolds were, however, found to be ductile and they were hard to halve with a cutter, yet being rather flexible.

8.7 *In vitro* degradation of synthetic polymer-based scaffolds

When using synthetic biodegradable polymers such as PLAs, the acidic degradation products of the polymer can be harmful to the surrounding tissue (Yang et al. 2001). Therefore, it would be preferable to have some buffering component in the system. Bioactive glasses and bioceramics are known to buffer the acidic degradation of PLAs (Huttunen et al. 2006; Yang et al. 2006; Niemelä et al. 2008; Niemelä et al. 2005). For the PLA70+TCP scaffolds, the acidic degradation products of PLA70 were not noticed during the hydrolysis. However, the hydrolysis time, 26 weeks, was relatively short for the polymer as the degradation of PLA70 is known to be much longer than the stud-

ied period (Niemelä et al. 2008). Also, the degradation of the used, relatively large filler particles of TCP was not noticed during the 26 weeks of hydrolysis. This was why no buffering effect of the used filler TCP was noticed during the hydrolysis in Publication III. However, the buffering effect of BGf in the PLGA+BGf composite scaffolds was noticed because the degradation of PLGA70 is relatively fast, as noted in Publication V. Therefore, the degradation and leaching of acidic by-products started relatively quickly. Also, the degradation rate of BGf fibres was found to be relatively the same as the matrix polymer, PLGA70, as no major change in BGf content was noticed during the hydrolysis.

The studied degradation time, 26 weeks, for PLA70+TCP composite scaffolds was chosen since this period of degradation was thought to mimic the period of natural healing of fractured bone, since at that point the bone-healing is finished *in vivo* (Yu et al. 2008; von Doernberg et al. 2006). The degradation of PLA70+TCP composites (as well as the plain PLA70/30 scaffolds) was, however, still in the early beginning at that point, since the weight loss of the studied scaffolds was maximally only 5%. However, the early degradation showed typical characteristics of a bulk-eroding synthetic polymer, as the weight loss starts in the inner parts. The inner parts become a very viscous liquid with oligomers, and later the outer layer becomes thinner as the degradation propagates towards the surface and weight loss occurs (Li et al. 1990). This phenomenon was also verified by the results of water penetrating the polymer matrix as the weight of the scaffold was increased at the time of 8 to 16 weeks in hydrolysis. This indicated water uptake by which the hydrolysis of aliphatic esters starts and is followed by hydrolytic splitting of the ester bonds (Shih 1995). The i.v. values of the polymer also dropped steadily during the hydrolysis and the thermal stability steadily decreased after the first four weeks in hydrolysis. These results also verified the bulk-degradation of the polymer component during hydrolysis. Interestingly the i.v. of the PLA70 was found to decrease even before the hydrolysis and indicates degradation of the polymer during the processing. However, the thermal stability of the PLA70 was found to be improved after the processing and during the first weeks in hydrolysis. The addition of the filler TCP did not increase the thermal stability of the scaffolds. The improvement in thermal stability after processing could be explained by the processing method, freeze-drying, which removed any excess water during processing. Furthermore, at the beginning of the hydrolysis, the early dissolution of resulting monomers and oligomers might also have improved the thermal stability.

The degradation of PLGA+BGf scaffolds varied highly between the plain PLGA and the PLGA+BGf composite scaffolds. High degradation, around 40 to 60%, was detected for all scaffolds. However, the plain PLGA scaffolds suffered from severe shrinking and twisting during the hydrolysis and had already started at the beginning of the hydrolysis in week 2. The phenomenon where the plain PLGA scaffolds lose their initial porous structure was also detected in a previous study (Orava et al. 2007) with porous PLGA scaffolds manufactured by solvent casting and pressure quenching with CO_2. The porous structure of PLGA+BGf composite scaffolds, on the other hand, remained open until the end of the hydrolysis. This demonstrates the ability of the highly po-

rous BGf fibre structure to stabilize the dimensional stability of the PLGA+BGf composite scaffolds. The M_w and M_n results of the PLGA component in plain PLGA and PLGA+BGf scaffolds verified the core accelerated bulk degradation to be the degradation mechanism for the PLGA+BGf scaffolds. Interestingly, in contrast with this result, solid poly(L-lactide-co-DL-lactide) (PLDLA)/BG fibre composites studied previously (Lehtonen et al. 2013b) did not follow the typical core-accelerated degradation mechanism, with a combination of surface and bulk erosion. This though might be due to the highly porous polymer structure of the studied scaffolds. Therefore, the diffusion of water into the matrix and into the BGf fibre surface is different when compared with solid scaffolds. The steady decrease of M_w, M_n, steady weight loss and the minor changes in T_g values supports the core-accelerated bulk-erosion mechanism as well. The TGA studies demonstrate that the degradation of BG fibres in the PLGA+BGf composites is at a relatively similar level than the degradation of PLGA in the matrix, as the BG content remained at the same level during the 10 weeks in hydrolysis. No further characterization of the BGf fibres was made. However, the studied BGf fibres have demonstrated bioactive characteristics when immersed in simulated body fluid with calcium phosphate formation occurring on the surface of the fibres (Lehtonen et al. 2013a).

8.8 The feasibility of the freeze-dried natural polymer-based scaffolds for cartilage tissue engineering

The natural polymer-based scaffolds in Publication IV were studied for cartilage tissue engineering. The feasibility of the scaffolds to be used for cartilage tissue engineering was demonstrated by seeding chondrocytes into the scaffolds. The cells were found to be viable after one week culture. The cells were evenly distributed on the surfaces of the scaffolds and attached to the collagen and chitosan porous structure as well as the PLA96 fibres. The cells expressed collagen type II in the cytoplasm, which verified that they retained their chondrogenic phenotype. However, there were high variations in the penetration of the cells into the scaffolds, as most of the cells remained at the top of the scaffolds. The penetration of the chondrocytes was improved in hybrid scaffolds PLA96 fibres. The higher penetration of chondrocytes was most likely due to higher porosity of hybrid scaffolds and the cells were able to penetrate into the more porous scaffolds easier. The penetration was the best in ColPLA and C2C1PLA scaffolds, and some penetration was also detected in ChiPLA and C1C1PLA scaffolds. This indicates that collagen in the scaffolds also improved the penetration of the cells. Higher wettability of collagen containing scaffolds most likely improved the penetration of the cells as well as the cell medium was able to go inside the structure of the scaffolds more easily. Seeding of the cells was done with a pipette onto the top surface of the scaffolds. The seeding of the cells by other methods such as injecting with a needle could also improve the even distribution of the cells into the scaffolds. The incorporation of chitosan to collagen hydrogel has been found to improve the viability and metabolic activity of chondrocytes of collagen+chitosan dense hydrogels (Chicatun et al. 2013). Therefore, to study the ability of the collagen+chitosan blend scaffolds for cartilage tissue engineering, the neutralisation of the chitosan component still

needs to be verified in order to find out the actual properties of the scaffolds with chitosan, C1C1 and C2C1, as a matrix.

For articular cartilage tissue engineering, earlier studies have demonstrated that neither PLA nor collagen has been an optimal scaffold for articular cartilage. The PLA matrix was shown to be too hard (Pulliainen et al. 2007) and collagen gels suffered from contraction (Pulkkinen et al. 2010). Therefore, it was predicted that a study that combines these two structures with freeze-drying would overcome these limitations. When using the PLA96 carded mesh as a skeleton for the hybrid and freeze-drying and cross-linking the collagen component, a more optimal structure could be achieved. With natural polymer-based scaffolds, the best results for tissue engineering application were found with ColPLA and C2C1PLA hybrid scaffolds, and it indicates the positive outcome of the hybridisation and potential for cartilage tissue engineering.

Our group investigated the collagen+PLA96 hybrid with PLA96 fibrous mesh (needle punched carded mesh) inside the collagen component (Muhonen et al. 2015, unpublished data) with good results. In the study, a needle punched fibrous structure was used because the needle punching gives the PLA96 carded mesh more mechanical stability compared with PLA96 carded mesh without the needle punching procedure, as studied in Publication IV. Recombinant human collagen type II (an optimal collagen for cartilage tissue engineering because collagen type II is the most abundant collagen in cartilage) together with PLA96 needle punched carded mesh were combined together into a structure where the PLA96 mesh was immersed in recombinant human collagen type II to form a homogenous scaffold structure with two highly porous 3D structures combined in the hybrid. We studied the hybrids *in vivo* in a porcine model to investigate the ability of the scaffold to repair full-thickness cartilage lesion. The scaffold was compared with spontaneous healing and a commercial biomaterial scaffold operated with a second-generation ACI together with autologous chondrocytes. The repair tissue was evaluated after 4 months. The results showed that hyaline-like repair tissue was formed more frequently with the studied recombinant human type II collagen+PLA96 needle punched carded mesh than with the commercial control scaffold or spontaneous healing. Biomechanically, both studied scaffolds resulted in better repair tissue than the spontaneous healing. In addition, adverse bone reactions were less frequent in recombinant human type II collagen+PLA96 needle punched carded mesh scaffolds than with the other groups studied.

8.9 The feasibility of the freeze-dried synthetic polymer-based scaffolds for bone and osteochondral tissue engineering

The synthetic polymer-based scaffolds, the PLA70+TCP and PLA70+BG composite scaffolds in Publications II and III, were studied for bone and osteochondral applications. The viability, distribution, proliferation and osteogenic differentiation of ASCs were studied on the scaffolds in Publication II. After 2 weeks in culture, the number of the cells was increased compared with the 3 h time

point. After 3 h, the cells were mainly attached to the porous bottom surface (where the cells were seeded), and after 2 weeks the cells were spread inside the scaffolds as well. Still, the majority of the cells were still in the region close to the surface and only a few cells were on the top surface of the scaffolds. The filler particles (TCP or BG) did not affect the morphology of the cells. The cell number was significantly higher in PLA70+TCP composite scaffolds, and PLA2TCP10 scaffolds had a significantly higher magnitude of ALP activity. The relative ALP activity increased in all scaffold types from week 1 to week 2. No significant difference was found between the two different filler ratios (10 or 20 wt% of TCP or BG) in the attachment, proliferation or differentiation of ASCs. The PLA70+TCP composite scaffolds significantly enhanced the ASC proliferation and total ALP activity compared with the other scaffolds (PLA70+BG and plain PLA70) and demonstrates their potential as bone tissue engineering scaffolds.

The feasibility of the PLGA+BGf scaffolds for bone tissue engineering still needs to be verified. We are subsequently performing *in vivo* studies in rabbit-model to study the suitability of these kinds of PLGA+BGf scaffolds for bone tissue regeneration. Earlier studies (Orava et al. 2007) have demonstrated the feasibility of PLGA+BG porous composites to show fast resorption of the scaffold with very good bone tissue regeneration when studied in a rat-model. Those scaffolds were, however, manufactured by solvent casting and pressure quenching with CO_2 with an inhomogeneous scaffold structure and with a higher pore size in the scaffolds. The pore size was 50–500 µm, and the used filler was BG particles.

8.10 Freeze-dried scaffolds for cartilage and osteochondral tissue engineering

For synthetic polymer-based scaffolds, the composite structure with TCP particles or BGf fibres as fillers resulted in a better outcome compared with plain polymer scaffolds. Also, the composites with TCP particles showed a better outcome than the scaffolds with BG particles as filler (Publications II and III). The use of a highly porous 3D fibrous structure as reinforcement seems to be an optimal way to overcome the limitations (low mechanical strength, poor dimensional stability or bioactivity) of both natural and synthetic polymer-based freeze-dried scaffolds (Publications IV and V). The more homogenous structure in Publication V with carded BG fibres immersed thoroughly inside the matrix polymer, PLGA70 would be a more favourable method than to use fibrous filler inside the freeze-dried polymer matrix of hybrids or composites.

The structure of the optimal composite scaffolds manufactured by freeze-drying could be the combination of two highly porous 3D structures: a highly porous polymer matrix and a highly porous fibrous mesh, as studied here. However, this will probably work optimally only for single tissue applications, i.e., for cartilage or bone tissue engineering. The solution for optimal osteochondral scaffolds is still unknown. It is assumed that these two components, a cartilage scaffold and a bone

scaffold, could be combined using freeze-drying. Using the freeze-drying technique, the combining of different layers (for cartilage and bone) is relatively easy (Levingstone et al. 2014). The two different layers could be fabricated separately and then glued together with a suitable polymer solution. Freeze-drying the structure again would then combine the layers. Alternatively, the different layers could be processed with a two-step process where the second layer is processed on top of the first layer to form a bi-layer osteochondral scaffold. One possibility is to use two different filler structures, one for bone and one for cartilage, on top of each other and then to combine them into one scaffold with the addition of a suitable polymer solution as a combined matrix by freeze-drying.

As the outcome of this thesis, the idea was to preferably use the two scaffolds, one for cartilage and one for bone, separately and to combine them if needed. With this method, the cultivation of the chondrogenic and osteogenic cells can be performed in separate media and environmental conditions. These two layers could then be combined during the operation. However, with this method poor adhesion between the two layers could be a challenge (Shimomura et al. 2014). Also, the size of the lesion varies and, therefore, it might even be impossible to manufacture a one size combined scaffold for osteochondral lesions. Therefore, the method to use two different scaffolds with the correct scaffold size for both lesions would be a preferable way to overcome the problem.

9 Summary and conclusions

Since osteochondral tissue engineering requires a scaffold for both cartilage and underlying bone (i.e. subchondral bone) for the regeneration of damaged tissues, there are several possibilities to achieve the goal. Using one scaffold for both tissues is the easiest method. However, the different characteristics of the different tissues are not always fulfilled with this technique. The use of two distinct scaffolds, one for cartilage and one for bone tissues could, therefore, be an optimal way to solve the problem.

Scaffolds suitable for cartilage (Publication IV), bone (Publications II, III, and V) and osteochondral tissue engineering (Publications II and III) were successfully manufactured using the freeze-drying technique. Some of the scaffolds with a heterogeneous structure (Publications II and III) could be used for either only bone or as combined scaffolds for osteochondral tissue engineering. The structure of all of the studied scaffolds was highly porous and interconnected pores were detected in all the scaffolds. The filler in the scaffolds were not found to affect the pore structure, pore size or interconnectivity of the pores. The interconnection between the filler particles or fibrous filler mesh was good in all the composite or hybrid scaffolds.

Cross-linking with EDC post freeze-drying was found to be the most effective way to cross-link collagen scaffolds (Publication I). The blending of collagen with chitosan was not found to improve the properties of the scaffolds (Publication IV). However, this was due to inadequate neutralization of chitosan. The natural polymer-based hybrids were found to have improved compressive stiffness compared with the plain scaffolds (Publication IV).

The TCP or BG particles in the PLA70 composite scaffolds were found to improve the osteoconductive properties of the scaffolds in Publications II and III. No significant difference was found between the different amounts of the filler in the composites. The composite structure in Publication V with a fibrous BG mesh in freeze-dried PLGA matrices was found to stabilise the structure of the composites, and the BGf buffered the acidic degradation products of PLGA in the composites.

The TCP particles in the structure of the PLA70 composite scaffolds were found to improve the cell proliferation and total ALP activity of ASCs when compared with plain PLA70 or PLA70+BG composite scaffolds in Publication II. The viability and attachment of chondrocytes were good in all the natural polymer-based scaffolds in Publication IV. However, the PLA96 fibrous mesh in the hybrid scaffolds increased the penetration of the cells and the best penetration was found to be in the ColPLA and C2C1PLA hybrid scaffolds.

The use of two highly porous 3D structures combined, a porous freeze-dried matrix polymer combined with a porous fibrous mesh (manufactured from polymer or bioactive glass) led to improved properties of the studied scaffolds (Publications IV and V). The studied sandwich structure with a

softer freeze-dried polymer component in the middle of the scaffolds (Publication IV) was found not to be an optimal structure. Therefore, a homogenous structure with filler thoroughly inside the scaffold (Publication V) could lead to improved structure.

Finding the optimal osteochondral scaffold is still in the future. However, if the optimal cartilage and bone scaffolds are developed and then combined, the possibility of developing an optimal osteochondral scaffold could be closer. The study of the optimal cartilage tissue engineering scaffold is still ongoing and the latest results are promising. However, the study of the optimal bone tissue engineering scaffold needs further evaluation. In addition, the method of using a two-component osteochondral scaffold with separate cartilage and bone layers still needs to be studied more extensively to find out if the most convenient method for osteochondral scaffold is to combine the two layers.

10 Suggestions for future work

Our latest study (Muhonen et al. 2015, unpublished data) led to the promising *in vivo* results when using the combination of recombinant human collagen type II and PLA96 needle punched carded mesh. We will take these scaffolds to the next experiments to apply them in **cartilage tissue engineering**.

For **bone tissue engineering** we will study how the above-mentioned structure of cartilage scaffold with porous freeze-dried polymer combined with needle punched carded mesh will act in bone. The literature indicates the pores in bone tissue engineering scaffolds should be bigger than 100 µm and our developed synthetic polymer-based scaffolds had lower pore sizes (compared to natural polymer based scaffolds). Therefore, it is necessary to further optimize the freeze-drying of synthetic polymer-based scaffolds to increase the pore sizes. Also, we found the synthetic polymer-based scaffolds rather hydrophobic. That is why we plan to improve hydrophilicity by combining the synthetic polymer matrix with BG fibrous mesh so that the BG fibres are on the surface of the scaffolds as well. As an alternative, the synthetic polymer can be replaced with collagen type I for freeze-dried component for better hydrophilicity and for better compatibility with bone. Although the natural polymers often suffer for inferior mechanical stability, collagen together with mechanically more stable BG fibrous mesh could give the required mechanical stability for the structure.

The study of **osteochondral tissue engineering** will continue by combining the cartilage and bone tissue engineering scaffolds to achieve osteochondral scaffold structure. We will compare the characteristics of two approaches: the two separate scaffolds (osteo-scaffold and cartilage-scaffold) combined in implantation or a single osteochondral scaffold. For an osteochondral scaffold and tissue engineering we need to further develop the manufacturing of the scaffolds and co-culture of chondrocytes and osteoblasts, or mesenchymal stem cells.

References

Aboudzadeh, N., Imani, M., Shokrgozar, M.A., Khavandi, A., Javadpour, J., Shafieyan, Y. & Farokhi, M. 2010. Fabrication and characterization of poly(D,L-lactide-co-glycolide)/ hydroxyapatite nanocomposite scaffolds for bone tissue regeneration. Journal of Biomedical Materials Research - Part A 94, 1, pp. 137-145.

Ahola, N., Veiranto, M., Männistö, N., Karp, M., Rich, J., Efimov, A., Seppälä, J. & Kellomäki, M. 2012. Processing and sustained in vitro release of rifampicin containing composites to enhance the treatment of osteomyelitis. Biomatter 2, 4, pp. 213-225.

Akkouch, A., Zhang, Z. & Rouabhia, M. 2011. A novel collagen/hydroxyapatite/poly(lactide-co-Îµ-caprolactone) biodegradable and bioactive 3D porous scaffold for bone regeneration. Journal of Biomedical Materials Research - Part A 96 A, 4, pp. 693-704.

Al-Munajjed, A.A. & O'Brien, F.J. 2009. Influence of a novel calcium-phosphate coating on the mechanical properties of highly porous collagen scaffolds for bone repair. Journal of the Mechanical Behavior of Biomedical Materials 2, 2, pp. 138-146.

Al-Munajjed, A.A., Plunkett, N.A., Gleeson, J.P., Weber, T., Jungreuthmayer, C., Levingstone, T., Hammer, J. & O'Brien, F.J. 2009. Development of a biomimetic collagen-hydroxyapatite scaffold for bone tissue engineering using a SBF immersion technique. Journal of Biomedical Materials Research - Part B Applied Biomaterials 90, 2, pp. 584-591.

Arpornmaeklong, P., Pripatnanont, P. & Suwatwirote, N. 2008. Properties of chitosan-collagen sponges and osteogenic differentiation of rat-bone-marrow stromal cells. International journal of oral and maxillofacial surgery 37, 4, pp. 357-366.

Ashby, M. 2013. Designing architectured materials. Scripta Materialia 68, 1, pp. 4-7.

Ashby, M.F. & Bréchet, Y.J.M. 2003. Designing hybrid materials. Acta Materialia 51, 19, pp. 5801-5821.

Bian, S., Lu, W., Xu, C., Fan, Y. & Zhang, X. 2014. In vitro cartilage tissue engineering using porous collagen/PLLA nanoparticle hybrid scaffold. Journal of Medical and Biological Engineering 34, 1, pp. 36-43.

Boccaccini, A.R., Blaker, J.J., Maquet, V., Day, R.M. & Jéróme, R. 2005. Preparation and characterisation of poly(lactide-co-grycolide) (PLGA) and PLGA/Bioglass® composite tubular foam scaffolds for tissue engineering applications. Materials Science and Engineering C 25, 1, pp. 23-31.

Boccaccini, A.R. & Maquet, V. 2003. Bioresorbable and bioactive polymer/Bioglass® composites with tailored pore structure for tissue engineering applications. Composites Science and Technology 63, 16, pp. 2417-2429.

Bohner, M. & Baumgart, F. 2004. Theoretical model to determine the effects of geometrical factors on the resorption of calcium phosphate bone substitutes. Biomaterials 25, 17, pp. 3569-3582.

Cao, H. & Xu, S. 2008. EDC/NHS-crosslinked type II collagen-chondroitin sulfate scaffold: Characterization and in vitro evaluation. Journal of Materials Science: Materials in Medicine 19, 2, pp. 567-575.

Castro, N.J., Hacking, S.A. & Zhang, L.G. 2012. Recent progress in interfacial tissue engineering approaches for osteochondral defects. Annals of Biomedical Engineering 40, 8, pp. 1628-1640.

Chen, G., Sato, T., Ushida, T., Hirochika, R., Shirasaki, Y., Ochiai, N. & Tateishi, T. 2003. The use of a novel PLGA fiber/collagen composite web as a scaffold for engineering of articular cartilage tissue with adjustable thickness. Journal of Biomedical Materials Research - Part A 67, 4, pp. 1170-1180.

Chen, G., Sato, T., Ushida, T., Ochiai, N. & Tateishi, T. 2004. Tissue Engineering of Cartilage Using a Hybrid Scaffold of Synthetic Polymer and Collagen. Tissue engineering 10, 3-4, pp. 323-330.

Chen, G., Tanaka, J. & Tateishi, T. 2006. Osteochondral tissue engineering using a PLGA-collagen hybrid mesh. Materials Science and Engineering C 26, 1, pp. 124-129.

Chen, G., Ushida, T. & Tateishi, T. 2002. Scaffold design for tissue engineering. Macromolecular Bioscience 2, 2, pp. 67-77.

Chen, J., Chen, H., Li, P., Diao, H., Zhu, S., Dong, L., Wang, R., Guo, T., Zhao, J. & Zhang, J. 2011. Simultaneous regeneration of articular cartilage and subchondral bone in vivo using MSCs induced by a spatially controlled gene delivery system in bilayered integrated scaffolds. Biomaterials 32, 21, pp. 4793-4805.

Chiang, H. & Jiang, C. 2009. Repair of articular cartilage dafects: Review and perspectives. Journal of the Formosan Medical Association 108, 2, pp. 87-101.

Chicatun, F., Pedraza, C.E., Muja, N., Ghezzi, C.E., McKee, M.D. & Nazhat, S.N. 2013. Effect of Chitosan incorporation and Scaffold geometry on chondrocyte function in dense collagen type i hydrogels. Tissue Engineering - Part A 19, 23-24, pp. 2553-2564.

Chomchalao, P., Pongcharoen, S., Sutheerawattananonda, M. & Tiyaboonchai, W. 2013. Fibroin and fibroin blended three-dimensional scaffolds for rat chondrocyte culture. BioMedical Engineering Online 12, 1, Article number 28.

Chung, C. & Burdick, J.A. 2008. Engineering cartilage tissue. Advanced Drug Delivery Reviews 60, 2, pp. 243-262.

Ciardelli, G., Gentile, P., Chiono, V., Mattioli-Belmonte, M., Vozzi, G., Barbani, N. & Giusti, P. 2010. Enzymatically crosslinked porous composite matrices for bone tissue regeneration. Journal of Biomedical Materials Research - Part A 92, 1, pp. 137-151.

Cunniffe, G.M., Dickson, G.R., Partap, S., Stanton, K.T. & O'Brien, F.J. 2010. Development and characterisation of a collagen nano-hydroxyapatite composite scaffold for bone tissue engineering. Journal of materials science: Materials in medicine 21, 8, pp. 2293-2298.

Dai, W., Kawazoe, N., Lin, X., Dong, J. & Chen, G. 2010. The influence of structural design of PLGA/collagen hybrid scaffolds in cartilage tissue engineering. Biomaterials 31, 8, pp. 2141-2152.

Di Martino, A., Sittinger, M. & Risbud, M.V. 2005. Chitosan: A versatile biopolymer for orthopaedic tissue-engineering. Biomaterials 26, 30, pp. 5983-5990.

Dimitriou, R., Jones, E., McGonagle, D. & Giannoudis, P.V. 2011. Bone regeneration: Current concepts and future directions. BMC Medicine 9, Article number 66.

Domard, A. & Domard, M. 2001. Chitosan: Structure-Properties Relationship and Biomedical Applications. In: Dumitrui, S. (ed.). Polymeric Biomaterials. 2nd ed. New York, NY, USA, Marcel Dekker Incorporated. pp. 187-212.

Doube, M., Klosowski, M.M., Arganda-Carreras, I., Cordelières, F.P., Dougherty, R.P., Jackson, J.S., Schmid, B., Hutchinson, J.R. & Shefelbine, S.J. 2010. BoneJ: Free and extensible bone image analysis in ImageJ. Bone 47, 6, pp. 1076-1079.

Duan, X. & Sheardown, H. 2005. Crosslinking of collagen with dendrimers. Journal of Biomedical Materials Research - Part A 75, 3, pp. 510-518.

Ellä, V. 2012. Effects of Processing Parameters on P(L/D)LA 96/4 Fibers and Fibrous Products for Medical Applications. Tampere University of Technology. 96 p.

Endogan Tanir, T., Hasirci, V. & Hasirci, N. 2014. Preparation and characterization of Chitosan and PLGA-based scaffolds for tissue engineering applications. Polymer Composites .

Ferreira, A.M., Gentile, P., Chiono, V. & Ciardelli, G. 2012. Collagen for bone tissue regeneration. Acta Biomaterialia 8, 9, pp. 3191-3200.

Ficai, M., Andronescu, E., Ficai, D., Voicu, G. & Ficai, A. 2010. Synthesis and characterization of COLL-PVA/HA hybrid materials with stratified morphology. Colloids and Surfaces B: Biointerfaces 81, 2, pp. 614-619.

Fisher, M.B. & Mauck, R.L. 2013. Tissue engineering and regenerative medicine: Recent innovations and the transition to translation. Tissue Engineering - Part B: Reviews 19, 1, pp. 1-13.

Flink, J.M. & Knudsen, H. 1983. An introduction to freeze drying. 1st ed. Denmark, Strandberg Bogtryk/Offset a.s.

Francis Suh, J. & Matthew, H.W.T. 2000. Application of chitosan-based polysaccharide biomaterials in cartilage tissue engineering: A review. Biomaterials 21, 24, pp. 2589-2598.

Franks, F. 1998. Freeze-drying of bioproducts: Putting principles into practice. European Journal of Pharmaceutics and Biopharmaceutics 45, 3, pp. 221-229.

Freyman, T.M., Yannas, I.V. & Gibson, L.J. 2001. Cellular materials as porous scaffolds for tissue engineering. Progress in Materials Science 46, 3-4, pp. 273-282.

Friess, W. & Lee, G. 1996. Basic thermoanalytical studies of insoluble collagen matrices. Biomaterials 17, 23, pp. 2289-2294.

Friess, W. 1998. Collagen - Biomaterial for drug delivery. European Journal of Pharmaceutics and Biopharmaceutics 45, 2, pp. 113-136.

Ge, Z., Li, C., Heng, B.C., Cao, G. & Yang, Z. 2012. Functional biomaterials for cartilage regeneration. Journal of Biomedical Materials Research - Part A 100 A, 9, pp. 2526-2536.

Gelse, K., Pöschl, E. & Aigner, T. 2003. Collagens - Structure, function, and biosynthesis. Advanced Drug Delivery Reviews 55, 12, pp. 1531-1546.

Gentile, P., Chiono, V., Tonda-Turo, C., Mattu, C., Baino, F., Vitale-Brovarone, C. & Ciardelli, G. 2012a. Bioresorbable glass effect on the physico-chemical properties of bilayered scaffolds for osteochondral regeneration. Materials Letters 89, pp. 74-76.

Gentile, P., Mattioli-Belmonte, M., Chiono, V., Ferretti, C., Baino, F., Tonda-Turo, C., Vitale-Brovarone, C., Pashkuleva, I., Reis, R.L. & Ciardelli, G. 2012b. Bioactive glass/polymer composite scaffolds mimicking bone tissue. Journal of Biomedical Materials Research - Part A 100 A, 10, pp. 2654-2667.

Gibson, L.J., Ashby, M. & Harley, B.A. 2010. Cellular Materials in Nature and Medicine. Cambridge, UK, Cambridge University Press. 309 p.

Gomes, M.E. & Reis, R.L. 2004. Biodegradable polymers and composites in biomedical applications: From catgut to tissue engineering Part 2 Systems for temporary replacement and advanced tissue regeneration. International Materials Reviews 49, 5, pp. 274-285.

Gordon, M.K. & Hahn, R.A. 2010. Collagens. Cell and tissue research 339, 1, pp. 247-257.

Griffon, D.J., Sedighi, M.R., Schaeffer, D.V., Eurell, J.A. & Johnson, A.L. 2006. Chitosan scaffolds: Interconnective pore size and cartilage engineering. Acta Biomaterialia 2, 3, pp. 313-320.

Groot, W., van Krieken, J., Sliekersl, O. & de Vos, S. 2010. Production and purification of lactic acid and lactide. In: Auras, R., Lim, L.T., Selke, S.E.M. & Tsuji, H. (ed.). Poly(lactic acid): Synthesis, structures, properties, processing, and applications. 1st ed. Hoboken, New Jersey, John Wiley & Sons, Inc. pp. 3-18.

Gunatillake, P.A., Adhikari, R. & Gadegaard, N. 2003. Biodegradable synthetic polymers for tissue engineering. European Cells and Materials 5, pp. 1-16.

Gupta, A.P. & Kumar, V. 2007. New emerging trends in synthetic biodegradable polymers - Polylactide: A critique. European Polymer Journal 43, 10, pp. 4053-4074.

Harley, B.A., Leung, J.H., Silva, E.C.C.M. & Gibson, L.J. 2007. Mechanical characterization of collagen-glycosaminoglycan scaffolds. Acta Biomaterialia 3, 4, pp. 463-474.

Harley, B.A., Lynn, A.K., Wissner-Gross, Z., Bonfield, W., Yannas, I.V. & Gibson, L.J. 2010a. Design of a multiphase osteochondral scaffold III: Fabrication of layered scaffolds with continuous interfaces. Journal of Biomedical Materials Research - Part A 92, 3, pp. 1078-1093.

Harley, B.A., Lynn, A.K., Wissner-Gross, Z., Bonfield, W., Yannas, I.V. & Gibson, L.J. 2010b. Design of a multiphase osteochondral scaffold. II. Fabrication of a mineralized collagen-glycosaminoglycan scaffold. Journal of Biomedical Materials Research - Part A 92, 3, pp. 1066-1077.

Heidemann, W., Jeschkeit, S., Ruffieux, K., Fischer, J.H., Wagner, M., Krüger, G., Wintermantel, E. & Gerlach, K.L. 2001. Degradation of poly(D,L)lactide implants with or without addition of calciumphosphates in vivo. Biomaterials 22, 17, pp. 2371-2381.

Hench, L.L. & Polak, J.M. 2002. Third-generation biomedical materials. Science 295, 5557, pp. 1014-1017.

Hiraoka, Y., Kimura, Y., Ueda, H. & Tabata, Y. 2003. Fabrication and Biocompatibility of Collagen Sponge Reinforced with Poly(glycolic acid) Fiber. Tissue engineering 9, 6, pp. 1101-1112.

Ho, M., Kuo, P., Hsieh, H., Hsien, T., Hou, L., Lai, J. & Wang, D. 2004. Preparation of porous scaffolds by using freeze-extraction and freeze-gelation methods. Biomaterials 25, 1, pp. 129-138.

Hokugo, A., Takamoto, T. & Tabata, Y. 2006. Preparation of hybrid scaffold from fibrin and biodegradable polymer fiber. Biomaterials 27, 1, pp. 61-67.

Holland, T.A & Mikos, A.G. 2006. Review: Biodegradable polymeric scaffolds. Improvements in bone tissue engineering through controlled drug delivery. Biodegradable polymers: Bone tissue engineering: Drug delivery. 102, pp. 161-185.

Hosseinkhani, H., Hosseinkhani, M., Tian, F., Kobayashi, H. & Tabata, Y. 2006. Ectopic bone formation in collagen sponge self-assembled peptide-amphiphile nanofibers hybrid scaffold in a perfusion culture bioreactor. Biomaterials 27, 29, pp. 5089-5098.

Hoyer, B., Bernhardt, A., Heinemann, S., Stachel, I., Meyer, M. & Gelinsky, M. 2012. Biomimetically mineralized salmon collagen scaffolds for application in bone tissue engineering. Biomacromolecules 13, 4, pp. 1059-1066.

Huang, X., Yang, D., Yan, W., Shi, Z., Feng, J., Gao, Y., Weng, W. & Yan, S. 2007. Osteochondral repair using the combination of fibroblast growth factor and amorphous calcium phosphate/poly(l-lactic acid) hybrid materials. Biomaterials 28, 20, pp. 3091-3100.

Hulbert, S.F., Young, F.A., Mathews, R.S., Klawitter, J.J., Talbert, C.D. & Stelling, F.H. 1970. Potential of ceramic materials as permanently implantable skeletal prostheses. Journal of Biomedical Materials Research 4, 3, pp. 433-456.

Hull, D. & Clyne, T.W. 1996. An introduction to composite materials. Second edition ed. Cambridge, UK, Cambridge University Press. 326 p.

Hunziker, E.B. 2002. Articular cartilage repair: Basic science and clinical progress. A review of the current status and prospects. Osteoarthritis and Cartilage 10, 6, pp. 432-463.

Hutmacher, D.W. 2000. Scaffolds in tissue engineering bone and cartilage. Biomaterials 21, 24, pp. 2529-2543.

Huttunen, M., Ashammakhi, N., Törmälä, P. & Kellomäki, M. 2006. Fibre reinforced bioresorbable composites for spinal surgery. Acta Biomaterialia 2, 5, pp. 575-587.

Ignatius, A., Blessing, H., Liedert, A., Schmidt, C., Neidlinger-Wilke, C., Kaspar, D., Friemert, B. & Claes, L. 2005. Tissue engineering of bone: Effects of mechanical strain on osteoblastic cells in type I collagen matrices. Biomaterials 26, 3, pp. 311-318.

International Standard, ISO 15814. 1999. Implants for surgery - copolymers and blends based on polylactide - in vitro degradation testing.

Itälä, A.I., Ylnen, H.O., Ekholm, C., Karlsson, K.H. & Aro, H.T. 2001. Pore diameter of more than 100 μm is not requisite for bone ingrowth in rabbits. Journal of Biomedical Materials Research 58, 6, pp. 679-683.

Iwasa, J., Engebretsen, L., Shima, Y. & Ochi, M. 2009. Clinical application of scaffolds for cartilage tissue engineering. Knee Surgery, Sports Traumatology, Arthroscopy 17, 6, pp. 561-577.

Jagur-Grodzinski, J. 2006. Polymers for tissue engineering, medical devices, and regenerative medicine. Concise general review of recent studies. Polymers for Advanced Technologies 17, 6, pp. 395-418.

Jayakumar, R., Ramachandran, R., Divyarani, V.V., Chennazhi, K.P., Tamura, H. & Nair, S.V. 2011. Fabrication of chitin-chitosan/nano TiO2-composite scaffolds for tissue engineering applications. International journal of biological macromolecules 48, 2, pp. 336-344.

Jia, L., Duan, Z., Fan, D., Mi, Y., Hui, J. & Chang, L. 2013. Human-like collagen/nano-hydroxyapatite scaffolds for the culture of chondrocytes. Materials Science and Engineering C 33, 2, pp. 727-734.

Jiang, L., Li, Y., Wang, X., Zhang, L., Wen, J. & Gong, M. 2008. Preparation and properties of nano-hydroxyapatite/chitosan/carboxymethyl cellulose composite scaffold. Carbohydrate Polymers 74, 3, pp. 680-684.

Jin, H., Kim, D., Kim, T., Shin, K., Jung, J.S., Park, H. & Yoon, S. 2012. In vivo evaluation of porous hydroxyapatite/chitosan-alginate composite scaffolds for bone tissue engineering. International journal of biological macromolecules 51, 5, pp. 1079-1085.

Jukola, H., Nikkola, L., Gomes, M.E., Chiellini, F., Tukiainen, M., Kellomäki, M., Chiellini, E., Reis, R.L. & Ashammakhi, N. 2008. Development of a bioactive glass fiber reinforced starch-polycaprolactone composite. Journal of Biomedical Materials Research - Part B Applied Biomaterials 87, 1, pp. 197-203.

Kane, R.J. & Roeder, R.K. 2012. Effects of hydroxyapatite reinforcement on the architecture and mechanical properties of freeze-dried collagen scaffolds. Journal of the Mechanical Behavior of Biomedical Materials 7, pp. 41-49.

Karageorgiou, V. & Kaplan, D. 2005. Porosity of 3D biomaterial scaffolds and osteogenesis. Biomaterials 26, 27, pp. 5474-5491.

Karkhaneh, A., Naghizadeh, Z., Shokrgozar, M.A. & Bonakdar, S. 2014. Evaluation of the chondrogenic differentiation of mesenchymal stem cells on hybrid biomimetic scaffolds. Journal of Applied Polymer Science 131, 16, .

Kellomäki, M., Puumanen, K., Waris, T. & Törmälä, P. 2000. In vivo degradation of composite membrane of P(e-CL/L-LA) 50/50 film and PLDLA 96/4 mesh. Materials for Medical Engineering: Euromat 2, pp. 73-79.

Kim, H., Knowles, J.C. & Kim, H. 2005. Hydroxyapatite and gelatin composite foams processed via novel freeze-drying and crosslinking for use as temporary hard tissue scaffolds. Journal of Biomedical Materials Research - Part A 72, 2, pp. 136-145.

Kim, I., Seo, S., Moon, H., Yoo, M., Park, I., Kim, B. & Cho, C. 2008. Chitosan and its derivatives for tissue engineering applications. Biotechnology Advances 26, 1, pp. 1-21.

Kinner, B., Capita, R.M., Spector, M. 2005. Regeneration of articular cartilage. Advantages in Biochemical Engineering/Biotechnology 94, pp. 91-123.

Kneser, U., Schaefer, D.J., Polykandriotis, E. & Horch, R.E. 2006. Tissue engineering of bone: The reconstructive surgeon's point of view. Journal of Cellular and Molecular Medicine 10, 1, pp. 7-19.

Ko, C., Huang, J., Huang, C. & Chu, I. 2009. Type II collagen-chondroitin sulfate-hyaluronan scaffold cross-linked by genipin for cartilage tissue engineering. Journal of Bioscience and Bioengineering 107, 2, pp. 177-182.

Kock, L., Van Donkelaar, C.C. & Ito, K. 2012. Tissue engineering of functional articular cartilage: The current status. Cell and tissue research 347, 3, pp. 613-627.

Kon, E., Delcogliano, M., Filardo, G., Pressato, D., Busacca, M., Grigolo, B., Desando, G. & Marcacci, M. 2010. A novel nano-composite multi-layered biomaterial for treatment of osteochondral lesions: Technique note and an early stability pilot clinical trial. Injury 41, 7, pp. 693-701.

Kricheldorf, H.R. 2001. Syntheses and application of polylactides. Chemosphere 43, 1, pp. 49-54.

Kumar, P.T.S., Srinivasan, S., Lakshmanan, V., Tamura, H., Nair, S.V. & Jayakumar, R. 2011. Synthesis, characterization and cytocompatibility studies of α-chitin hydrogel/nano hydroxyapatite composite scaffolds. International journal of biological macromolecules 49, 1, pp. 20-31.

Langer, R. 2000. Tissue engineering. Molecular Therapy 1, 1, pp. 12-15.

Lee, C.R., Grodzinsky, A.J. & Spector, M. 2001. The effects of cross-linking of collagen-glycosaminoglycan scaffolds on compressive stiffness, chondrocyte-mediated contraction, proliferation and biosynthesis. Biomaterials 22, 23, pp. 3145-3154.

Lee, J., Cuddihy, M.J. & Kotov, N.A. 2008. Three-dimensional cell culture matrices: State of the art. Tissue Engineering - Part B: Reviews 14, 1, pp. 61-86.

Lee, S.B., Kim, Y.H., Chong, M.S. & Lee, Y.M. 2004. Preparation and characteristics of hybrid scaffolds composed of β-chitin and collagen. Biomaterials 25, 12, pp. 2309-2317.

Lee, S.J., Lim, G.J., Lee, J., Atala, A. & Yoo, J.J. 2006. In vitro evaluation of a poly(lactide-co-glycolide)-collagen composite scaffold for bone regeneration. Biomaterials 27, 18, pp. 3466-3472.

Lehtonen, T.J., Tuominen, J.U. & Hiekkanen, E. 2013a. Dissolution behavior of high strength bioresorbable glass fibers manufactured by continuous fiber drawing. Journal of the Mechanical Behavior of Biomedical Materials 20, pp. 376-386.

Lehtonen, T.J., Tuominen, J.U. & Hiekkanen, E. 2013b. Resorbable composites with bioresorbable glass fibers for load-bearing applications. in vitro degradation and degradation mechanism. Acta Biomaterialia 9, 1, pp. 4868-4877.

Levingstone, T.J., Matsiko, A., Dickson, G.R., O'Brien, F.J. & Gleeson, J.P. 2014. A biomimetic multi-layered collagen-based scaffold for osteochondral repair. Acta Biomaterialia 10, 5, pp. 1996-2004.

Li, S.M., Garreau, H. & Vert, M. 1990. Structure-property relationships in the case of the degradation of massive aliphatic poly-(α-hydroxy acids) in aqueous media - Part 1: Poly(dl-lactic acid). Journal of Materials Science: Materials in Medicine 1, 3, pp. 123-130.

Li, X., Yang, Y., Fan, Y., Feng, Q., Cui, F. & Watari, F. 2014. Biocomposites reinforced by fibers or tubes as scaffolds for tissue engineering or regenerative medicine. Journal of Biomedical Materials Research - Part A 102, 5, pp. 1580-1594.

Lim, L.T., Cink, K. & Vanyo, T. 2010. Processing of poly(lactic acid). In: Auras, R., Lim, L.T., Selke, S.E.M. & Tsuji, H. (ed.). Poly(lactic acid): Synthesis, structures, properties, processing, and applications. 1st ed. Hoboken, New Jersey, John Wiley & Sons, Inc. pp. 191-215.

Lin, Y., Tan, F., Marra, K.G., Jan, S. & Liu, D. 2009. Synthesis and characterization of collagen/hyaluronan/chitosan composite sponges for potential biomedical applications. Acta Biomaterialia 5, 7, pp. 2591-2600.

Liu, C., Xia, Z. & Czernuszka, J.T. 2007. Design and development of three-dimensional scaffolds for tissue engineering. Chemical Engineering Research and Design 85, 7 A, pp. 1051-1064.

Liuyun, J., Yubao, L. & Chengdong, X. 2009. Preparation and biological properties of a novel composite scaffold of nano-hydroxyapatite/chitosan/carboxymethyl cellulose for bone tissue engineering. Journal of Biomedical Science 16, 1, Article number 65.

Liverani, L., Roether, J.A., Nooeaid, P., Trombetta, M., Schubert, D.W. & Boccaccini, A.R. 2012. Simple fabrication technique for multilayered stratified composite scaffolds suitable for interface tissue engineering. Materials Science and Engineering A 557, pp. 54-58.

Lu, H., Oh, H.H., Kawazoe, N., Yamagishi, K. & Chen, G. 2012. PLLA-collagen and PLLA-gelatin hybrid scaffolds with funnel-like porous structure for skin tissue engineering. Science and Technology of Advanced Materials 13, 6, Article number 064210.

Ma, J., Wang, H., He, B. & Chen, J. 2001. A preliminary in vitro study on the fabrication and tissue engineering applications of a novel chitosan bilayer material as a scaffold of human neofetal dermal fibroblasts. Biomaterials 22, 4, pp. 331-336.

Ma, L., Gao, C., Mao, Z., Zhou, J., Shen, J., Hu, X. & Han, C. 2003. Collagen/chitosan porous scaffolds with improved biostability for skin tissue engineering. Biomaterials 24, 26, pp. 4833-4841.

Ma, P.X. 2004. Scaffolds for tissue fabrication. Materials Today 7, 5, pp. 30-40.

Madihally, S.V. & Matthew, H.W.T. 1999. Porous chitosan scaffolds for tissue engineering. Biomaterials 20, 12, pp. 1133-1142.

Malafaya, P.B., Silva, G.A. & Reis, R.L. 2007. Natural-origin polymers as carriers and scaffolds for biomolecules and cell delivery in tissue engineering applications. Advanced Drug Delivery Reviews 59, 4-5, pp. 207-233.

Mano, J.F., Silva, G.A., Azevedo, H.S., Malafaya, P.B., Sousa, R.A., Silva, S.S., Boesel, L.F., Oliveira, J.M., Santos, T.C., Marques, A.P., Neves, N.M. & Reis, R.L. 2007. Natural origin biodegradable systems in tissue engineering and regenerative medicine: Present status and some moving trends. Journal of the Royal Society Interface 4, 17, pp. 999-1030.

Maquet, V., Boccaccini, A.R., Pravata, L., Notingher, I. & Jérôme, R. 2004. Porous poly(α-hydroxyacid)/Bioglass® composite scaffolds for bone tissue engineering. I: Preparation and in vitro characterisation. Biomaterials 25, 18, pp. 4185-4194.

Martin, I., Miot, S., Barbero, A., Jakob, M. & Wendt, D. 2007. Osteochondral tissue engineering. Journal of Biomechanics 40, 4, pp. 750-765.

Menzies, K.L. & Jones, L. 2010. The impact of contact angle on the biocompatibility of biomaterials. Optometry and Vision Science 87, 6, pp. 387-399.

Meyer, U. & Wiesmann, H.P. (ed.). 2006. Bone and cartilage engineering. Springer. 264 p.

Miki, T., Masaka, K., Imai, Y. & Enomoto, S. 2000. Experience with freeze-dried PGLA/HA/rhBMP-2 as a bone graft substitute. Journal of Cranio-Maxillofacial Surgery 28, 5, pp. 294-299.

Mikos, A.G. & Temenoff, J.S. 2000. Formation of highly porous biodegradable scaffolds for tissue engineering. Electronic Journal of Biotechnology 3, 2, pp. 114-119.

Miles, C.A., Avery, N.C., Rodin, V.V. & Bailey, A.J. 2005. The increase in denaturation temperature following cross-linking of collagen is caused by dehydration of the fibres. Journal of Molecular Biology 346, 2, pp. 551-556.

Mistry, A.S. & Mikos, A.G. 2005. Tissue engineering strategies for bone regeneration. Advances in Biochemical Engineering/Biotechnology 94, pp. 1-22.

Muhonen, V., Salonius, E., Järvinen, E., Haaparanta, A.M., Paatela, T., Meller, A., Hannula, M., Björkman, M., Pyhältö, T., Aula, A.S., Ellä, V., Vasara, A., Töyräs, J., Kellomäki, M., Kiviranta, I. 2015. Autologous chondrocyte implantation with recombinant human type II collagen / polylactide scaffold enhances articular cartilage repair in a porcine model, *to be submitted*.

Mohamad Yunos, D., Bretcanu, O. & Boccaccini, A. 2008. Polymer-bioceramic composites for tissue engineering scaffolds. Journal of Materials Science 43, 13, pp. 4433-4442.

Moutos, F.T. & Guilak, F. 2008. Composite scaffolds for cartilage tissue engineering. Biorheology 45, 3-4, pp. 501-512.

Muzzarelli, R.A.A. 2009. Chitins and chitosans for the repair of wounded skin, nerve, cartilage and bone. Carbohydrate Polymers 76, 2, pp. 167-182.

Nair, L.S. & Laurencin, C.T. 2007. Biodegradable polymers as biomaterials. Progress in Polymer Science (Oxford) 32, 8-9, pp. 762-798.

Nair, L.S. & Laurencin, C.T. 2006. Polymers as biomaterials for tissue engineering and controlled drug delivery. 2006. Advances in Biochemical Engineering/Biotechnology, 102, pp. 47-90.

Nanda, H.S., Chen, S., Zhang, Q., Kawazoe, N. & Chen, G. 2014. Collagen scaffolds with controlled insulin release and controlled pore structure for cartilage tissue engineering. BioMed Research International 2014, Article number 623805.

Navarro, M., Aparicio, C., Charles-Harris, M., Ginebra, M.P., Engel, E. & Planell, J.A. 2006. Development of a biodegradable composite scaffold for bone tissue engineering: Physicochemical, topographical, mechanical, degradation, and biological properties. Advances in Polymer Science, 200, 1, pp. 209-231.

Nettles, D.L., Elder, S.H. & Gilbert, J.A. 2002. Potential use of chitosan as a cell scaffold material for cartilage tissue engineering. Tissue engineering 8, 6, pp. 1009-1016.

Niemelä, T., Niiranen, H., Kellomäki, M. & Törmälä, P. 2005. Self-reinforced composites of bioabsorbable polymer and bioactive glass with different bioactive glass contents. Part I: Initial mechanical properties and bioactivity. Acta Biomaterialia 1, 2, pp. 235-242.

Niemelä, T., Niiranen, H. & Kellomäki, M. 2008. Self-reinforced composites of bioabsorbable polymer and bioactive glass with different bioactive glass contents. Part II: In vitro degradation. Acta Biomaterialia 4, 1, pp. 156-164.

Niemelä, T. 2005. Effect of ß-tricalcium phosphate addition on the in vitro degradation of self-reinforced poly-L,D-lactide. Polymer Degradation and Stability 89, 3, pp. 492-500.

Nikkola, L., Vapalahti, K., Huolman, R., Seppälä, J., Harlin, A. & Ashammakhi, N. 2008. Multilayer implant with triple drug releasing properties. Journal of Biomedical Nanotechnology 4, 3, pp. 331-338.

Nitzsche, H., Lochmann, A., Metz, H., Hauser, A., Syrowatka, F., Hempel, E., Müller, T., Thurn-Albrecht, T. & Mäder, K. 2010. Fabrication and characterization of a biomimetic composite scaffold for bone defect repair. Journal of Biomedical Materials Research - Part A 94, 1, pp. 298-307.

Nooeaid, P., Salih, V., Beier, J.P. & Boccaccini, A.R. 2012. Osteochondral tissue engineering: Scaffolds, stem cells and applications. Journal of Cellular and Molecular Medicine 16, 10, pp. 2247-2270.

Nukavarapu, S.P. & Dorcemus, D.L. 2013. Osteochondral tissue engineering: Current strategies and challenges. Biotechnology Advances 31, 5, pp. 706-721.

Oprita, E.I., Moldovan, L., Craciunescu, O. & Zarnescu, O. 2008. In vitro behaviour of osteoblast cells seeded into a COL/β-TCP composite scaffold. Central European Journal of Biology 3, 1, pp. 31-37.

Orava, E., Korventausta, J., Rosenberg, M., Jokinen, M. & Rosling, A. 2007. In vitro degradation of porous poly(dl-lactide-co-glycolide) (PLGA)/bioactive glass composite foams with a polar structure. Polymer Degradation and Stability 92, 1, pp. 14-23.

Panseri, S., Russo, A., Cunha, C., Bondi, A., Di Martino, A., Patella, S. & Kon, E. 2012. Osteochondral tissue engineering approaches for articular cartilage and subchondral bone regeneration. Knee Surgery, Sports Traumatology, Arthroscopy 20, 6, pp. 1182-1191.

Panzavolta, S., Fini, M., Nicoletti, A., Bracci, B., Rubini, K., Giardino, R. & Bigi, A. 2009. Porous composite scaffolds based on gelatin and partially hydrolyzed α-tricalcium phosphate. Acta Biomaterialia 5, 2, pp. 636-643.

Panzavolta, S., Torricelli, P., Amadori, S., Parrilli, A., Rubini, K., Della Bella, E., Fini, M. & Bigi, A. 2013. 3D interconnected porous biomimetic scaffolds: In vitro cell response. Journal of Biomedical Materials Research - Part A 101, 12, pp. 3560-3570.

Park, S., Park, J., Kim, H.O., Song, M.J. & Suh, H. 2002. Characterization of porous collagen/hyaluronic acid scaffold modified by 1-ethyl-3-(3-dimethylaminopropyl)carbodiimide cross-linking. Biomaterials 23, 4, pp. 1205-1212.

Pasqui, D., Torricelli, P., De Cagna, M., Fini, M. & Barbucci, R. 2014. Carboxymethyl cellulose - Hydroxyapatite hybrid hydrogel as a composite material for bone tissue engineering applications. Journal of Biomedical Materials Research - Part A 102, 5, pp. 1568-1579.

Patrascu, J.M., Krüger, J.P., Böss, H.G., Ketzmar, A., Freymann, U., Sittinger, M., Notter, M., Endres, M. & Kaps, C. 2013. Polyglycolic acid-hyaluronan scaffolds loaded with bone marrow-derived mesenchymal stem cells show chondrogenic differentiation in vitro and cartilage repair in the rabbit model. Journal of Biomedical Materials Research - Part B Applied Biomaterials 101, 7, pp. 1310-1320.

Pattnaik, S., Nethala, S., Tripathi, A., Saravanan, S., Moorthi, A. & Selvamurugan, N. 2011. Chitosan scaffolds containing silicon dioxide and zirconia nano particles for bone tissue engineering. International journal of biological macromolecules 49, 5, pp. 1167-1172.

Peltola, S.M., Melchels, F.P.W., Grijpma, D.W. & Kellomäki, M. 2008. A review of rapid prototyping techniques for tissue engineering purposes. Annals of Medicine 40, 4, pp. 268-280.

Pieper, J.S., Oosterhof, A., Dijkstra, P.J., Veerkamp, J.H. & Van Kuppevelt, T.H. 1999. Preparation and characterization of porous crosslinked collagenous matrices containing bioavailable chondroitin sulphate. Biomaterials 20, 9, pp. 847-858.

Pieper, J.S., Van Der Kraan, P.M., Hafmans, T., Kamp, J., Buma, P., Van Susante, J.L.C., Van Den Berg, W.B., Veerkamp, J.H. & Van Kuppevelt, T.H. 2002. Crosslinked type II collagen matrices: Preparation, characterization, and potential for cartilage engineering. Biomaterials 23, 15, pp. 3183-3192.

Pitt, G.G., Gratzl, M.M., Kimmel, G.L., Surles, J. & Sohindler, A. 1981. Aliphatic polyesters II. The degradation of poly (DL-lactide), poly (e-caprolactone), and their copolymers in vivo. Biomaterials 2, 4, pp. 215-220.

Pon-On, W., Charoenphandhu, N., Teerapornpuntakit, J., Thongbunchoo, J., Krishnamra, N. & Tang, I. 2014. Mechanical properties, biological activity and protein controlled release by poly(vinyl alcohol)-bioglass/chitosan-collagen composite scaffolds: A bone tissue engineering applications. Materials Science and Engineering C 38, 1, pp. 63-72.

Powell, H.M. & Boyce, S.T. 2006. EDC cross-linking improves skin substitute strength and stability. Biomaterials 27, 34, pp. 5821-5827.

Pulkkinen, H.J., Tiitu, V., Valonen, P., Jurvelin, J.S., Lammi, M.J. & Kiviranta, I. 2010. Engineering of cartilage in recombinant human type II collagen gel in nude mouse model in vivo. Osteoarthritis and Cartilage 18, 8, pp. 1077-1087.

Pulliainen, O., Vasara, A.I., Hyttinen, M.M., Tiitu, V., Valonen, P., Kellomäki, M., Jurvelin, J.S., Peterson, L., Lindahl, A., Kiviranta, I. & Lammi, M.J. 2007. Poly-L-D-lactic acid scaffold in the repair of porcine knee cartilage lesions. Tissue engineering 13, 6, pp. 1347-1355.

Puppi, D., Chiellini, F., Piras, A.M. & Chiellini, E. 2010. Polymeric materials for bone and cartilage repair. Progress in Polymer Science (Oxford) 35, 4, pp. 403-440.

Ramshaw, J.A.M., Peng, Y.Y., Glattauer, V. & Werkmeister, J.A. 2009. Collagens as biomaterials. Journal of Materials Science: Materials in Medicine 20, SUPPL. 1, pp. S3-S8.

Risbud, M.V. & Sittinger, M. 2002. Tissue engineering: Advances in in vitro cartilage generation. Trends in biotechnology 20, 8, pp. 351-356.

Roether, J.A., Gough, J.E., Boccaccini, A.R., Hench, L.L., Maquet, V. & Jérôme, R. 2002. Novel bioresorbable and bioactive composites based on bioactive glass and polylactide foams for bone tissue engineering. Journal of Materials Science: Materials in Medicine 13, 12, pp. 1207-1214.

Sagar, N., Soni, V.P. & Bellare, J.R. 2012. Influence of carboxymethyl chitin on stability and biocompatibility of 3D nanohydroxyapatite/gelatin/carboxymethyl chitin composite for bone tissue engineering. Journal of Biomedical Materials Research - Part B Applied Biomaterials 100 B, 3, pp. 624-636.

Salgado, A.J., Coutinho, O.P. & Reis, R.L. 2004. Bone tissue engineering: State of the art and future trends. Macromolecular Bioscience 4, 8, pp. 743-765.

Sato, T., Chen, G., Ushida, T., Ishii, T., Ochiai, N. & Tateishi, T. 2001. Tissue-engineered cartilage by in vivo culturing of chondrocytes in PLGA-collagen hybrid sponge. Materials Science and Engineering C 17, 1-2, pp. 83-89.

Schagemann, J.C., Chung, H.W., Mrosek, E.H., Stone, J.J., Fitzsimmons, J.S., O'Driscoll, S.W. & Reinholz, G.G. 2010. Poly-ε-caprolactone/gel hybrid scaffolds for cartilage tissue engineering. Journal of Biomedical Materials Research - Part A 93, 2, pp. 454-463.

Schindelin, J., Arganda-Carreras, I., Frise, E., Kaynig, V., Longair, M., Pietzsch, T., Preibisch, S., Rueden, C., Saalfeld, S., Schmid, B., Tinevez, J., White, D.J., Hartenstein, V., Eliceiri, K., Tomancak, P. & Cardona, A. 2012. Fiji: An open-source platform for biological-image analysis. Nature Methods 9, 7, pp. 676-682.

Schoof, H., Apel, J., Heschel, I. & Rau, G. 2001. Control of pore structure and size in freeze-dried collagen sponges. Journal of Biomedical Materials Research 58, 4, pp. 352-357.

Seo, Y. & Park, J. 2010. Tissue engineered scaffold utilizing the reinforced technique. Biotechnology and Bioprocess Engineering 15, 4, pp. 527-533

Shah Mohammadi, M., Bureau, M.N. & Nazhat, S.N. 2014. Polylactic acid (PLA) biomedical foams for tissue engineering. 2014. Biomedical Foams for Tissue Engineering Applications, pp. 313-334.

Shah, S.S., Cha, Y. & Pitt, C.G. 1992. Poly (glycolic acid-co-dl-lactic acid): diffusion or degradation controlled drug delivery? Journal of Controlled Release 18, 3, pp. 261-270.

Shen, X., Chen, L., Cai, X., Tong, T., Tong, H. & Hu, J. 2011. A novel method for the fabrication of homogeneous hydroxyapatite/collagen nanocomposite and nanocomposite scaffold with hierarchical porosity. Journal of Materials Science: Materials in Medicine 22, 2, pp. 299-305.

Shen, X., Tong, H., Jiang, T., Zhu, Z., Wan, P. & Hu, J. 2007. Homogeneous chitosan/carbonate apatite/citric acid nanocomposites prepared through a novel in situ precipitation method. Composites Science and Technology 67, 11-12, pp. 2238-2245.

Shih, C. 1995. Chain-end scission in acid catalyzed hydrolysis of poly (d,l-lactide) in solution. Journal of Controlled Release 34, 1, pp. 9-15.

Shimomura, K., Moriguchi, Y., Murawski, C.D., Yoshikawa, H. & Nakamura, N. 2014. Osteochondral Tissue Engineering with Biphasic Scaffold: Current Strategies and Techniques. Tissue Engineering Part B: Reviews 20, 5, pp. 468-476.

Singh, D., Tripathi, A., Zo, S., Singh, D. & Han, S.S. 2014. Synthesis of composite gelatin-hyaluronic acid-alginate porous scaffold and evaluation for in vitro stem cell growth and in vivo tissue integration. Colloids and Surfaces B: Biointerfaces 116, pp. 502-509.

Sionkowska, A. & Kozłowska, J. 2010. Characterization of collagen/hydroxyapatite composite sponges as a potential bone substitute. International journal of biological macromolecules 47, 4, pp. 483-487.

Södergård, A. & Stolt, M. 2002. Properties of lactic acid based polymers and their correlation with composition. Progress in Polymer Science (Oxford) 27, 6, pp. 1123-1163.

Stevens, B., Yang, Y., Mohandas, A., Stucker, B. & Nguyen, K.T. 2008. A review of materials, fabrication methods, and strategies used to enhance bone regeneration in engineered bone tissues. Journal of Biomedical Materials Research - Part B Applied Biomaterials 85, 2, pp. 573-582.

Sun, Y., Xing, Z., Xue, Y., Mustafa, K., Finne-Wistrand, A. & Albertsson, A. 2014. Surfactant as a critical factor when tuning the hydrophilicity in three-dimensional polyester-based scaffolds: Impact of hydrophilicity on their mechanical properties and the cellular response of human osteoblast-like cells. Biomacromolecules 15, 4, pp. 1259-1268.

Tamaddon, M., Walton, R.S., Brand, D.D. & Czernuszka, J.T. 2013. Characterisation of freeze-dried type II collagen and chondroitin sulfate scaffolds. Journal of Materials Science: Materials in Medicine 24, 5, pp. 1153-1165.

Tanase, C.E., Popa, M.I. & Verestiuc, L. 2011. Biomimetic bone scaffolds based on chitosan and calcium phosphates. Materials Letters 65, 11, pp. 1681-1683.

Tang, S., Vickers, S.M., Hsu, H. & Spector, M. 2007. Fabrication and characterization of porous hyaluronic acid-collagen composite scaffolds. Journal of Biomedical Materials Research - Part A 82, 2, pp. 323-335.

Temenoff, J.S. & Mikos, A.G. 2000. Review: Tissue engineering for regeneration of articular cartilage. Biomaterials 21, 5, pp. 431-440.

Tripathi, A., Saravanan, S., Pattnaik, S., Moorthi, A., Partridge, N.C. & Selvamurugan, N. 2012. Bio-composite scaffolds containing chitosan/nano-hydroxyapatite/nano-copper-zinc for bone tissue engineering. International journal of biological macromolecules 50, 1, pp. 294-299.

Tsang, V.L. & Bhatia, S.N. 2006. Fabrication of three-dimensional tissues. Advantages in Biochemical Engineeering/Biotechnology, 103, pp. 189-205.

Tsuji, H. 2010. Hydrolytic degradation. In: Auras, R., Lim, L.T., Selke, S.E.M. & Tsuji, H. (ed.). Poly(lactic acid): Synthesis, structures, properties, processing, and applications. 1st ed. Hoboken, New Jersey, John Wiley & Sons, Inc. pp. 345-381.

Ulery, B.D., Nair, L.S. & Laurencin, C.T. 2011. Biomedical applications of biodegradable polymers. Journal of Polymer Science, Part B: Polymer Physics 49, 12, pp. 832-864.

Van Vlierberghe, S., Dubruel, P. & Schacht, E. 2011. Biopolymer-based hydrogels as scaffolds for tissue engineering applications: A review. Biomacromolecules 12, 5, pp. 1387-1408.

Venkatesan, J., Ryu, B., Sudha, P.N. & Kim, S. 2012. Preparation and characterization of chitosan-carbon nanotube scaffolds for bone tissue engineering. International journal of biological macromolecules 50, 2, pp. 393-402.

Vinatier, C., Mrugala, D., Jorgensen, C., Guicheux, J. & Noël, D. 2009. Cartilage engineering: a crucial combination of cells, biomaterials and biofactors. Trends in biotechnology 27, 5, pp. 307-314.

Von Doernberg, M., von Rechenberg, B., Bohner, M., Grünenfelder, S., Van Lenthe, G.H., Müller, R., Gasser, B., Mathys, R., Baroud, G. & Auer, J. 2006. In vivo behavior of calcium phosphate scaffolds with four different pore sizes. Biomaterials 27, 30, pp. 5186-5198.

Von Heimburg, D., Zachariah, S., Kühling, H., Heschel, I., Schoof, H., Hafemann, B. & Pallua, N. 2001. Human preadipocytes seeded on freeze-dried collagen scaffolds investigated in vitro and in vivo. Biomaterials 22, 5, pp. 429-438.

Wang, X., Sang, L., Luo, D. & Li, X. 2011. From collagen-chitosan blends to three-dimensional scaffolds: The influences of chitosan on collagen nanofibrillar structure and mechanical property. Colloids and Surfaces B: Biointerfaces 82, 1, pp. 233-240.

Wang, X.H., Cui, F.Z., Feng, Q.L., Li, J.C. & Zhang, Y.H. 2003. Preparation and Characterization of Collagen/Chitosan Matrices as Potential Biomaterials. Journal of Bioactive and Compatible Polymers 18, 6, pp. 453-467.

Wang, Y., Yang, C., Chen, X. & Zhao, N. 2006. Development and characterization of novel biomimetic composite scaffolds based on bioglass-collagen-hyaluronic acid-phosphatidylserine for tissue engineering applications. Macromolecular Materials and Engineering 291, 3, pp. 254-262.

Weigel, T., Schinkel, G. & Lendlein, A. 2006. Design and preparation of polymeric scaffolds for tissue engineering. Expert Review of Medical Devices 3, 6, pp. 835-851.

Williams, B.R., Gelman, R.A., Poppke, D.C. & Piez, K. 1978. Collagen fibril formation. Optimal in vitro conditions and preliminary kinetic results. Journal of Biological Chemistry 253, 18, pp. 6578-6585.

Wu, X., Black, L., Santacana-Laffitte, G. & Patrick Jr., C.W. 2007. Preparation and assessment of glutaraldehyde-crosslinked collagen-chitosan hydrogels for adipose tissue engineering. Journal of Biomedical Materials Research - Part A 81, 1, pp. 59-65.

Xia, W., Liu, W., Cui, L., Liu, Y., Zhong, W., Liu, D., Wu, J., Chua, K. & Cao, Y. 2004. Tissue engineering of cartilage with the use of chitosan-gelatin complex scaffolds. Journal of Biomedical Materials Research - Part B Applied Biomaterials 71, 2, pp. 373-380.

Xie, E., Hu, Y., Chen, X., Bai, X., Li, D., Ren, L. & Zhang, Z. 2008. In vivo bone regeneration using a novel porous bioactive composite. Applied Surface Science 255, 2, pp. 545-547.

Xu, C., Lu, W., Bian, S., Liang, J., Fan, Y. & Zhang, X. 2012. Porous collagen scaffold reinforced with surfaced activated PLLA nanoparticles. The Scientific World Journal 2012, Article number 695137.

Xu, C., Su, P., Chen, X., Meng, Y., Yu, W., Xiang, A.P. & Wang, Y. 2011. Biocompatibility and osteogenesis of biomimetic Bioglass-Collagen-Phosphatidylserine composite scaffolds for bone tissue engineering. Biomaterials 32, 4, pp. 1051-1058.

Yang, C. 2012. Enhanced physicochemical properties of collagen by using EDC/NHS-crosslinking. Bulletin of Materials Science 35, 5, pp. 913-918.

Yang, C.R., Wang, Y.J., Chen, X.F. & Zhao, N.R. 2005. Biomimetic fabrication of BCP/COL/HCA scaffolds for bone tissue engineering. Materials Letters 59, 28, pp. 3635-3640.

Yang, F., Cui, W., Xiong, Z., Liu, L., Bei, J. & Wang, S. 2006. Poly(l,l-lactide-co-glycolide)/tricalcium phosphate composite scaffold and its various changes during degradation in vitro. Polymer Degradation and Stability 91, 12, pp. 3065-3073.

Yang, S., Leong, K., Du, Z. & Chua, C. 2001. The design of scaffolds for use in tissue engineering. Part I. Traditional factors. Tissue engineering 7, 6, pp. 679-689.

Yao, Q., Nooeaid, P., Detsch, R., Roether, J.A., Dong, Y., Goudouri, O., Schubert, D.W. & Boccaccini, A.R. 2014. Bioglass®/chitosan-polycaprolactone bilayered composite scaffolds intended for osteochondral tissue engineering. Journal of Biomedical Materials Research - Part A, 102, 12, pp.4510-4518.

Yaylaoglu, M.B., Yildiz, C., Korkusuz, F. & Hasirci, V. 1999. A novel osteochondral implant. Biomaterials 20, 16, pp. 1513-1520.

Yu, D., Li, Q., Mu, X., Chang, T. & Xiong, Z. 2008. Bone regeneration of critical calvarial defect in goat model by PLGA/TCP/rhBMP-2 scaffolds prepared by low-temperature rapid-prototyping technology. International journal of oral and maxillofacial surgery 37, 10, pp. 929-934.

Zhang, J., Liu, G., Wu, Q., Zuo, J., Qin, Y. & Wang, J. 2012. Novel Mesoporous Hydroxyapatite/Chitosan Composite for Bone Repair. Journal of Bionic Engineering 9, 2, pp. 243-251.

Zhang, K., Zhang, Y., Yan, S., Gong, L., Wang, J., Chen, X., Cui, L. & Yin, J. 2013. Repair of an articular cartilage defect using adipose-derived stem cells loaded on a polyelectrolyte complex scaffold based on poly(l-glutamic acid) and chitosan. Acta Biomaterialia 9, 7, pp. 7276-7288.

Zhang, Y., Ni, M., Zhang, M. & Ratner, B. 2003. Calcium phosphate-chitosan composite scaffolds for bone tissue engineering. Tissue engineering 9, 2, pp. 337-345.

Zhang, Y., Wu, C., Friis, T. & Xiao, Y. 2010. The osteogenic properties of CaP/silk composite scaffolds. Biomaterials 31, 10, pp. 2848-2856.

Zhang, Y. & Zhang, M. 2001. Microstructural and mechanical characterization of chitosan scaffolds reinforced by calcium phosphates. Journal of Non-Crystalline Solids 282, 2-3, pp. 159-164.

Zhang, Y. & Zhang, M. 2002. Three-dimensional macroporous calcium phosphate bioceramics with nested chitosan sponges for load-bearing bone implants. Journal of Biomedical Materials Research 61, 1, pp. 1-8.

Zhou, J., Xu, C., Wu, G., Cao, X., Zhang, L., Zhai, Z., Zheng, Z., Chen, X. & Wang, Y. 2011. In vitro generation of osteochondral differentiation of human marrow mesenchymal stem cells in novel collagen-hydroxyapatite layered scaffolds. Acta Biomaterialia 7, 11, pp. 3999-4006.

Zhu, C., Fan, D., Duan, Z., Xue, W., Shang, L., Chen, F. & Luo, Y. 2009a. Initial investigation of novel human-like collagen/chitosan scaffold for vascular tissue engineering. Journal of Biomedical Materials Research - Part A 89, 3, pp. 829-840.

Zhu, Y., Liu, T., Song, K., Jiang, B., Ma, X. & Cui, Z. 2009b. Collagen-chitosan polymer as a scaffold for the proliferation of human adipose tissue-derived stem cells. Journal of Materials Science: Materials in Medicine 20, 3, pp. 799-808.

Zhu, Y., Wan, Y., Zhang, J., Yin, D. & Cheng, W. 2014. Manufacture of layered collagen/chitosan-polycaprolactone scaffolds with biomimetic microarchitecture. Colloids and Surfaces B: Biointerfaces 113, pp. 352-360.

APPENDIX I

Different freeze-dried scaffolds types, the used materials (matrix and filler) and amount of components, cross-linking method, the type of the molud in processing (the material used for the mould and the size of the mould), possible sterilization method, abbreviations for different scaffold types, and their related publications.

Scaffold materials	Matrix material	Filler	Cross-linking	Used mould and size [Ø/height]	Sterilized	Abbreviation	Publica-tion
Natural polymer-based scaffolds							
Collagen	0.3 wt% collagen	No	No	PS[a], 21.5 mm/5 mm	No	Col0.3NoE	I
		No	EDC cross-linking prior to freeze-drying	PS, 21.5 mm/5 mm	No	Col0.3(E)	I
		No	EDC cross-linking post freeze-drying	PS, 21.5 mm/5 mm	No	Col0.3E	I
	0.5 wt% collagen	No	No	PS, 21.5 mm/5 mm	No	Col0.5NoE	I
		No	EDC cross-linking prior to freeze-drying	PS, 21.5 mm/5 mm	No	Col0.5(E)	I
		No	EDC cross-linking post freeze-drying	PS, 21.5 mm/5 mm	No	Col0.5E	I
	1.0 wt% collagen	No	No	PS, 21.5 mm/5 mm or PTFE[b], 8 mm/4 mm	No	Col1.0NoE	I
		No	EDC cross-linking prior to freeze-drying	PS, 21.5 mm/5 mm	No	Col1.0(E)	I
		No	EDC cross-linking post freeze-drying	PS, 21.5 mm/5 mm	No	Col1.0E	I
		No	EDC+NHS cross-linking post freeze-drying	PTFE, 8 mm/3 mm	No	Col	IV
	2.0 wt% collagen	No	No	PS, 21.5 mm/5 mm	No	Col2.0	I
		No	EDC cross-linking prior to freeze-drying	PS, 21.5 mm/5 mm	No	Col2.0(E)	I
		No	EDC cross-linking post freeze-drying	PS, 21.5 mm/5 mm	No	Col2.0E	I
Chitosan	1.0 wt% chitosan	No	No	PTFE, 8 mm/4 mm	No	Chi	IV
Collagen+Chitosan	1.0 wt% collagen and chitosan 1:1 (v/v)	No	EDC+NHS cross-linking post freeze-drying	PTFE, 8 mm/4 mm	No	C1C1	IV
	1.0 wt% collagen and chitosan 2:1 (v/v)	No	EDC+NHS cross-linking post freeze-drying	PTFE, 8 mm/4 mm	No	C2C1	IV
Collagen+PLA96	0.5 wt% collagen	PLA96 mesh	EDC+NHS cross-linking post freeze-drying	PTFE, 8 mm/4 mm	No	ColPLA	IV
Chitosan+PLA96	0.5 wt% chitosan	PLA96 mesh	EDC+NHS cross-linking post freeze-drying	PTFE, 8 mm/4 mm	No	ChiPLA	IV
Collagen+Chitosan+PLA96	0.5 wt% collagen and chitosan 1:1 (v/v)	PLA96 mesh	EDC+NHS cross-linking post freeze-drying	PTFE, 8 mm/4 mm	No	C1C1PLA	IV
	0.5 wt% collagen and chitosan 2:1 (v/v)	PLA96 mesh	EDC+NHS cross-linking post freeze-drying	PTFE, 8 mm/4 mm	No	C2C1PLA	IV
Synthetic polymer-based scaffolds							
PLA70	2.0 wt% PLA70/30	No	No	PTFE, 15 mm/3 mm	Gamma 25 kGy[c]	PLA2	II, III
	3.0 wt% PLA70/30	No	No	PTFE, 15 mm/3 mm	No	PLA3	III
PLA70+TCP	2.0 wt% PLA70/30	5 wt% β-TCP	No	PTFE, 15 mm/3 mm	No	PLA2TCP5	III
	2.0 wt% PLA70/30	10 wt% β-TCP	No	PTFE, 15 mm/3 mm	Gamma 25 kGy	PLA2TCP10	II, III
	2.0 wt% PLA70/30	20 wt% β-TCP	No	PTFE, 15 mm/3 mm	Gamma 25 kGy	PLA2TCP20	II, III
	3.0 wt% PLA70/30	5 wt% β-TCP	No	PTFE, 15 mm/3 mm	No	PLA3TCP5	III
	3.0 wt% PLA70/30	10 wt% β-TCP	No	PTFE, 15 mm/3 mm	No	PLA3TCP10	III
	3.0 wt% PLA70/30	20 wt% β-TCP	No	PTFE, 15 mm/3 mm	No	PLA3TCP20	III
PLA70+BG	2.0 wt% PLA70/30	10 wt% BaG0127	No	PTFE, 15 mm/3 mm	Gamma 25 kGy	PLA2BG10	II
	2.0 wt% PLA70/30	20 wt% BaG0127	No	PTFE, 15 mm/3 mm	Gamma 25 kGy	PLA2BG20	II
PLGA1	5.0 wt% PLGA1	No	No	PTFE, 15 mm/3 mm	Gamma 25 kGy	PLGA1	V
PLGA2	5.0 wt% PLGA1	No	No	PTFE, 15 mm/3 mm	Gamma 25 kGy	PLGA2	V
PLGA1+BGf1	3 wt% PLGA1	BGf1 mesh	No	PTFE, 15 mm/3 mm	Gamma 25 kGy	PLGA1BG1	V
PLGA2+BGf2	3 wt% PLGA1	BGf2 mesh	No	PTFE, 15 mm/3 mm	Gamma 25 kGy	PLGA2BG2	V

[a]PS = polystyrene, [b]PTFE = Polytetrafluoroethylene (Teflon), [c]Gamma 25 kGy = Gamma irradiation 25 kGy

APPENDIX IIA

Schematic diagram of the fabrication processes of natural polymer-based scaffolds.

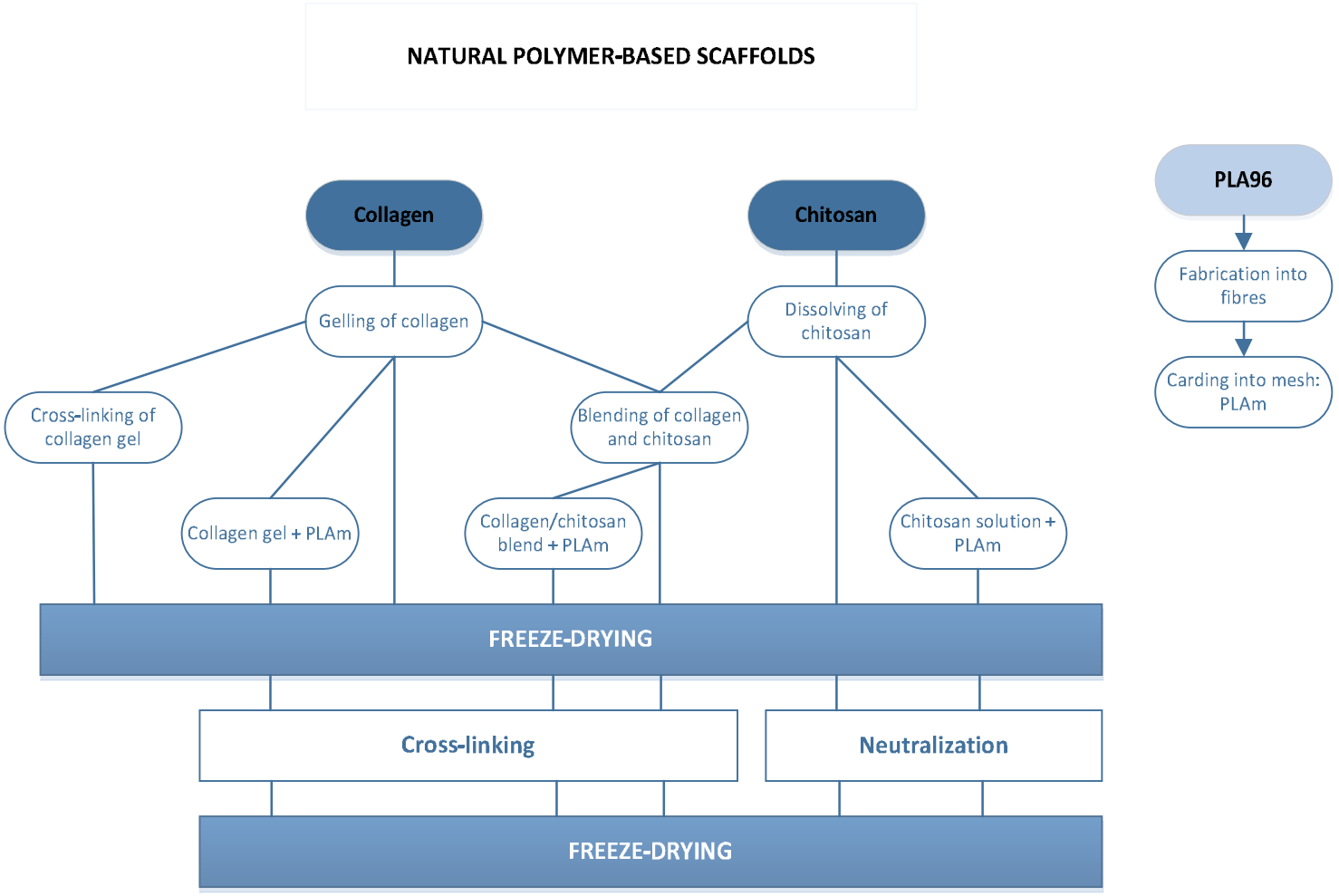

APPENDIX IIB

Schematic diagram of the fabrication processes of synthetic polymer-based scaffolds.

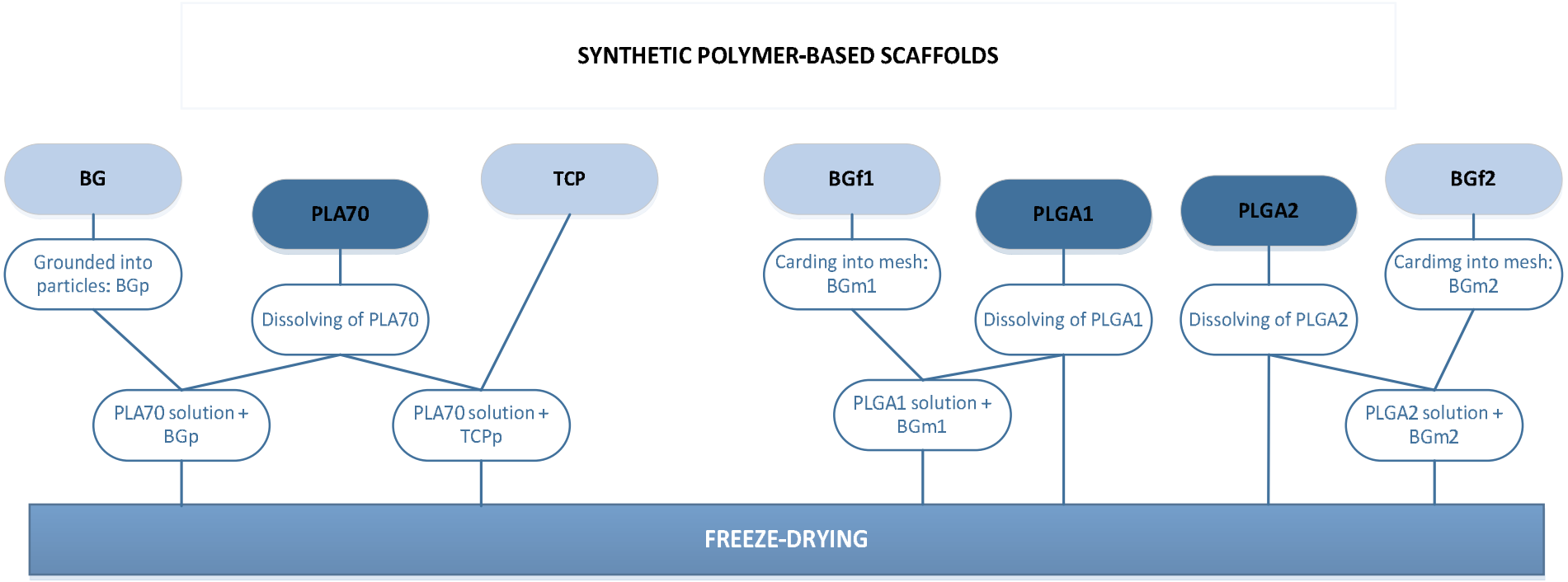

ORIGINAL PUBLICATIONS

Publication I

Haaparanta, AM., Koivurinta, J., Hämäläinen, ER. and Kellomäki, M.

The effect of cross-linking time on a porous freeze-dried collagen scaffold using 1-ethyl-3-(3-dimethylaminopropyl)carbodiimide as a cross-linker

Journal of Applied Biomaterials & Biomechanics, **6** (2008), 89-94

Publication II

Haimi, S., Suuriniemi, N., Haaparanta, AM., Ellä, V., Lindroos, B., Huhtala, H., Räty, S., Kuokkanen, H., Sándor, GK., Kellomäki, M., Miettinen, S. and Suuronen, R.

Growth and osteogenic differentiation of adipose stem cells on PLA/bioactive glass and PLA/β-TCP scaffolds

Tissue Engineering, **15** (2009), 1473-1480

TISSUE ENGINEERING: Part A
Volume 15, Number 7, 2009

DOI: 10.1089/ten.tea.2008.0241

Growth and Osteogenic Differentiation of Adipose Stem Cells on PLA/Bioactive Glass and PLA/β-TCP Scaffolds

Suvi Haimi, M.Sc.,[1,*] Niina Suuriniemi, M.Sc.,[1,*] Anne-Marie Haaparanta, M.Sc.,[2] Ville Ellä, M.Sc.,[2] Bettina Lindroos, M.Sc.,[1] Heini Huhtala, M.Sc.,[3] Sari Räty, M.D.,[4] Hannu Kuokkanen, M.D., Ph.D.,[5] George K. Sándor, M.D., D.D.S., Ph.D.,[1] Minna Kellomäki, Dr. Tech.,[2] Susanna Miettinen, M.Sc.,[1,*] and Riitta Suuronen, M.D., D.D.S., Ph.D.[1,2,6,*]

The aim of this study was to compare the effects of novel three-dimensional composite scaffolds consisting of a bioactive phase (bioactive glass or β-tricalcium phosphate [β-TCP] 10 and 20 wt%) incorporated within a polylactic acid (PLA) matrix on viability, distribution, proliferation, and osteogenic differentiation of human adipose stem cells (ASCs). The viability and distribution of ASCs on the bioactive composite scaffolds was evaluated using Live/Dead fluorescence staining, environmental scanning electron microscopy, and scanning electron microscopy. There were no differences between the two concentrations of bioactive glass and β-TCP in PLA scaffolds on proliferation and osteogenic differentiation of ASCs. After 2 weeks of culture, DNA content and alkaline phosphatase (ALP) activity of ASCs cultured on PLA/β-TCP composite scaffolds were higher relative to other scaffold types. Interestingly, the cell number was significantly lower, but the relative ALP/DNA ratio of ASCs was significantly higher in PLA/bioactive glass scaffolds than in other three scaffold types. These results indicate that the PLA/β-TCP composite scaffolds significantly enhance ASC proliferation and total ALP activity compared to other scaffold types. This supports the potential future use of PLA/β-TCP composites as effective scaffolds for tissue engineering and as bone replacement materials.

Introduction

One approach for bone tissue engineering involves harvesting of autologous stem cells from the patient, which are at first cultured on a scaffold *in vitro*, and then implanted with the scaffold in the defect of the patient, where optimally the bone should regenerate at the rate at which the scaffold resorbs.[1–3]

Mesenchymal stem cells (MSCs) have recently received widespread attention in the field of tissue engineering. MSCs can be derived from different types of tissues, but generally bone marrow–derived MSCs or adipose stem cells (ASCs) are used in bone tissue applications. ASCs can differentiate into osteoblastic cells, among other mesenchymal lineages *in vitro*, when treated with appropriate inducing factors.[4,5] ASCs are an ideal cell source for bone tissue engineering applications because they are abundant, their procurement causes minimal morbidity, and their expansion is rapid *in vitro*.[6–8]

Polylactic acid (PLA) polymers have been widely investigated as tissue engineering scaffolds due to their excellent mechanical properties and degradation profile even though they are not generally considered osteoconductive.[9–11] Composite scaffolds that include bioceramic or bioactive glass phases are one solution to improve the bioactivity. Bioactive glass is a well-known bone substitute material in clinical use because it is remarkably biocompatible, biodegradable, and osteoconductive, and provokes no significant inflammatory response.[12–15] On the surfaces of the bioactive glasses, a layer of calcium phosphate is formed in the presence of body fluids. *In vivo* and *in vitro* studies have demonstrated that the development of this bioactive layer stimulates the adjacent tissues to form new bone (i.e., osteoinduction) in

[1]Regea Institute for Regenerative Medicine, University of Tampere, Tampere, Finland.
[2]Department of Biomedical Engineering, Tampere University of Technology, Tampere, Finland.
[3]Tampere School of Public Health, University of Tampere, Tampere, Finland.
[4]Department of Gastroenterology and Alimentary Tract Surgery, Tampere University Hospital, Tampere, Finland.
[5]Department of Plastic Surgery, Tampere University Hospital, Tampere, Finland.
[6]Department of Eye, Ear, and Oral Diseases, Tampere University Hospital, Tampere, Finland.
*These authors contributed equally to this work.

the absence of any osteogenic supplements.[13,16–18] Another well-known bone substitute material is β-tricalcium phosphate (β-TCP), which has been studied extensively and used clinically as bone substitute material because of its similar molecular composition to human bone.[19–21] Among the bioceramics, β-TCP has excellent osteoconductivity, bioactivity, and an ability to form a strong bone–calcium phosphate interface.[22] However, clinical applications of β-TCP and bioactive glass are limited due to their brittleness and low mechanical strength.[23,24] Our hypothesis was that the incorporation of bioactive glass or β-TCP into a biodegradable PLA will result in an osteoconductive composite scaffold that supports both cell proliferation as well as differentiation into osteoblasts in a mechanically stable construct.

Even though there are many studies on different bioactive glass and β-TCP/biodegradable polymer composites,[25–29] only the effect of the concentration of bioactive glass or β-TCP in the composite on cell activity has been evaluated. However, no systematic comparison between PLA/β-TCP and PLA/bioactive glass composite scaffolds has been done. In the present study, we investigated and compared the effects of two novel biomaterial composite scaffolds, PLA/β-TCP and PLA/bioactive glass, upon human ASC morphology, proliferation, and osteogenic differentiation.

Materials and Methods

Material fabrication

Poly(L/D, L-lactide) (PLA) 70/30 (PURAC biochem bv, Gronichem, Netherlands) with inherent viscosity of ~3.1 dL/g was used as a matrix polymer. β-TCP (Beta Whitlockite; Plasma Biotal, Tideswell, UK) and bioactive glass (BaG0127; 5% Na_2O, 7.5% K_2O, 3% MgO, 25% CaO and 59.5% SiO_2; Åbo Akademi, Turku, Finland) were used as the filler materials. The particle size distribution of porous β-TCP granules was 75–106 μm, and the bioactive glass was ground down to 75–125 μm.

Table 1A. PLA/β-TCP Composite Scaffolds

	PLA (wt%)	*β-TCP (wt%)*
PLA	100	0
PLA/10 β-TCP	90	10
PLA/20 β-TCP	80	20

Table 1B. PLA/Bioactive Glass Composite Scaffolds

	PLA (wt%)	*Bioactive glass (wt%)*
PLA	100	0
PLA/10 bioactive glass	90	10
PLA/20 bioactive glass	80	20

The PLA solution of concentration of 2.0 wt% was prepared by dissolution of PLA in 1,4-dioxane (Sigma-Aldrich, Helsinki, Finland). Either filler was added into the PLA solution. The PLA filler ratios used are shown in Table 1. The solutions were frozen at −30°C before freeze-drying. The solution was placed into custom-made Teflon molds (Ø15 mm and height 3 mm) and frozen at −30°C for 24 h before 24 h freeze-drying. As a control, plain PLA scaffolds were prepared with the same technique like composite scaffolds. After freeze-drying, all the samples were held in room temperature under vacuum for a minimum of 48 h before sterilization with gamma irradiation at 25 kGy.

Scaffold characterization

The typical porous structure of the scaffolds is shown in the scanning electron microscopy (SEM) micrographs

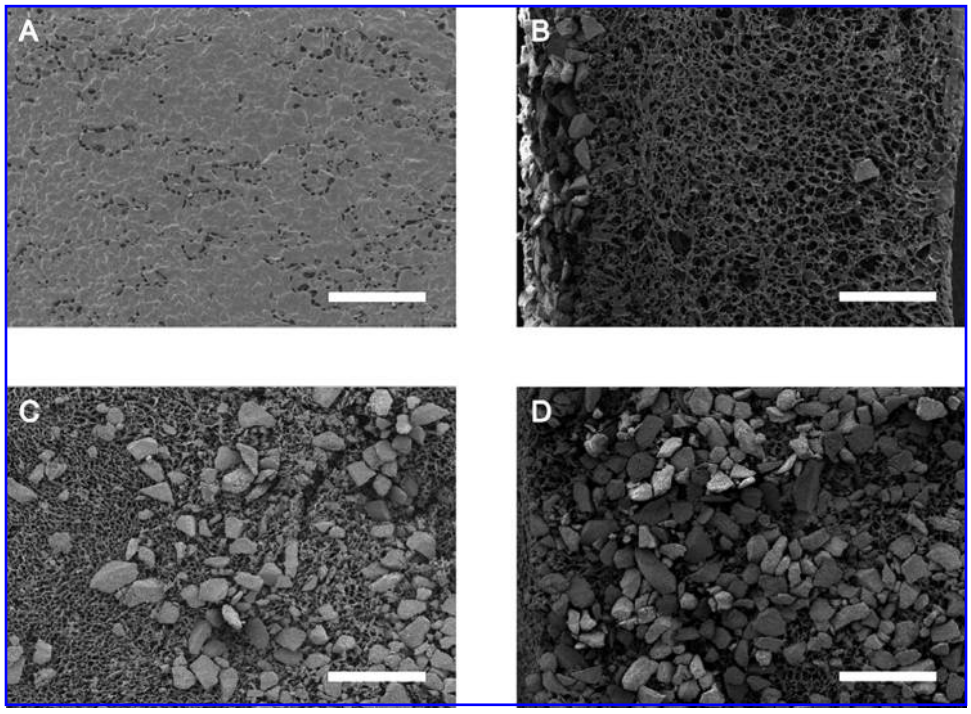

FIG. 1. SEM images of (**A**) dense top surface of PLA scaffold, (**B**) cross section of PLA/20 β-TCP scaffold, (**C**) porous bottom surface of PLA/10 β-TCP scaffold, and (**D**) porous bottom surface of PLA/20 β-TCP scaffold. Scale bars: 500 μm.

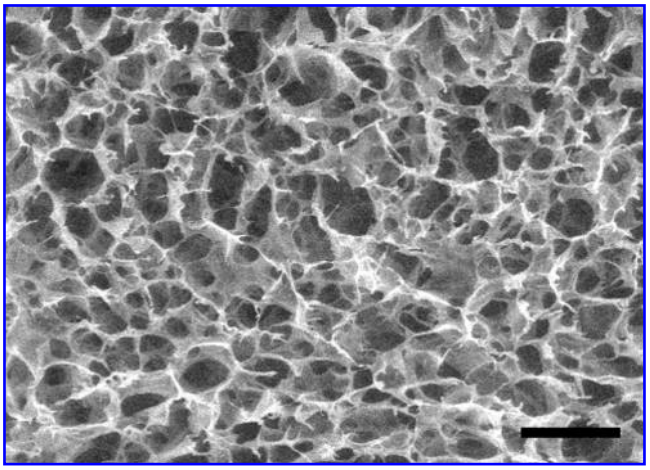

FIG. 2. E-SEM image of porous bottom surface of PLA scaffold. Scale bar: 100 μm.

(Fig. 1). Two different functional surfaces were formed during the freeze-drying of the scaffolds. The denser top surface of the scaffolds (Fig. 1A), also referred as the skin layer, was formed on all scaffold types when the frozen solvent sublimated from the top surface during the freeze-drying process. The structures of the bioactive glass and β-TCP composite scaffolds were similar; therefore, only the β-TCP SEM images are shown here. The β-TCP and bioactive glass granules were dispersed into the porous bottom surface during manufacturing (Fig. 1B–D). However, some granules can be seen in the middle of the scaffold (Fig. 1B). The granule distribution on the porous surface and the difference between 10 and 20 wt% of filler material are shown in Figure 1C and D. The interconnectivity of the pores is shown in Figure 2.

ASC isolation and culture

The study was conducted in accordance with the Ethics Committee of the Pirkanmaa Hospital District, Tampere, Finland. The ASCs were isolated from adipose tissue samples collected at operations and from liposuctions obtained from six donors (mean age = 44 ± 7). The adipose tissue samples were received from the Department of Plastic Surgery and from the Department of Gastroenterology and Alimentary Tract Surgery, Tampere University Hospital. The adipose tissue was digested with collagenase type I (1.5 mg/mL; Invitrogen, Paisley, UK). ASCs were expanded in T-75 polystyrene flasks (Nunc, Roskilde, Denmark) in maintenance medium consisting of Dulbecco's modified Eagle's medium/F-12 1:1 (Invitrogen), 10% fetal bovine serum (Invitrogen), 1% L-glutamine (GlutaMAX I; Invitrogen), and 1% antibiotics/antimycotic (100 U/mL penicillin, 0.1 mg/mL streptomycin, and 0.25 μg/mL amphotericin B; Invitrogen). Cells from passages 4 to 7 were used for all experiments.

Flow cytometric surface marker expression analysis

After primary culture in T-75 flasks, the ASCs were harvested and analyzed by a fluorescence-activated cell sorter (FACSAria; BD Biosciences, Erembodegem, Belgium). Monoclonal antibodies (MAb) against CD9-PE, CD10-PE-Cy7, CD13-PE, CD29-APC, CD49d-PE, CD90-APC, CD106-PE-Cy5, and CD166-PE (BD Biosciences); CD45-FITC (Miltenyi Biotech, Bergisch Gladbach, Germany); CD31-FITC, CD34-APC, and CD44-FITC (Immunotools, Friesoythe, Germany); and CD105-PE (R&D Systems, Minneapolis, MN) were used. MAb against STRO-1 (R&D Systems) and human fibroblast surface protein (hFSP; Sigma-Aldrich, St. Louis, MO) were conjugated with IgM-PE (CalTag Laboratories, Burlingame, CA). A total of 10,000 cells per sample were used, and positive expression was defined as a level of fluorescence that was 99% of the corresponding unstained cell sample.

Cell seeding and culture of ASC-seeded composite scaffolds

In each experiment, three to four patient samples were pooled together to yield enough cells for one experiment. Each scaffold was pretreated with maintenance medium for 48 h at 37°C. The porous surfaces of the scaffolds were seeded with 350,000 cells in a 0.175 mL drop. The cells were allowed to attach to the scaffolds for 3 h at 37°C in 5% carbon dioxide before additional medium was added. The cell-seeded scaffolds were cultured in maintenance medium until analyses.

Cell attachment and growth

Cell attachment and viability were studied using Live/Dead staining. Briefly, ASC–biomaterial constructs were incubated for 45 min at room temperature with a mixture of 5 μM CellTracker™ green (5-chloromethylfluorescein diacetate; Molecular Probes, Eugene, OR) and 2.5 μM ethidium homodimer-1 (Molecular Probes). The viable cells (green fluorescence) and necrotic cells (red fluorescence) were examined using a fluorescence microscope.

Cell morphology evaluation

After the cells were cultured for 2 weeks, the scaffolds were fixed in 5% glutaraldehyde (Sigma-Aldrich) in 0.1 M phosphate buffer, pH 7.4, for 48 h. After phosphate buffered saline rinsing, the samples were dehydrated through a series of increasing concentrations of ethanol (70%, 96%, and 100%). After the final dehydration step in absolute ethanol, the samples were transferred to liquid carbon dioxide and dried in a critical point dryer. A gold–palladium coating was sputtered on the specimens for SEM observations. Two parallel scaffolds of each type were observed using a scanning electron microscope (Jeol JSM-5500, Sundbyberg, Sweden).

Additionally, Philips XL30 E-SEM-TMP environmental scanning electron microscope (BioMater Centre, University of Kuopio, Finland) was used to evaluate the microstructure and morphology of the biomaterial scaffolds seeded with ASCs. The environmental scanning electron microscopy (E-SEM) images were taken using beam intensity at 8.0–12.0 kV and the gaseous secondary electron detectors at 1.0–4.0 torr.

Cell proliferation and quantitative analysis of alkaline phosphatase activity

The DNA content of ASC–biomaterial constructs was measured using a CyQUANT® Cell proliferation assay kit (Molecular Probes–Invitrogen) as described earlier.[30] The quantitative alkaline phosphatase (ALP) measurement was

performed according to the Sigma ALP procedure as described earlier.[30]

Statistical analysis

Statistical analysis of the results was performed with SPSS, version 13. The effect of scaffold material and time of culture (1 week vs. 2 weeks) were studied using a paired Student's *t*-test. The effects between β-TCP and bioactive glass composite material on the DNA content and ALP activity were compared using a one-way ANOVA, after checking for normal distribution and homogeneity of variance. *Post hoc* tests were performed to detect significant differences between groups. Data were reported as mean ± standard deviation values, and $p < 0.05$ was considered significant. The experiments were repeated three times.

Results

Flow cytometric surface marker expression analysis of ASCs

The FACS analysis demonstrated that the ASCs express the surface markers CD9, CD29, CD34, CD49d, CD105, CD166, CD44, CD10, CD13, CD90, STRO-1, and hFSP. The ASCs were negative for the hematopoietic markers CD31 and CD45 and for the vascular cell adhesion molecule CD106.

Cell attachment and growth on scaffolds

By 2 weeks, the number of viable cells had increased compared to the 3-h time point (data not shown), as observed by Live/Dead staining. At the 3-h time point the cells were attached only on the region close to surface, that is, cell seeding area. No difference was observed in different scaffold types at 3 h. The spreading of the cells inside the scaffolds had changed during the 2-week culturing period. Generally, in each scaffold type the cells had migrated from the porous bottom surface toward the inner parts of the scaffolds, which confirmed the interconnectivity of the pores, but only a few cells were found on the dense top surface. The cell density at the region close to the porous surface was higher than at the core of each scaffold type. At the region close to the surface, cells had formed cluster structures between the pores in all other scaffold types but not in PLA/20 β-TCP, where the cells had spread more evenly (Fig. 3). There was no difference between different scaffold types on cell number or the cell viability in visual inspection.

Cell morphology

After the 2-week cell culture period, SEM and E-SEM imaging were used to examine the cell morphology and spreading on the cell–biomaterial interface (Fig. 4). The cell

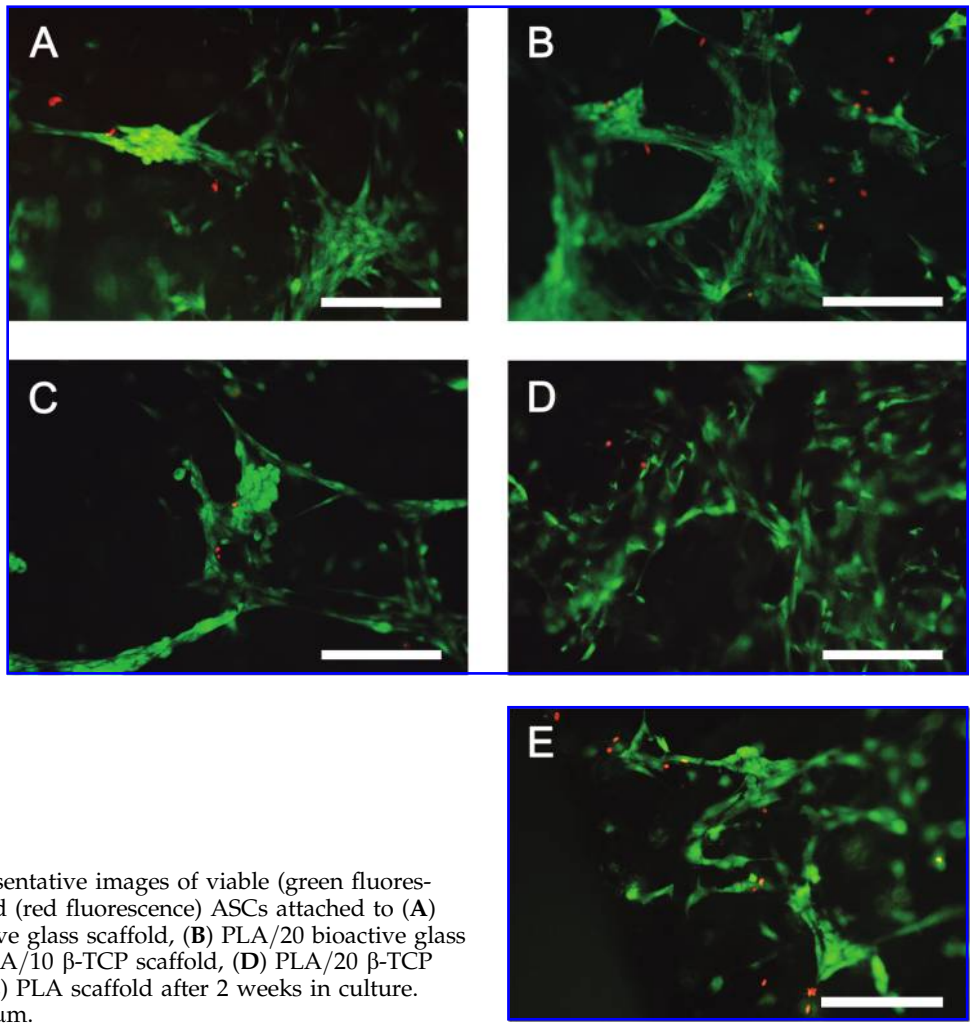

FIG. 3. Representative images of viable (green fluorescence) and dead (red fluorescence) ASCs attached to (**A**) PLA/10 bioactive glass scaffold, (**B**) PLA/20 bioactive glass scaffold, (**C**) PLA/10 β-TCP scaffold, (**D**) PLA/20 β-TCP scaffold, and (**E**) PLA scaffold after 2 weeks in culture. Scale bars: 200 μm.

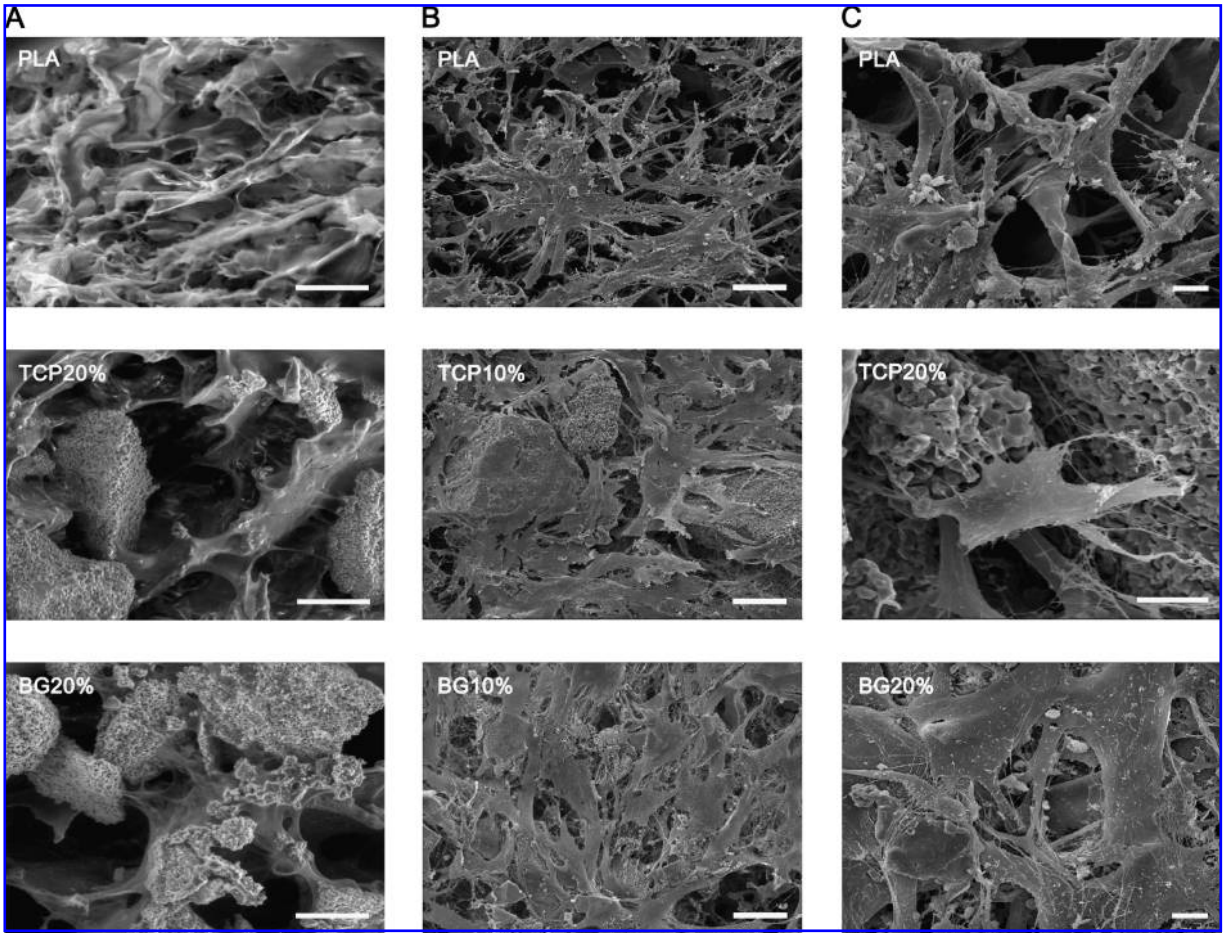

FIG. 4. (**A**) E-SEM images of ASCs on the PLA, PLA/20 β-TCP (TCP), and PLA/bioactive glass (BG) 20 wt% (scale bars: 50 μm). (**B**) SEM micrographs of ASCs on the PLA, PLA/10β-TCP, and PLA/10 bioactive glass (scale bars: 50 μm). (**C**) SEM micrographs of ASCs on the PLA, PLA/20β-TCP, and PLA/20 bioactive glass (scale bars: 10 μm).

morphology was unaffected by β-TCP or bioactive glass component in the scaffolds. During the 2-week culture period, ASCs started to colonize the scaffolds without forming a homogenous monolayer. Images with higher magnification (Fig. 3C) show ASCs stretching and forming projections on the porous surface of the scaffolds. The β-TCP and bioactive glass granules were clearly distinguished on the porous surface of the scaffolds, and the ASCs were forming bridges between the granules on the PLA/β-TCP and PLA/bioactive glass composite scaffolds (Fig. 4A). ASCs were also detected inside the pores in different scaffolds. In each scaffold type the majority of ASCs were spread at the region close to the porous surface, which supports the observations made in Live/Dead staining.

Cell proliferation

The number of cells present on the scaffolds was assessed by measuring the total DNA content (Fig. 5). After 2 weeks of culture, the cell number was significantly higher in both PLA/β-TCP scaffolds than in other three scaffold types. Conversely, DNA content of ASC cultured on PLA/bioactive glass scaffolds was significantly lower compared to the other scaffold types. There was no significant difference detected between the two concentrations of both β-TCP and bioactive glass (i.e., 10 wt% vs. 20 wt%).

ASC differentiation

The effects of the five different scaffold types on the early differentiation of ASCs into osteogenic pathway were evaluated by quantitative measurement of ALP activity. At 2 weeks the relative ALP activity of ASCs cultured on PLA/10 β-TCP scaffolds had the same magnitude as ASCs cultured on PLA/20 β-TCP scaffolds, but it was significantly higher than that of the other scaffold types (PLA, $p = 0.017$; bioactive glass 10 wt%, $p = 0.023$; and bioactive glass 20 wt%, $p = 0.022$; Fig. 6). At 2 weeks the relative ALP activity of ASCs cultured on PLA/bioactive glass and PLA scaffold was comparable, but it is due to the lower cell number in PLA/bioactive glass scaffolds than in PLA scaffolds. These results indicate that relative ALP/DNA ratio was higher on PLA/bioactive glass scaffolds than in PLA and PLA/β-TCP scaffolds.

The effect of culturing period on ASCs proliferation and differentiation

We studied the effect of culturing period on ASC proliferation, and we found no increase of relative DNA content when the cells were cultured on bioactive glass composites for 2 weeks compared to 1 week (data not shown). In contrast, the DNA content of ASCs cultured on PLA/β-TCP

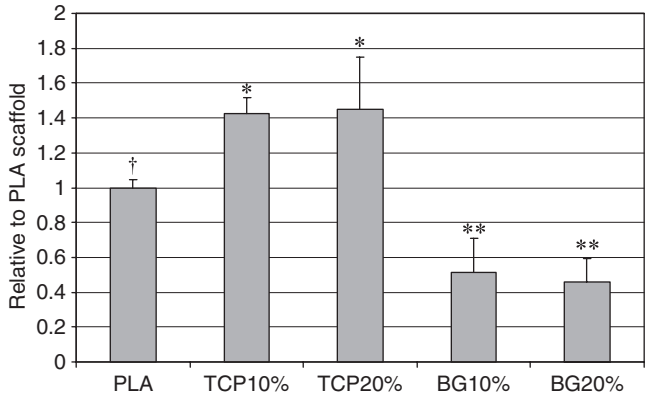

FIG. 5. Relative DNA content of ASCs cultured for 2 weeks on PLA, PLA/β-TCP (TCP), and PLA/bioactive glass (BG) scaffolds. Results are expressed as mean + SD relative DNA content in three experiments ($n = 4$). *$p < 0.005$ with respect to PLA, bioactive glass 10 and 20 wt%; **$p < 0.005$ with respect to PLA, β-TCP 10 and 20 wt%; $^{\dagger}p < 0.005$ with respect to β-TCP 10 and 20 wt% and bioactive glass 10 and 20 wt%.

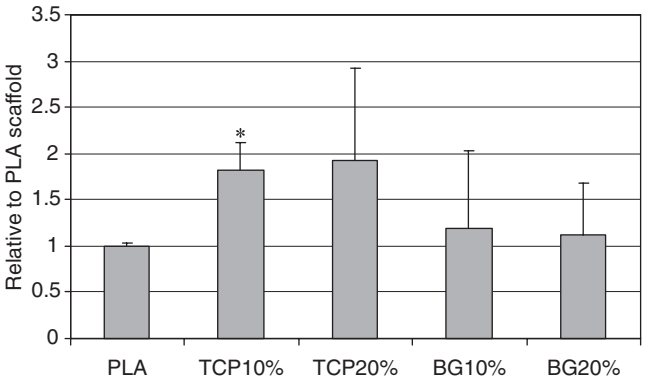

FIG. 6. Relative ALP activity of ASCs cultured for 2 weeks on PLA, PLA/β-TCP (TCP), and PLA/bioactive glass (BG) scaffolds. Results are expressed as mean + SD relative ALP activity in three experiments ($n = 4$). *$p < 0.005$ with respect to PLA, bioactive glass 10 and 20 wt%.

composites and PLA scaffolds was increased at 2 weeks; however, no significant difference between 1 and 2 weeks was detected.

ASCs cultured on PLA and bioactive glass composite scaffolds produced two times higher levels of ALP activity at 2 weeks than at 1 week (data not shown). A significant increase at the 2-week time point was only seen when ASCs were cultured on PLA/20 β-TCP scaffolds, although ALP activity of ASCs cultured on PLA/10 β-TCP scaffolds was also three times higher at 2 weeks than at 1 week.

Discussion

To our knowledge, this is the first reported study that compares the *in vitro* effects of PLA/β-TCP and PLA/bioactive glass composite scaffolds on ASC attachment, proliferation, and osteogenic differentiation. We also studied the effect of culturing period on proliferation and ALP activity of ASC cultured on different scaffold types in two time points.

The identity of ACSs was confirmed using FACS analysis. The FACS analysis results were consistent with previous results for MSCs.[31] A culture system using ASCs was chosen because these cells have the ability to differentiate into osteoblasts, similar to bone marrow–derived MSCs. A second advantage of using ACSs is that unlike bone marrow MSCs, their use is not limited by a low harvest number of cells.[6,32]

Live/Dead staining and SEM imaging showed that the cell density at the region close to the surface was higher than at the core of each scaffold type, which is attributed to the heterogenic structure of the composite scaffolds. The bioactive glass and β-TCP particles were clustered on the porous side of the composite scaffold, which made this region of the scaffold more hydrophilic. It is not surprising that the hydrophilic nature of this region enhanced the cell attachment and growth compared to other more hydrophobic parts of the scaffold. These results are also in agreement with previously published *in vitro* experiments, which have confirmed the positive effect of increasing concentration of bioactive glass particles on poly(DL-lactide) (PDLLA) scaffolds to promote osteoblast and osteoblast-like cell adhesion and growth.[28,33] In PLA scaffolds the cells spread also to the region close to the porous surface, which may be explained by the overall hydrophobicity of the scaffold.

Our SEM results show that the cell morphology was unaffected by β-TCP or bioactive glass component in the scaffold material. This result differs from the findings of Tsigkou *et al.*,[17] where the authors found that human fetal osteoblasts were less spread and elongated on PDLLA and PDLLA-bioactive glass 5 wt% composite films, whereas cells on PDLLA-bioactive glass 40 wt% composite films were elongated but with multiple protrusions spreading over the bioactive glass particles.

Bioactive glass has been studied intensively for over three decades in the bone regeneration applications. Specific bioactive glass compositions have been shown to promote proliferation and differentiation of human osteoblasts and rat MSCs into osteogenic lineages.[34–36] These publications have shown that bioactive glasses are superior scaffold materials in inducing osteogenic differentiation, although contradictory results also exist. Reilly *et al.* have recently shown that the positive effects of bioactive glass on bone growth in human patients are not mediated by accelerated differentiation of MSCs.[37] In addition, a poly(lactide-co-glycolide) (PLGA) scaffold coated with bioactive glass had no effect on ALP activity or osteocalcin production of human MSCs compared with uncoated scaffolds.[38] Our findings suggest that bioactive glass particles do not induce total ALP activity of ASCs more than PLA alone, although the relative ALP activity of a single cell, that is, ALP/DNA ratio on PLA/bioactive glass scaffolds, was higher than in other scaffolds. This result is in contrast to Mayr-Wohlfart *et al.*, who demonstrated that osteoblast-like cells grown on α-TCP have significantly higher ALP/DNA ratio than on bioactive glass.[39]

It has been shown that adding increasing percentages of β-TCP to a lactic acid polymer matrix stimulates the proliferation and differentiation of human MSCs and osteogenous cells.[27,40] While it is difficult to compare our results with those of others who have used different composites,

our results are similar to previous work which showed that proliferation and total ALP activity of ASCs was significantly higher in PLA/β-TCP scaffolds than in PLA scaffolds.

In the present study, no significant differences between the effects of the two concentrations of bioactive glass and β-TCP were found on ASC attachment, proliferation, and differentiation. This may be explained by the heterogeneous structure of the composite scaffold. If the filler particles would have been homogeneously arranged on the scaffold, the difference between the filler concentration may have been more evident.

Interestingly, the results of the effect of the culturing period on ASC proliferation showed that the cell number was at the same level on PLA/bioactive composite scaffolds, while the cell number was increased in three other scaffold types (in PLA/10 β-TCP significantly) at 2 weeks compared to 1 week. The relative ALP activity of ACSs, however, increased with time in all scaffold types.

This study demonstrated that, of the studied scaffolds, PLA/bioactive glass scaffolds supported proliferation of ASCs the weakest, although ASCs exhibited the strongest differentiation capacity when cultured on PLA/bioactive glass scaffolds. An ideal scaffold for bone tissue engineering should, however, promote both cell proliferation and osteogenic differentiation. Our results show that PLA/β-TCP composite scaffolds significantly enhance ASC proliferation and total ALP activity compared to PLA alone or composite forms of PLA/bioactive glass scaffolds. We conclude that PLA/β-TCP composite scaffolds demonstrate significant potential in future hard tissue engineering.

Acknowledgments

The authors thank Ms. Miia Juntunen and Ms. Minna Salomäki for excellent technical assistance. Special thanks to Mr. Tuomas Huttunen for graphic processing and consultation and to Arto Koistinen in the BioMater Centre, University of Kuopio, for the outstanding technical assistance and guidance of the E-SEM equipment. Thanks also to Professor Lauri Pelliniemi from Laboratory of Electron Microscopy, University of Turku. This research was supported by the competitive research funding of the Pirkanmaa Hospital District, the Finnish Funding Agency for Technology and Innovation (TEKES), the Finnish Cultural Foundation and the City of Tampere.

Disclosure Statement

No competing financial interests exist.

References

1. Jones, J.R., Tsigkou, O., Coates, E.E., Stevens, M.M., Polak, J.M., and Hench, L.L. Extracellular matrix formation and mineralization on a phosphate-free porous bioactive glass scaffold using primary human osteoblast (HOB) cells. Biomaterials **28**(9), 1653–1663, 2007.
2. Ohgushi, H., and Caplan, A.I. Stem cell technology and bioceramics: from cell to gene engineering. J Biomed Mater Res **48**(6), 913–927, 1999.
3. Takezawa, T. A strategy for the development of tissue engineering scaffolds that regulate cell behavior. Biomaterials **24**(13), 2267–2275, 2003.
4. Zuk, P.A., Zhu, M., Ashjian, P., de Ugarte, D.A., Huang, J.I., Mizuno, H., *et al.* Human adipose tissue is a source of multipotent stem cells. Mol Biol Cell **13**(12), 4279–4295, 2002.
5. Zuk, P.A., Zhu, M., Mizuno, H., Huang, J., Futrell, J.W., Katz, A.J., *et al.* Multilineage cells from human adipose tissue: implications for cell-based therapies. Tissue Eng **7**(2), 211–228, 2001.
6. Hattori, H., Sato, M., Masuoka, K., Ishihara, M., Kikuchi, T., Matsui, T., *et al.* Osteogenic potential of human adipose tissue-derived stromal cells as an alternative stem cell source. Cells Tissues Organs **178**(1), 2–12, 2004.
7. Slater, B., Kwan, M., Wan, D., and Longaker, M. From adiposity to bone. Int Congr Ser **1302,** 79–88, 2007.
8. Strem, B.M., and Hedrick, M.H. The growing importance of fat in regenerative medicine. Trends Biotechnol **23**(2), 64–66, 2005.
9. Navarro, M., Ginebra, M.P., Planell, J.A., Zeppetelli, S., and Ambrosio, L. Development and cell response of a new biodegradable composite scaffold for guided bone regeneration. J Mater Sci Mater Med **15**(4), 419–422, 2004.
10. Ren, J., Ren, T., Zhao, P., Huang, Y., and Pan, K. Repair of mandibular defects using MSCs-seeded biodegradable polyester porous scaffolds. J Biomater Sci Polym Ed **18**(5), 505–517, 2007.
11. Wang, S., Cui, W., and Bei, J. Bulk and surface modifications of polylactide. Anal Bioanal Chem **381**(3), 547–556, 2005.
12. Hench, L.L., and Andersson, O. Bioactive glasses. In: Hench, L.L., and Wilson, J., eds. In an Introduction to Bioceramics. Singapore: World Scientific, 1993, pp. 41–62.
13. Hench, L.L., and Paschall, H.A. Direct chemical bond of bioactive glass-ceramic materials to bone and muscle. J Biomed Mater Res **7**(3), 25–42, 1973.
14. Jarcho, M. Calcium phosphate ceramics as hard tissue prosthetics. Clin Orthop Relat Res **157**, 259–278, 1981.
15. Kitsugi, T., Yamamuro, T., Nakamura, T., Kotani, S., Kokubo, T., and Takeuchi, H. Four calcium phosphate ceramics as bone substitutes for non-weight-bearing. Biomaterials **14**(3), 216–224, 1993.
16. Hench, L.L., and Paschall, H.A. Histochemical responses at a biomaterial's interface. J Biomed Mater Res **8**(3), 49–64, 1974.
17. Tsigkou, O., Hench, L.L., Boccaccini, A.R., Polak, J.M., and Stevens, M.M. Enhanced differentiation and mineralization of human fetal osteoblasts on PDLLA containing Bioglass composite films in the absence of osteogenic supplements. J Biomed Mater Res A **80**(4), 837–851, 2007.
18. Vrouwenvelder, W.C., Groot, C.G., and de Groot, K. Histological and biochemical evaluation of osteoblasts cultured on bioactive glass, hydroxylapatite, titanium alloy, and stainless steel. J Biomed Mater Res **27**(4), 465–475, 1993.
19. Dorozhkin, S.V., and Epple, M. Biological and medical significance of calcium phosphates. Angew Chem Int Ed Engl **41**(17), 3130–3146, 2002.
20. Hench, L.L., and Wilson, J. Surface-active biomaterials. Science **226**(4675), 630–636, 1984.
21. Sun, H., Wu, C., Dai, K., Chang, J., and Tang, T. Proliferation and osteoblastic differentiation of human bone marrow-derived stromal cells on akermanite-bioactive ceramics. Biomaterials **27**(33), 5651–5657, 2006.
22. LeGeros, R.Z. Properties of osteoconductive biomaterials: calcium phosphates. Clin Orthop Relat Res **395**, 81–98, 2002.

23. Hench, L.L. The story of Bioglass. J Mater Sci Mater Med **17**(11), 967–978, 2006.
24. Wang, M. Developing bioactive composite materials for tissue replacement. Biomaterials **24**(13), 2133–2151, 2003.
25. Kim, S.S., Sun Park, M., Jeon, O., Yong Choi, C., and Kim, B.S. Poly(lactide-co-glycolide)/hydroxyapatite composite scaffolds for bone tissue engineering. Biomaterials **27**(8), 1399–1409, 2006.
26. Niemeyer, P., Krause, U., Fellenberg, J., Kasten, P., Seckinger, A., Ho, A.D., *et al.* Evaluation of mineralized collagen and alpha-tricalcium phosphate as scaffolds for tissue engineering of bone using human mesenchymal stem cells. Cells Tissues Organs **177**(2), 68–78, 2004.
27. Takahashi, Y., Yamamoto, M., and Tabata, Y. Osteogenic differentiation of mesenchymal stem cells in biodegradable sponges composed of gelatin and beta-tricalcium phosphate. Biomaterials **26**(17), 3587–3596, 2005.
28. Verrier, S., Blaker, J.J., Maquet, V., Hench, L.L., and Boccaccini, A.R. PDLLA/Bioglass composites for soft-tissue and hard-tissue engineering: an *in vitro* cell biology assessment. Biomaterials **25**(15), 3013–3021, 2004.
29. Yang, X.B., Webb, D., Blaker, J., Boccaccini, A.R., Maquet, V., Cooper, C., *et al.* Evaluation of human bone marrow stromal cell growth on biodegradable polymer/bioglass composites. Biochem Biophys Res Commun **342**(4), 1098–1107, 2006.
30. Lindroos, B., Mäenpää, K., Ylikomi, T., Oja, H., Suuronen, R., and Miettinen, S. Characterisation of human dental stem cells and buccal mucosa fibroblasts. Biochem Biophys Res Commun, **368**(2), 329–335, 2008.
31. Gronthos, S., Franklin, D.M., Leddy, H.A., Robey, P.G., Storms, R.W., and Gimble, J.M. Surface protein characterization of human adipose tissue-derived stromal cells. J Cell Physiol **189**(1), 54–63, 2001.
32. Strem, B.M., Hicok, K.C., Zhu, M., Wulur, I., Alfonso, Z., Schreiber, R.E., *et al.* Multipotential differentiation of adipose tissue-derived stem cells. Keio J Med **54**(3), 132–141, 2005.
33. Boccaccini, A.R., Notingher, I., Maquet, V., and Jerome, R. Bioresorbable and bioactive composite materials based on polylactide foams filled with and coated by bioglass particles for tissue engineering applications. J Mater Sci Mater Med **14**(5), 443–450, 2003.
34. Bosetti, M., and Cannas, M. The effect of bioactive glasses on bone marrow stromal cells differentiation. Biomaterials **26**(18), 3873–3879, 2005.
35. Bosetti, M., Zanardi, L., Hench, L., and Cannas, M. Type I collagen production by osteoblast-like cells cultured in contact with different bioactive glasses. J Biomed Mater Res A **64**(1), 189–195, 2003.
36. Xynos, I.D., Hukkanen, M.V., Batten, J.J., Buttery, L.D., Hench, L.L., and Polak, J.M. Bioglass 45S5 stimulates osteoblast turnover and enhances bone formation *in vitro*: implications and applications for bone tissue engineering. Calcif Tissue Int **67**(4), 321–329, 2000.
37. Reilly, G.C., Radin, S., Chen, A.T., and Ducheyne, P. Differential alkaline phosphatase responses of rat and human bone marrow derived mesenchymal stem cells to 45S5 bioactive glass. Biomaterials **28**(28), 4091–4097, 2007.
38. Leach, J.K., Kaigler, D., Wang, Z., Krebsbach, P.H., and Mooney, D.J. Coating of VEGF-releasing scaffolds with bioactive glass for angiogenesis and bone regeneration. Biomaterials **27**(17), 3249–3255, 2006.
39. Mayr-Wohlfart, U., Fiedler, J., Gunther, K.P., Puhl, W., and Kessler, S. Proliferation and differentiation rates of a human osteoblast-like cell line (SaOS-2) in contact with different bone substitute materials. J Biomed Mater Res **57**(1), 132–139, 2001.
40. Aunoble, S., Clement, D., Frayssinet, P., Harmand, M.F., and Le Huec, J.C. Biological performance of a new beta-TCP/PLLA composite material for applications in spine surgery: *in vitro* and *in vivo* studies. J Biomed Mater Res A **78**(2), 416–422, 2006.

Address correspondence to:
Suvi Haimi, M.Sc.
Regea Institute for Regenerative Medicine
University of Tampere
Biokatu 12
33520 Tampere
Finland

E-mail: suvi.haimi@regea.fi

Received: April 22, 2008
Accepted: October 1, 2008
Online Publication Date: December 10, 2008

Publication III

Haaparanta, AM., Haimi, S., Ellä, V., Hopper, N., Miettinen, S., Suuronen, R. and Kellomäki, M.

Porous polylactide/β-tricalcium phosphate composite scaffolds for tissue engineering applications

Journal of Tissue Engineering and Regenerative Medicine, **4** (2010), 366-373

Publication IV

Haaparanta, AM., Järvinen, E., Cengiz, IF., Ellä, V., Kokkonen, HT., Kiviranta, I. and Kellomäki, M.

Preparation and characterization of collagen/PLA, chitosan/PLA, and collagen/chitosan/PLA hybrid scaffolds for cartilage tissue engineering

Journal of materials Science: Materials in Medicine, **25** (2014), 1129-1136

Publication V

Haaparanta, AM., Uppstu, P., Hannula, M., Ellä, V., Rosling A. and Kellomäki, M.

Improved dimensional stability with bioactive glass fibre skeleton in poly(lactide-co-glycolide) porous scaffolds for tissue engineering

Submitted to
Materials Science and Engineering C: Materials for Biological Applications (2015)

Tampereen teknillinen yliopisto
PL 527
33101 Tampere

Tampere University of Technology
P.O.B. 527
FI-33101 Tampere, Finland

ISBN 978-952-15-3484-3
ISSN 1459-2045